

EUROPEAN ORGANISATION FOR NUCLEAR RESEARCH (CERN)



Submitted to: Phys. Lett. B.

CERN-EP-2025-155
18th July 2025

Search for the Higgs boson decay to a Z boson and a photon in pp collisions at $\sqrt{s} = 13$ TeV and 13.6 TeV with the ATLAS detector

The ATLAS Collaboration

A search for the Higgs boson decay to a Z boson and a photon in the $\ell\ell\gamma$ ($\ell = e, \mu$) final state is performed using pp collisions at $\sqrt{s} = 13.6$ TeV recorded with the ATLAS detector at the Large Hadron Collider during 2022–2024, corresponding to an integrated luminosity of 165 fb^{-1} . The signal yield, normalised to the Standard Model prediction, is measured to be $\mu = 0.9^{+0.7}_{-0.6}$, compared to an expected value of $\mu = 1.0 \pm 0.7$. This corresponds to an observed (expected) signal significance of 1.4 (1.5) standard deviations for the background-only hypothesis. This result is combined with that of a similar search performed with 140 fb^{-1} of $\sqrt{s} = 13$ TeV pp collisions to provide the most stringent expected sensitivity to date to this rare decay, namely an observed (expected) signal strength of $\mu = 1.3^{+0.6}_{-0.5}$ ($\mu = 1.0^{+0.6}_{-0.5}$), corresponding to an observed (expected) significance of 2.5 (1.9) standard deviations. The measurement is consistent with the Standard Model expectation.

1 Introduction

A new boson with properties consistent with those of the Standard Model (SM) Higgs boson (H) was independently observed in 2012 by the ATLAS and CMS Collaborations [1, 2] at the Large Hadron Collider (LHC) [3]. Measurements of its couplings to SM particles, its spin, and its parity have, to date, shown no significant deviation from the SM predictions [4–7]. The combined ATLAS and CMS determination of its mass from LHC Run-1 data yields $m_H = 125.09 \pm 0.24$ GeV [8], a value that is consistent with recent Run-2 measurements [9–11].

Within the SM, the Higgs boson decay to a Z boson and a photon ($H \rightarrow Z\gamma$) proceeds via loop-induced processes, leading to a predicted branching ratio of $\text{BR}(H \rightarrow Z\gamma) = (1.54^{+0.10}_{-0.11}) \times 10^{-3}$ for $m_H = 125.09$ GeV [12], similar to that for $H \rightarrow \gamma\gamma$, $\text{BR}(H \rightarrow \gamma\gamma) = (2.27^{+0.07}_{-0.06}) \times 10^{-3}$ [12]. Extensions to the SM, such as models with additional colourless charged scalars, fermions, or vector bosons, can alter this rate via contributions in the loops [13–19], making the ratio $\text{BR}(H \rightarrow Z\gamma)/\text{BR}(H \rightarrow \gamma\gamma)$ a particularly sensitive probe of new physics. Similarly, scenarios in which the Higgs boson is composite or arises from alternative symmetry-breaking sectors may yield significantly different $H \rightarrow Z\gamma$ branching fractions [20–22]. Moreover, the observation of $H \rightarrow Z\gamma$ decay would complete the suite of established Higgs boson decays into pairs of electroweak gauge bosons ($\gamma\gamma$, ZZ^* , WW^*), consolidating the role played by the Higgs boson in electroweak symmetry breaking. Consequently, precise measurements of this rare decay provide a sensitive probe for the SM and its extensions.

The $Z(\rightarrow \ell\ell)\gamma$ final state ($\ell = e, \mu$), despite its reduced branching ratio, offers the best sensitivity to the $H \rightarrow Z\gamma$ process, as it can be efficiently triggered on and clearly distinguished from background events produced in proton–proton (pp) collisions. Furthermore, it benefits from full kinematic reconstruction and excellent invariant mass resolution. Both the ATLAS and CMS Collaborations have performed searches for the $H \rightarrow Z(\rightarrow \ell\ell)\gamma$ decay using the Run-2 pp collision dataset, corresponding to an integrated luminosity of about 140 fb^{-1} at $\sqrt{s} = 13$ TeV for each experiment. Compared to the background-only hypothesis, ATLAS observed a signal significance of 2.2σ (1.2σ expected) with a measured signal strength, defined by the ratio of the signal yield to the SM prediction, $\mu = 2.0^{+1.0}_{-0.9}$ [23], while CMS reported a signal significance of 2.7σ (1.2σ expected) with $\mu = 2.4 \pm 0.9$ [24]. The combination of these searches yielded the first evidence of $H \rightarrow Z\gamma$ decays with a significance of 3.4σ (1.6σ expected) with $\mu = 2.2 \pm 0.7$ [25]. All results were consistent with the SM expectation.

This letter presents a search for $H \rightarrow Z\gamma$ decays in the $\ell\ell\gamma$ final state using pp collision data collected with the ATLAS detector at $\sqrt{s} = 13.6$ TeV during 2022–2024 in Run 3, corresponding to an integrated luminosity of 165 fb^{-1} . Compared to the Run-2 analysis [23], this study benefits from an increased Higgs boson production cross-section at higher centre-of-mass energy, and from a larger data and simulated background samples. Furthermore, the event selection is optimised with relaxed transverse-momentum (p_T) thresholds for muons and photons. In addition, 13 mutually exclusive event categories are defined, including for the first time a dedicated multi-lepton category designed to target Higgs boson production in association with a vector boson or top quarks. The remaining 12 categories employ a multivariate classifier based on XGBoost [26] to maximise the sensitivity, replacing the previous approach mostly based on rectangular selections on simple kinematic variables. A simultaneous fit to the reconstructed $Z\gamma$ invariant mass distributions across all categories is performed to extract the overall $H \rightarrow Z\gamma$ signal yield. Finally, the result is combined with the Run-2 measurement to increase the sensitivity to this rare decay.

2 ATLAS detector

The ATLAS experiment [27, 28] at the LHC is a multipurpose particle detector with a forward–backward symmetric cylindrical geometry and near 4π coverage in solid angle¹. It consists of an inner tracking detector (ID) surrounded by a thin superconducting solenoid providing a 2 T axial magnetic field, electromagnetic (EM) and hadronic calorimeters, and a muon spectrometer (MS). The inner tracking detector covers the pseudo-rapidity range $|\eta| < 2.5$. It consists of silicon pixels, silicon microstrips, and transition radiation tracking detectors. Lead/liquid-argon (LAr) sampling calorimeters provide electromagnetic (EM) energy measurements with high granularity within the region $|\eta| < 3.2$. A steel/scintillator-tile hadronic calorimeter covers the central pseudo-rapidity range ($|\eta| < 1.7$). The endcap and forward regions are instrumented with LAr calorimeters for EM and hadronic energy measurements up to $|\eta| = 4.9$. The muon spectrometer surrounds the calorimeters and is based on three large superconducting air-core toroidal magnets with eight coils each. The field integral of the toroids ranges between 2.0 and 6.0 T m across most of the detector. The muon spectrometer includes a system of precision tracking chambers up to $|\eta| = 2.7$ and fast detectors for triggering up to $|\eta| = 2.4$. The luminosity is primarily measured by the LUCID-2 detector, which is located close to the beam pipe. A two-level trigger system was used to select events [29, 30]. The first-level trigger is implemented in hardware and uses a subset of the detector information to accept events at a rate close to 100 kHz. This is followed by a software-based trigger that reduced the accepted rate of complete events to 3 kHz on average, depending on the data-taking conditions. A software suite [31] is used in data simulation, in the reconstruction and analysis of real and simulated data, in detector operations, and in the trigger and data acquisition systems of the experiment.

3 Data and simulation samples

The analysis presented in this letter uses pp collision data at $\sqrt{s} = 13.6$ TeV collected by the ATLAS experiment from 2022 to 2024 during LHC Run 3. Events were collected using unscaled single- and dilepton triggers [32, 33] with a variety of p_T thresholds. The lowest-threshold single-electron and single-muon triggers required $p_T > 26$ GeV and $p_T > 24$ GeV, respectively. The dielectron trigger required two electrons with $p_T > 17$ GeV each. The dimuon triggers employed a symmetric 14 GeV–14 GeV configuration in 2022–2024 and an asymmetric 22 GeV–8 GeV configuration in 2023–2024. To maintain high efficiency at high instantaneous luminosity, these low-threshold triggers were supplemented by higher- p_T triggers with looser identification or isolation requirements. The trigger selections yield an efficiency of 96% for the $ee\gamma$ final state and 93% for the $\mu\mu\gamma$ final state for events passing the offline selection requirements that will be described in Section 4. After data quality requirements, the total integrated luminosity amounts to 165 fb^{-1} . The average number of inelastic pp interactions per bunch crossing (pile-up) increased from 42 in 2022 to 58 in 2024, with the peak instantaneous luminosity reaching $2.3 \times 10^{34} \text{ cm}^{-2}\text{s}^{-1}$.

The optimisation of the analysis strategy and the modelling of the relevant physics processes rely on simulation Monte Carlo (MC) samples that represent both the Higgs boson signal and the dominant

¹ ATLAS uses a right-handed coordinate system with its origin at the nominal interaction point (IP) in the centre of the detector and the z -axis along the beam pipe. The x -axis points from the IP to the centre of the LHC ring, and the y -axis points upwards. Polar coordinates (r, ϕ) are used in the transverse plane, ϕ being the azimuthal angle around the z -axis. The pseudorapidity is defined in terms of the polar angle θ as $\eta = -\ln \tan(\theta/2)$ and is equal to the rapidity $y = \frac{1}{2} \ln \left(\frac{E+p_z}{E-p_z} \right)$ in the relativistic limit. Angular distance is measured in units of $\Delta R \equiv \sqrt{(\Delta y)^2 + (\Delta \phi)^2}$.

background processes. These samples, unless explicitly stated otherwise, undergo the full simulation of the ATLAS detector response using the GEANT4 framework [34], as implemented in the ATLAS simulation infrastructure [35].

The Higgs boson mass is set to $m_H = 125$ GeV for all simulated samples, with a corresponding total decay width of $\Gamma_H = 4.1$ MeV, as recommended in Ref. [12]. The simulated samples are normalised to the SM production cross-sections, evaluated at a Higgs boson mass of $m_H = 125.09$ GeV. These include production via gluon–gluon fusion (ggF) [12, 36–47], vector boson fusion (VBF) [12, 48–50], associated production with a vector boson (VH , where $V = W, Z$) [12, 51–58], associated production with a top-quark pair ($t\bar{t}H$) [12, 59–62], and associated production with a bottom-quark pair ($b\bar{b}H$) [63–65]. Other Higgs boson production mechanisms were not considered, as their contributions to the total Higgs boson production cross-section are at the level of 0.1% or less. The $H \rightarrow Z\gamma$ branching ratio and its uncertainty were taken from Ref. [12].

The production of the Higgs boson was simulated using the POWHEG Box v2 MC event generator [66–70] and the PDF4LHC21 parton distribution functions (PDF) set [71], following the setup summarised in Table 1. The $H \rightarrow Z\gamma$ decay, as well as parton shower, hadronisation, and the modelling of the underlying event, were performed using PYTHIA 8 [72]. Contributions from $H \rightarrow \mu\mu$ decays, where the reconstructed photon originates from QED final-state radiation (FSR), were evaluated using samples produced with a similar setup and are considered as a potential background in this analysis. The impact of interference between Higgs boson decays with the same final-state signature ($H \rightarrow \ell\ell\gamma$ with non-resonant dilepton) is expected to be negligible in the SM [73]. Additional samples of the $H \rightarrow Z\gamma$ signals were generated using HERWIG 7 [74] for decay and parton shower simulation and are used to evaluate uncertainties associated with the parton shower modelling.

In this analysis, the dominant backgrounds arise from non-resonant production of a Z boson in association with a photon ($Z\gamma$) or jets, where a jet is misidentified as a photon ($Z + \text{jets}$). Additional background contributions stem from diboson (VV) production, where V denotes either a W or a Z boson. These additional background contributions are relevant only for the event category containing additional leptons.

A large $Z\gamma$ background sample was generated at next-to-leading-order (NLO) accuracy in QCD using the SHERPA 2.2.14 generator [75], with one to three additional partons in the final state at LO. The simulation employed the NNPDF3.0 next-to-next-to-leading-order (NNLO) PDF set [76], and a fast simulation of the calorimeter response was applied [77].

The EW production of a Z boson in association with a photon and two jets ($Z\gamma jj$) was simulated at LO accuracy in EW using MADGRAPH 3.5.5 [78] with the NNPDF2.3LO PDF set [79], where both jets originate from partons emitted at EW vertices. QCD-induced diagrams were explicitly excluded, resulting in no additional partons from QCD in the final state and ensuring orthogonality with the $Z\gamma$ sample generated with SHERPA. The hadronisation, parton shower, and the modelling of the underlying event were simulated using PYTHIA 8 with the A14 set of tuned parameters [80].

The background from $Z + \text{jets}$ was estimated from data using a control region of events in which the photon candidates fail the nominal criteria and pass looser identification or isolation requirements.

Diboson backgrounds resulting in three- and four-lepton final states were also modelled using SHERPA 2.2.14, employing the NNPDF3.0NNLO PDF set. The sample was generated at NLO accuracy in QCD with up to three additional partons at LO accuracy.

The effect of pile-up was modeled by overlaying simulated hard-scattering events with inelastic pp interactions from a mix of EPOS 2.0.1.4 [81] and PYTHIA 8. EPOS events were generated with the LHC

tune[82], and PYTHIA with the A3 tune [83] and the NNPDF2.3LO PDF set. PYTHIA simulated pileup events containing high- p_T jets, prompt photons, or leptons from b -hadron decays, while EPOS accounted for the remaining minimum-bias contribution. The individual samples were first reweighted to ensure a smooth transition across jet p_T , and the combined sample was reweighted to match the distribution of the number of interactions per bunch crossing observed in data. To improve the agreement between simulation and data, correction factors were applied to account for differences in reconstruction and identification efficiencies. These include corrections to the trigger, reconstruction, identification, and isolation efficiencies for electrons and muons, as well as the identification and selection of photons and jets. Additional corrections were applied to the energy and momentum scale and resolution of reconstructed objects to reflect the detector performance.

Table 1: Higgs boson signal MC samples produced with POWHEG Box V2 along with the techniques used to generate the events and their precision in α_s for the event generation (gen.). The version of PYTHIA 8, its parameter tune, and the PDF set, which are used for modelling the Higgs boson decay, parton shower, hadronisation, and the underlying event, are listed. The precision of the total cross-section used in the sample normalisation is also reported.

Process	Technique	QCD (gen.)	PYTHIA 8 & tune	PDF set	Normalisation
ggF	POWHEG [68, 69]	NNLO*	8.310 [72], A14 [80]	PDF4LHC21 [84]	NNLO (QCD), NLO (EW) [36–47]
VBF	POWHEG	NLO	8.310, A14	PDF4LHC21	NNLO (QCD), NLO (EW) [48–50]
$q\bar{q} \rightarrow ZH$	POWHEG & MiNLO [85]	NLO	8.310, A14	PDF4LHC21	NNLO (QCD), NLO (EW) [56, 58, 86]
$gg \rightarrow ZH$	POWHEG	LO	8.310, A14	PDF4LHC21	NLO (EW) [58, 87, 88]
WH	POWHEG & MiNLO [85]	NLO	8.310, A14	PDF4LHC21	NNLO (QCD), NLO (EW) [56, 58, 86]
$t\bar{t}H$	POWHEG	NLO	8.310, A14	PDF4LHC21	NNLO (QCD), NLO (EW) [59–62, 89]
$b\bar{b}H$	POWHEG (4FS)	NLO	8.310, A14	PDF4LHC21	NNLO (QCD), NLO (EW) [63–65, 90]

* NNLO accuracy achieved only for inclusive ggF observables.

4 Event selection and reconstruction

Events passing the trigger selection described in Section 3 are required to include at least one photon and two same-flavour, opposite-charge leptons, all associated with the primary vertex, defined as the inner-detector track vertex with the highest $\sum p_T^2$ of tracks with $p_T > 500$ MeV [91].

Muon candidates are reconstructed by combining the tracks in the ID and MS [92, 93]. They need to satisfy *medium* identification criteria, lie within $|\eta| < 2.5$, and have $p_T > 5$ GeV. Electrons are reconstructed from topological clusters of EM calorimeter cells matched to ID tracks [94–96]. They are required to pass a *loose* identification selection based on a likelihood discriminant using calorimeter shower shapes and track parameters, lie within $|\eta| < 2.47$ (excluding the transition region between the barrel and endcap EM calorimeters $1.37 < |\eta| < 1.52$), and have $p_T > 10$ GeV. To ensure leptons originate from the primary vertex and to suppress heavy-flavour backgrounds, all leptons are required to satisfy $|\Delta z_0 \cdot \sin \theta| < 0.5$ mm, where Δz_0 is the longitudinal impact parameter relative to the primary vertex and θ is the track polar angle. Moreover, the transverse-impact-parameter significance $|d_0|/\sigma_{d_0}$ needs to be < 3 for muons and < 5 for electrons, with d_0 measured relative to the beam line and σ_{d_0} its fit uncertainty.

Photon candidates are built from topological clusters of EM calorimeter cells [94–96]. They have to satisfy *tight* identification criteria based on calorimeter shower shape variables, $|\eta| < 2.37$ (excluding $1.37 < |\eta| < 1.52$), and have $p_T > 10$ GeV (relaxed from 15 GeV in Run 2 [23]). To increase the rejection of background from non-prompt and hadronic production, the lepton and photon candidates are required to

pass isolation criteria, based on the energy deposits in the calorimeter and the total p_T of charged-particle tracks from the primary vertex, measured in cones surrounding the direction of the particle candidates.

Jets are reconstructed from particle flow objects [97] clustered via the anti- k_t algorithm ($R = 0.4$) [98–100]. They are required to satisfy $p_T > 25$ GeV and $|y| < 4.4$. To suppress jets originating from pile-up, a central [101] or forward jet-vertex-tagger [102] is applied.

Overlap removal discards the lower- p_T electron when two electron candidates share the same track or satisfy $|\Delta\eta| < 0.075$ and $|\Delta\phi| < 0.125$. Electrons within $\Delta R < 0.02$ of muons are also removed. To suppress bremsstrahlung photons emitted by leptons, photons within $\Delta R < 0.3$ of leptons are discarded. Finally, jets within $\Delta R < 0.2$ of leptons or photons are removed.

Z boson candidates are reconstructed from opposite-charge and same-flavour lepton pairs. In the muon channel, the highest p_T collinear FSR photon ($\Delta R < 0.15$) is added to the corresponding muon to improve the di-muon mass resolution. A kinematic fit [23] then corrects the lepton four-momenta to constrain the dilepton mass to the known Z boson mass, accounting for its finite natural width. This procedure improves the $\ell\ell\gamma$ mass resolution of the signal MC samples by 17% for electrons and 11% for muons, including the effect of FSR. Candidates must satisfy $|m_{\ell\ell} - m_Z| < 10$ GeV, where $m_Z = 91.2$ GeV [103]. If multiple Z boson candidates are found, the dilepton pair with $m_{\ell\ell}$ closest to m_Z is selected, resulting in a 98% efficiency for correctly matching to the true Z boson in the ggF signal sample. The leptons associated with the Z boson candidate are additionally required to be geometrically matched to the corresponding trigger-level leptons that fired the event. They are required to satisfy an offline p_T threshold set 1–2 GeV above the nominal trigger requirement to ensure that the trigger is maximally efficient.

The Higgs boson candidate is reconstructed by combining the selected Z boson and the highest- p_T photon. The invariant mass of the $\ell\ell\gamma$ system ($m_{Z\gamma}$) must lie within 110–160 GeV to suppress contributions from on-shell Z boson events. In addition, the photon p_T is required to be larger than 0.09 times $m_{Z\gamma}$. This requirement further reduces the background, while not introducing a sharp turn-on in the $m_{Z\gamma}$ spectrum near m_H as would the use of an absolute minimum p_T^γ requirement with similar background rejection. This criterion, relaxed from the Run-2 value of 0.12 thanks to the calibrations of identification and isolation efficiencies for photons with lower p_T , enhances the selection efficiency. The overall reconstruction and selection efficiency (including detector acceptance) for the SM $H \rightarrow Z(\rightarrow \ell\ell)\gamma$ events ranges from 20% to 26%, depending on the production mode.

5 Event categorisation

To maximise the sensitivity to an $H \rightarrow Z\gamma$ signal, events are classified into 13 exclusive event categories. Events are first categorised into four primary regions: Lepton, VBF, High relative photon p_T , and Low relative photon p_T . This classification is based on lepton and jet multiplicities as well as kinematic properties. The VBF and both the High and Low relative photon p_T regions are further subdivided into mutually exclusive categories according to the output of XGBoost-based [26] boosted decision trees (BDT) and the lepton flavour. To avoid sculpting of the $m_{Z\gamma}$ distribution, the BDT inputs are selected to have minimal correlation with $m_{Z\gamma}$, and the classifiers are trained within narrow mass windows: 120–130 GeV for the VBF and High relative photon p_T regions, and 123–127 GeV for the Low relative photon p_T region. This categorisation strategy is designed to maximise the combined number counting significance, while requiring at least two background events in the signal region ($120 < m_{Z\gamma} < 130$ GeV) of each category. This requirement translates into a minimum number of background events in the full fit region that is

large enough to ensure sufficient statistical precision for the background estimate. The event classification scheme is illustrated in Figure 1 and more details are provided in the following paragraphs.

Events with at least three leptons ($N_{\text{lepton}} \geq 3$) are assigned to the Lepton category. This category is enriched in VH and $t\bar{t}H$ production modes, accounting for 56% and 35% of the signal yield in this category, respectively. The dominant backgrounds arise from Z + jets, multi-lepton diboson, and non-resonant $Z\gamma$ processes.

Events failing the Lepton region and containing at least two jets ($N_{\text{jet}} \geq 2$) are selected for the VBF region. If more than two jets are present in an event, the two highest- p_T jets are considered. A dedicated BDT was trained using 25 kinematic variables to separate the VBF signal from the non-resonant $Z\gamma$, and the EW $Z\gamma jj$, as well as to reduce the contamination from ggF. The variables are summarised in Table 2. Events in the VBF region are classified into tight (VBFT) and loose (VBFL) categories based on the BDT score, with the VBFT category exhibiting higher significance. The VBF fraction of the total signal yield is 89% and 64%, respectively, in the VBFT and VBFL categories.

Table 2: Summary of input variables used in the BDT training for the VBF, HRelpT- ee , HRelpT- $\mu\mu$, LRelpT- ee , and LRelpT- $\mu\mu$ analysis regions. The same set of input variables is employed in the four relative photon p_T regions.

Input variable	Description	VBF	relative photon p_T
N_{jet}	Number of jets	✓	✓
$p_T^{j_1}, \eta_{j_1}$	p_T , and η of the leading jet (j_1)	✓	✓
m_{j_1}	Mass of the leading jet	✓	
ϕ_{j_1}	Azimuthal angle of the leading jet		✓
$m_{j_2}, p_T^{j_2}, \eta_{j_2}$	Mass, p_T , and η of the subleading jet (j_2)	✓	
$m_{j_1 j_2}, p_T^{j_1 j_2}, \Delta\eta_{j_1 j_2}$	Dijet invariant mass, p_T , and η separation	✓	
η_γ	Pseudorapidity of the photon	✓	✓
p_T^γ	Transverse momentum of the photon	✓	
$p_T^{\ell\ell}$	Transverse momentum of the dilepton system	✓	
$\eta_{\ell\ell}, \eta_{\ell\ell\gamma}$	Pseudorapidity of the dilepton and $\ell\ell\gamma$ systems	✓	✓
$p_T^{\ell\ell\gamma}$	Transverse momentum of the $\ell\ell\gamma$ system	✓	
$p_T^{\ell\ell\gamma}/m_{\ell\ell\gamma}, p_T^\gamma/m_{\ell\ell\gamma}$	Relative p_T of the $\ell\ell\gamma$ and the photon		✓
$p_T^{\ell\ell}/m_{\ell\ell\gamma}$	Relative p_T of the dilepton system		✓
p_T^t	Component of $\vec{p}_T^{\ell\ell\gamma}$ perpendicular to the difference between $\vec{p}_T^{\ell\ell}$ and \vec{p}_T^γ ($p_T^t = \vec{p}_T^{\ell\ell\gamma} \times \hat{t} $, with $\hat{t} \propto \vec{p}_T^{\ell\ell} - \vec{p}_T^\gamma$) [104, 105]	✓	✓
$\Delta\phi_{\ell\ell,\gamma}$	Azimuthal separation between the $\ell\ell$ system and the photon	✓	✓
$\Delta\phi_{\ell\ell\gamma,j_1}$	Azimuthal separation between the $\ell\ell\gamma$ system and the leading jet	✓	✓
$\Delta\phi_{\ell\ell\gamma,j_1 j_2}$	Azimuthal separation between the $\ell\ell\gamma$ system and the dijet system	✓	
$\Delta\eta_{\ell\ell,\gamma}$	Pseudorapidity separation of the dilepton and the photon	✓	✓
$\Delta R_{\gamma \text{ or } \ell\ell, j}^{\text{min}}$	Minimum ΔR to j_1/j_2 from the photon or the dilepton system	✓	✓
$\cos\theta^*(\ell^+)$	Cosine of the polar angle of the ℓ^+ in the $\ell\ell$ rest frame	✓	✓
$\cos\theta(\ell\ell)$ in $\ell\ell\gamma$	Cosine of the polar angle of the $\ell\ell$ in the $\ell\ell\gamma$ rest frame	✓	✓
$\eta_{\text{Zeppenfeld}}$	Pseudorapidity difference between the $\ell\ell\gamma$ system and the dijet system, defined as $ \eta_{\ell\ell\gamma} - (\eta_{j_1} + \eta_{j_2})/2 $ [106]	✓	

Events not selected for the VBF region and satisfying $p_T^\gamma/m_{Z\gamma} \geq 0.4$ enter the High relative photon p_T region, dominated by ggF production. Separate BDTs are trained for the ee and $\mu\mu$ channels using

17 variables, as shown in Table 2. BDTs are trained using the simulated ggF and VBF signal events and the non-resonant $Z\gamma$ background events. For each lepton flavour, events are grouped into tight and loose categories using optimised BDT thresholds, yielding four categories (HRelpT- ee T, HRelpT- ee L, HRelpT- $\mu\mu$ T, HRelpT- $\mu\mu$ L) with ggF signal fractions above 70%.

Remaining events that are not selected in the VBF region and with $p_T^\gamma/m_{Z\gamma} < 0.4$, are placed into the Low relative photon p_T region, where the signal yield is also dominated by ggF with a fraction above 90%. BDTs trained separately for ee and $\mu\mu$ channels use the same input variables as in the High relative photon p_T region. The training samples consist of the simulated ggF signal events, the non-resonant $Z\gamma$ background, and the data-driven Z +jets background events. Background components are constructed and normalised as detailed in Section 6. Each channel is split into tight, medium, and loose categories, according to their BDT score, forming six in total: LRelpT- ee T, LRelpT- ee M, LRelpT- ee L, LRelpT- $\mu\mu$ T, LRelpT- $\mu\mu$ M, and LRelpT- $\mu\mu$ L.

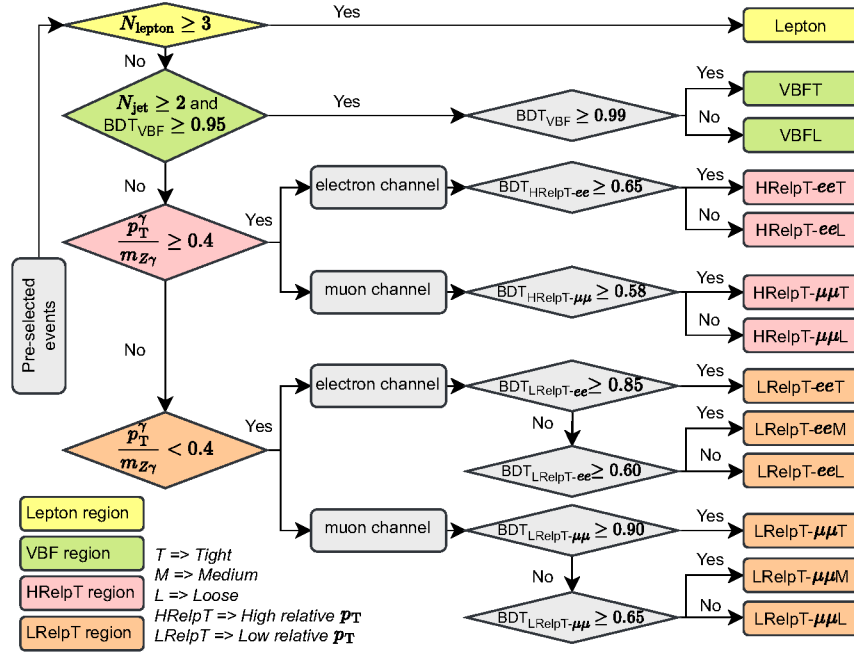


Figure 1: Schematic of the event categorisation based on kinematic selections and multivariate algorithms. Events are classified into four regions: Lepton (yellow), VBF (green), high relative photon p_T (HRelpT, pink), and low relative photon p_T (LRelpT, orange). The Lepton region is defined based on the number of lepton candidates, while the VBF region is split into loose and tight categories using a BDT output. The HRelpT and LRelpT regions are further divided into various categories based on the lepton flavour and dedicated BDT classifiers. In total, 13 mutually exclusive categories are defined.

Table 3 provides an overview of the expected signal and background composition in each analysis category, as determined from a signal-plus-background fit to the Asimov dataset (Section 8) to illustrate the sensitivity. The expected signal (S_{68}^{exp}), background (B_{68}^{exp}), and observed data (N_{68}) yields are quoted in an $m_{Z\gamma}$ window around the peak, with a width (w_{68}) corresponding to the interval expected to contain 68% of the signal. The resulting expected sensitivity, $S_{68}^{\text{exp}}/\sqrt{S_{68}^{\text{exp}} + B_{68}^{\text{exp}}}$, varies across categories, reaching a maximum of 0.91 in the VBFT category. The combined sensitivity, obtained by summing the contributions from all categories in quadrature, is 1.81. The inclusive sensitivity is used solely for category optimisation and is not intended to represent the final sensitivity derived from the full statistical analysis.

Table 3: Expected signal (S_{68}^{exp}), background (B_{68}^{exp}) and observed event yields in data (N_{68}) in a window of width w_{68} , expected to contain 68% of the signal. The expected signal and backgrounds are extracted from a signal-plus-background fit to the Asimov dataset (Section 8). The signal uncertainty reflects the impact in μ , while the background uncertainty accounts for the statistical uncertainty from the fit. The expected sensitivity is given by $S_{68}^{\text{exp}} / \sqrt{S_{68}^{\text{exp}} + B_{68}^{\text{exp}}}$. The last row shows the inclusive results, calculated by summing the contributions from all categories. The inclusive sensitivity is derived by combining the category sensitivities in quadrature.

Category	S_{68}^{exp}	B_{68}^{exp}	N_{68}	w_{68} [GeV]	$S_{68}^{\text{exp}} / \sqrt{S_{68}^{\text{exp}} + B_{68}^{\text{exp}}}$
Lepton	1.5 ± 1.1	76.3 ± 2.8	78	4.4	0.17
VBFT	1.5 ± 1.1	1.2 ± 0.4	3	3.8	0.91
VBFL	2.8 ± 2.0	27.6 ± 1.8	23	4.0	0.51
HRelpT- ee T	1.2 ± 0.8	6.6 ± 0.9	11	3.1	0.43
HRelpT- ee L	3.0 ± 2.1	54.10 ± 1.8	77	4.0	0.40
HRelpT- $\mu\mu$ T	2.4 ± 1.7	20.3 ± 1.7	33	3.9	0.50
HRelpT- $\mu\mu$ L	2.4 ± 1.7	56.5 ± 1.7	72	4.1	0.31
LRelpT- ee T	9 ± 6	234 ± 6	251	3.8	0.57
LRelpT- ee M	29 ± 20	$2\,591 \pm 19$	3\,806	4.1	0.56
LRelpT- ee L	24 ± 17	$13\,260 \pm 50$	17\,435	4.5	0.21
LRelpT- $\mu\mu$ T	4.9 ± 3.4	96 ± 4	127	3.9	0.49
LRelpT- $\mu\mu$ M	34 ± 24	$2\,545 \pm 19$	3\,133	4.1	0.67
LRelpT- $\mu\mu$ L	37 ± 26	$16\,960 \pm 40$	19\,331	4.4	0.28
Inclusive	150 ± 110	$35\,930 \pm 70$	44\,380	4.0	1.81

6 Signal and background modelling

The signal and background yields are determined by an unbinned extended maximum-likelihood fit to the reconstructed $m_{Z\gamma}$ spectrum in data, employing analytic functions for both components. The shape of the $H \rightarrow Z\gamma$ signal is modelled by a double-sided Crystal Ball (DSCB) function, comprising a Gaussian core with power-law tails on both sides to capture both the detector resolution and non-Gaussian effects [107]. In each category, the DSCB parameters (mean μ_{CB} , width σ_{CB} , and four parameters describing the tails) are determined from a fit to a combination of all signal samples. The mean is shifted by 90 MeV to correct for the generated Higgs boson mass of 125 GeV to the measured value of 125.09 GeV. The overall signal normalisation and acceptance are taken directly from the same simulation. A small contribution from $H \rightarrow \mu\mu$ decays (up to 3.8% of $H \rightarrow Z\gamma$ signal in certain categories) is likewise modelled with its own DSCB template, with normalisation fixed to the SM prediction.

For all selected events, the backgrounds arise primarily from non-resonant $Z\gamma$ production and Z +jets events in which a jet is misidentified as a photon. The diboson contribution remains below 0.2% and is therefore neglected in the inclusive background estimate. The relative fractions of $Z\gamma$ and Z +jets components are determined inclusively via a two-dimensional sideband method, applied to a dataset obtained after loosening the nominal photon identification and isolation requirements. The sideband populations of the dataset are used to extract the $Z\gamma$ purity in data [108]. This yields a $Z\gamma$ fraction of $0.49^{+0.05}_{-0.10}$, compared to $0.78^{+0.04}_{-0.09}$ in Run 2 [23]. The reduction reflects three combined effects: the increased pile-up in Run 3, the lowered photon p_T threshold in the event selection, which admits more jets faking photons, and the smaller

ratio of SM $Z\gamma$ to Z + jets cross-sections at $\sqrt{s} = 13.6$ TeV.

The background $m_{Z\gamma}$ distribution is modelled based on fits to a dedicated background template that combines the $Z\gamma$ and Z + jets components. After the inclusive fractions of $Z\gamma$ and Z + jets events are determined, they are extrapolated to each event category using efficiencies from the $Z\gamma$ fast-simulation MC and data-driven Z + jets samples. To reduce statistical fluctuations in the control region, the ratio of Z + jets to $Z\gamma$ shapes as a function of $m_{Z\gamma}$ is smoothed by fitting a low-order polynomial or exponential-polynomial function. This smoothed ratio is applied to the $Z\gamma$ template to define the Z + jets background shape. In the VBF categories, a similar smoothing is employed on the ratio of $Z\gamma$ + (Z + jets) to the larger EW $Z\gamma jj$ simulation to define the total background template. In the Lepton category, the 35% contribution from diboson backgrounds, taken from simulation, is added to the template. Finally, in each category, the overall background normalization is scaled to data in the $m_{Z\gamma}$ sidebands (excluding the interval 120–130 GeV). The resulting templates are compatible with the $m_{Z\gamma}$ distribution of data.

To determine the background model that accurately represents the data without inducing artificial signal features, a spurious signal (SS) study [23] is performed. In each category, several analytic function families, such as power laws, Bernstein polynomials, exponential polynomials, and logarithmic polynomials of the form $(1 - x^{1/3})^f x^{\sum_{i=0}^N p_i \log(x)^i}$, with $x = m_{Z\gamma}/\sqrt{s}$ and f a free parameter, are fitted to the background template. Each function is tested over three fit ranges (110–155 GeV, 115–160 GeV, 110–160 GeV). The function-range combinations are required to satisfy two criteria:

- The $|SS|$ is defined as the absolute value of the maximum fitted signal yield obtained from a background-only template when varying m_H between 120 and 130 GeV in steps of 1 GeV. It is required that one of $|SS - 1\sigma|$, SS , or $|SS + 1\sigma|$ is less than $0.2\Delta S$, where σ is the error of the SS , and ΔS is the expected signal statistical uncertainty.
- The χ^2 -probability of the background-only fit $> 1\%$.

When there is more than one function–range combination that passes these criteria, the one with the fewest free parameters is chosen. If more than one has the same number of parameters, the one with the smallest $|SS|$ is chosen. If no candidate satisfies both criteria, the fit window is progressively narrowed (to a minimum width of 35 GeV) until a valid model is found; if still unsuccessful, the combination with the lowest $|SS|$ is adopted. A Wald test [109, 110] is then applied to data sidebands to compare nested functions: if a lower-degree function is statistically compatible without significantly increasing $|SS|$, it replaces the nominal model to guard against over-fitting. To account for uncertainties in the relative $Z\gamma$ and Z + jets fractions, variations of those fractions by plus or minus their uncertainties are used to build alternative templates. Repeating the SS study on these templates leaves the chosen function–range combination unchanged in every category, and the maximum $|SS|$ across the three templates is assigned as the systematic uncertainty on the background model.

Once the function is selected, a smoothing technique based on Gaussian Process Regression [110, 111] is applied to each category’s template. The $|SS|$ is then re-evaluated. This reduces the effect of residual statistical fluctuations without introducing any shape bias and does not affect the choice of any function–range combination in any categories. Unlike the signal models, whose parameters are fixed from simulation, the background model parameters are extracted directly from a fit to the $m_{Z\gamma}$ distribution in data. As an additional validation, a template is built as the sum of the SM signal template and the background template in each category, and is then fitted. The resulting best-fit signal strength in every category is compatible with the SM prediction, confirming the robustness of the background models.

7 Systematic uncertainties

Systematic uncertainties impact the fit results by affecting either the normalization or the shape of the $m_{Z\gamma}$ invariant mass distributions. Experimental uncertainties are evaluated using Run-3 data and MC events. Despite the large simulation background samples and smoothing procedures, the spurious signal, uncorrelated across event categories, retains a large contribution from statistical fluctuations of the input samples. It results in an 11% impact on the signal strength μ , which is small with respect to the statistical uncertainty.

Signal shape modelling uncertainties vary by category and are driven by the calibration of the electron and photon energy, as well as the muon momentum. The uncertainty in the electron and photon energy resolution and in the muon momentum resolution leads to a less than 5% mass resolution (σ_{CB}) uncertainty. The uncertainty in the electron and photon energy scale (and in the muon momentum scale) leads to a less than 0.3% (0.1%) uncertainty in the peak position (μ_{CB}). Overall, these uncertainties affect the measured signal strength by less than 2%.

The 60% uncertainty in the $H \rightarrow \mu\mu$ contribution, taken from the Run-2 ATLAS measurement [112], contributes a 2% uncertainty in the expected signal strength. Additional uncertainties in the signal yield arising from reconstruction, identification, and isolation corrections are smaller than 3% for photons, electrons, and muons [95, 96]. The jet-related uncertainties, including those from jet reconstruction and in situ calibration, are each below 2%. A conservative uncertainty of 10% is assigned to the reconstruction and calibration of forward jets. All of the jet uncertainties translate into a 4% impact on the signal strength. The uncertainty related to the pile-up effects is negligible. The overall uncertainty in the integrated luminosity for each dataset using the LUCID-2 detector [113] is 4%² for 2022–2024. Additional uncertainties arising from the triggers are below 2% across the analysis categories. Combining all experimental systematics, excluding the spurious signal uncertainty, yields a total 9% uncertainty in the signal strength.

Theory uncertainties affecting the expected signal yield arise from multiple sources. Uncertainties in the production cross-section and kinematic distributions, primarily due to missing higher-order QCD corrections, contribute up to 12%, depending on the analysis category, and are dominated by variations in the renormalisation and factorisation scales. Parton shower modelling introduces additional uncertainties ranging from 3% to 29%, with the largest values observed in VBF categories; in non-VBF categories, the uncertainty typically ranges from 0.3% to 10%. The uncertainty in the Higgs boson branching ratio to $Z\gamma$ is 7% [12]. The total impact of theory uncertainties on the signal strength is estimated to be 12%. Table 4 summarises the symmetrised impacts of individual uncertainty sources on the expected and observed signal strengths. The total uncertainty is dominated by the statistical component, with an expected impact of 0.70. Systematic uncertainties contribute 0.17, the spurious signal and theory modelling effects being the leading sources.

² The integrated luminosity for the 2024 dataset is derived from the relative yields of $Z \rightarrow ee$ and $Z \rightarrow \mu\mu$ events relative to those measured in 2022/2023, yielding a preliminary uncertainty of 5%. When combined with the 2% uncertainty assigned to the 2022/2023 integrated luminosity [114, 115], a luminosity-weighted uncertainty of 4% is obtained for the Run-3 dataset.

Table 4: Breakdown of the symmetrised impacts from individual sources of uncertainty on the expected and observed signal strengths. Uncertainties are grouped by source type to illustrate their relative contributions.

Uncertainty source	$\Delta\mu$	
	Expected	Observed
Statistical uncertainty	0.70	0.64
Systematic uncertainty	0.17	0.17
Spurious signal (background modelling)	0.11	0.10
QCD scale, PDF+ α_S , parton shower	0.09	0.06
Branching ratio ($H \rightarrow Z\gamma$)	0.08	0.05
Luminosity	0.05	0.03
Photon efficiency	0.05	0.03
Jet	0.04	0.07
Electron and photon energy scale and resolution	0.02	0.02
Electron efficiency	0.02	0.02
Muon	0.02	< 0.01
Trigger	0.02	< 0.01
Total	0.72	0.67

8 Results

8.1 Run-3 only

The results are extracted via an unbinned, simultaneous maximum-likelihood fit [116] to the $m_{Z\gamma}$ distributions across all categories, each with its own optimised mass window determined as described in Section 6, following the methodology of previous $H \rightarrow Z\gamma$ searches [23, 117]. The likelihood function is built by incorporating both the signal strength of $H \rightarrow Z\gamma$ and the nuisance parameters (NPs), which characterise the effects of systematic uncertainties on the signal normalisation and shape, as well as background normalisation and shape parameters.

The measured signal strength is $\mu = 0.9^{+0.7}_{-0.6}(\text{stat.})^{+0.2}_{-0.1}(\text{syst.}) = 0.9^{+0.7}_{-0.6}$ for $m_H = 125.09$ GeV. Under the SM signal hypothesis, the expected signal strength is $\mu_{\text{exp}} = 1.0 \pm 0.7(\text{stat.})^{+0.2}_{-0.1}(\text{syst.}) = 1.0 \pm 0.7$. The corresponding Asimov dataset [116] is generated under the hypothesis of SM signal plus background. The result is statistically compatible with the SM expectation. The observed significance under the background-only hypothesis is 1.4σ , close to the expected significance of 1.5σ . Among the event categories, the VBFT category provides the highest expected sensitivity. In all cases, the uncertainties are dominated by the statistical contribution, while the most significant systematic uncertainty impact arises from the modelling of the background (spurious signal). The measurement using individual signal strengths for each category is consistent with the result obtained from the global signal strength, with a p -value of 0.37.

Figure 2 (a) presents the $m_{Z\gamma}$ distribution of selected events in the Run-3 dataset, weighted by $\ln(1+S_{68}/B_{68})$, where S_{68} and B_{68} are the signal and background yields in each category, estimated from the fit to the data, in an $m_{Z\gamma}$ window expected to contain 68% of the signal. The combined models, obtained by weighting the individual category models, are overlaid. The negative profiled-likelihood-ratio values as a function of the signal strength μ are shown in Figure 3.

Overall, this analysis achieves an expected significance improvement of 28% relative to the previous ATLAS result [23]. This gain is primarily driven by the advanced event selection and categorisation,

which contributes 15%. The remaining improvement is from the larger dataset and a more favourable signal-to-background ratio at $\sqrt{s} = 13.6$ TeV.

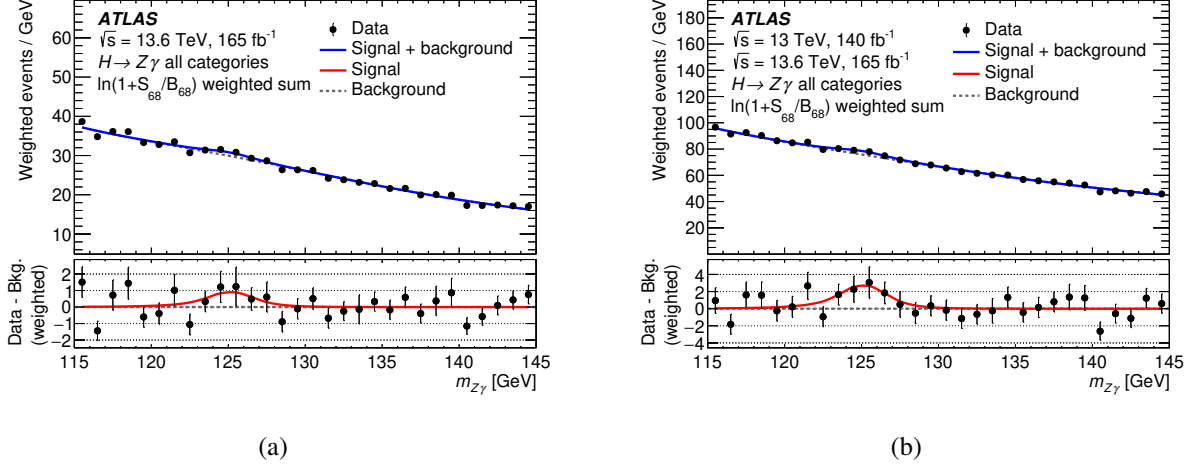


Figure 2: $Z\gamma$ invariant mass distributions of weighted data events across all categories for (a) Run-3 only and (b) the combined Run-2 and Run-3 dataset. The black points represent the data, with statistical uncertainties shown as error bars. Each event is weighted by $\ln(1 + S_{68}/B_{68})$, where S_{68} and B_{68} are the signal and background yields in each category, estimated from the fit to the data, in an $m_{Z\gamma}$ window expected to contain 68% of the signal. The signal-plus-background fit (solid blue curve) and the background model (dashed line) are overlaid. In the bottom panels, the residuals between the data and the background model (black dots with error bars) are compared to the signal model (red solid line). All curves represent the weighted sum of the individual category models.

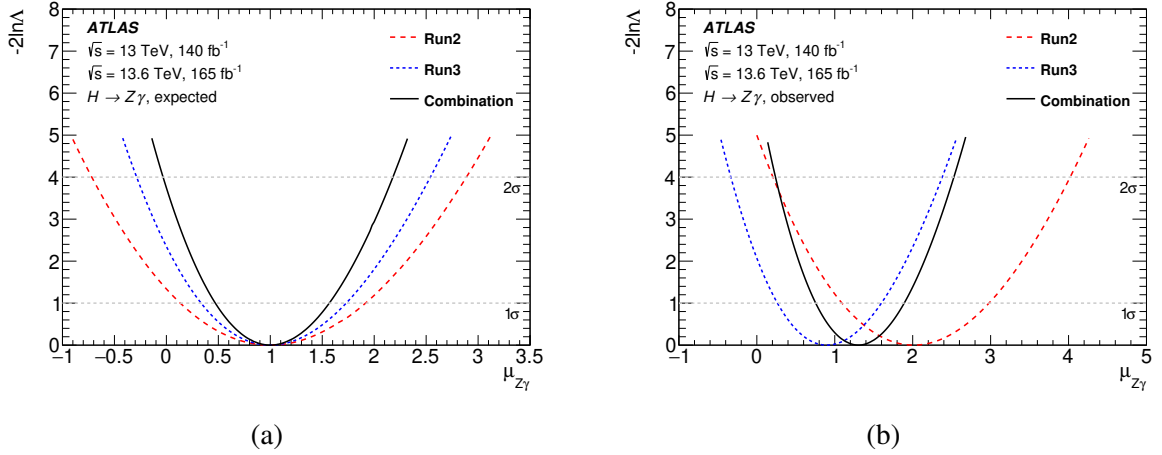


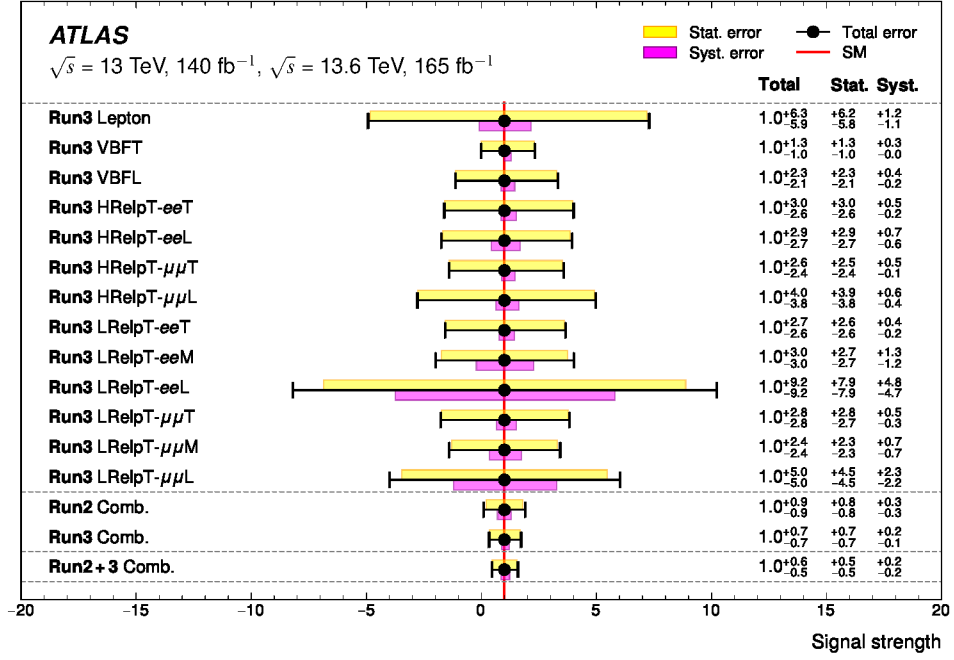
Figure 3: Profiled likelihood scan of the signal strength for the (a) expected and (b) observed results. Both plots show the results obtained by this analysis of the Run-3 dataset (dashed blue line), by the previous analysis of the Run-2 dataset [23] (long dashed red line), and their combination (solid black line).

8.2 Run-2 and Run-3 combination

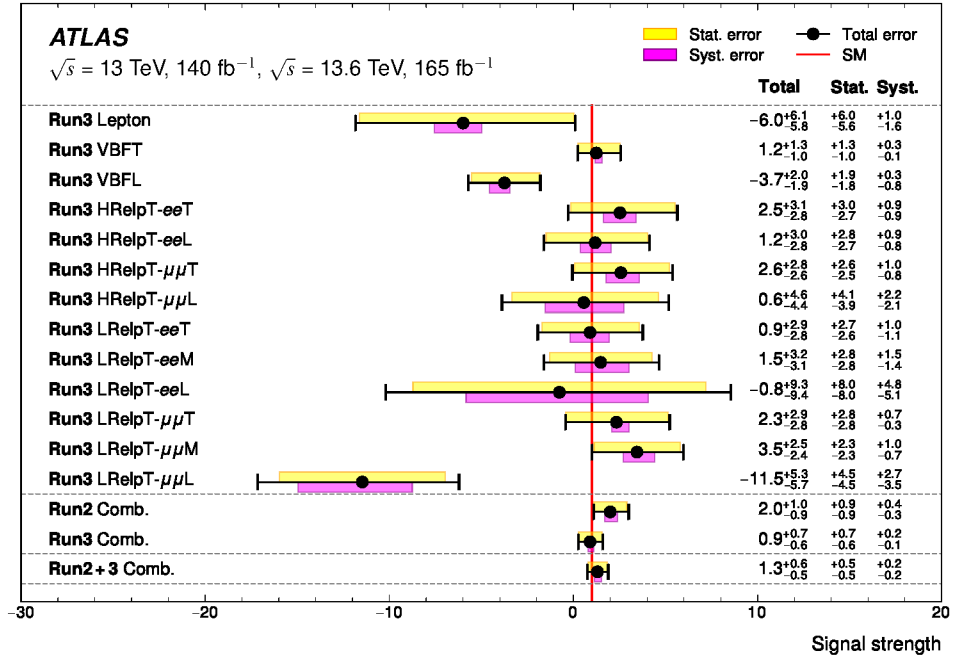
These results based on Run-3 data are combined with those from the previous ATLAS search for $H \rightarrow Z\gamma$ decays using Run-2 data [23]. The theoretical uncertainties, including branching ratios, QCD scale, and α_s

uncertainties, are treated as fully correlated across both datasets. The PDF uncertainties are uncorrelated due to the distinct PDF sets used in Run 2 and Run 3. Due to the different data-taking conditions, most experimental uncertainties are treated as uncorrelated between the two runs, in particular, the uncertainties related to the trigger, luminosity, electron, photon, and spurious signal. All of the uncertainty sources from muons and jets are correlated, except for the uncorrelated in situ calibration uncertainties. The impact of the correlation scheme on the final results was studied and found to be negligible, as the overall uncertainty is dominated by the statistical contributions. The joint likelihood is constructed as the product of the individual likelihood functions from the Run-2 and Run-3 analyses. Correlated systematic sources share a common NP with a Gaussian constraint in the combined fit.

Figure 2 (b) presents the weighted $m_{Z\gamma}$ distribution with the fitted signal and background models overlaid, and Figure 3 shows the likelihood scan of the combined signal strength. The observed combined fit has a best-fit signal strength of $\mu = 1.3 \pm 0.5(\text{stat.}) \pm 0.2(\text{syst.}) = 1.3^{+0.6}_{-0.5}$ with an expected $\mu = 1.0 \pm 0.5(\text{stat.}) \pm 0.2(\text{syst.}) = 1.0^{+0.6}_{-0.5}$. The significance of the observed (expected) excess above the background-only hypothesis is 2.5σ (1.9σ). Relative to the Run-2 analysis, the combined expected significance improves by 61%. Figure 4 shows the signal strength results in each Run-3 category, the stand-alone Run-2 and Run-3 measurements, and their combination. The Run-2 and Run-3 measurements are compatible, with a p -value of 0.33. Assuming the SM production cross-sections, the combination provides the most stringent expected sensitivity to date for determining the $H \rightarrow Z\gamma$ branching fraction, surpassing the ATLAS + CMS Run-2 combination [25]. Under this assumption, the observed (expected) branching fraction is $(2.0^{+0.9}_{-0.8}) \times 10^{-3}$ ($(1.5^{+0.9}_{-0.8}) \times 10^{-3}$), compared with the SM prediction of $(1.54^{+0.10}_{-0.11}) \times 10^{-3}$.



(a)



(b)

Figure 4: (a) Expected and (b) observed best-fit signal strengths and corresponding uncertainties in each category of the Run-3 analysis, their combined values, the results of the previous Run-2 analysis, and the overall combination. The black points with horizontal error bars correspond to the central values and total uncertainties, while the upper yellow (lower magenta) bands indicate the statistical (systematic) uncertainties. The red vertical line denotes the SM prediction.

9 Conclusion

A search for the Higgs boson decay to $Z\gamma$ in the $\ell\ell\gamma$ final state is performed using proton–proton collision data recorded with the ATLAS detector at $\sqrt{s} = 13.6$ TeV during 2022–2024, corresponding to an integrated luminosity of 165 fb^{-1} . A simultaneous unbinned maximum-likelihood fit to the reconstructed invariant mass of the $Z\gamma$ system across all event categories gives an observed (expected) signal yield normalised to the SM prediction, $\mu = 0.9^{+0.7}_{-0.6}$ ($\mu = 1.0 \pm 0.7$). This corresponds to an observed (expected) signal significance of 1.4 (1.5) standard deviations. The statistical uncertainty is the dominant source of error. Compared to a similar search performed with Run-2 data [23], the expected significance improves by 28%, with 15% arising from the enhanced event selection and categorisation strategies, and the remainder from increased integrated luminosity and larger cross-sections.

This measurement is further combined with the Run-2 result to yield the most stringent expected sensitivity to date for the $H \rightarrow Z\gamma$ decay, surpassing the ATLAS + CMS Run-2 combination [25]. In the combined fit, the observed (expected) signal yield normalised to the SM prediction is $\mu = 1.3^{+0.6}_{-0.5}$ ($\mu = 1.0^{+0.6}_{-0.5}$), corresponding to an observed (expected) signal significance of 2.5 (1.9) standard deviations. The combination improves the expected significance by 61% with respect to the Run-2 measurement. The measurement is consistent with the SM expectation, indicating no significant deviation from the predicted Higgs boson behaviour in the $Z\gamma$ channel.

Acknowledgements

We thank CERN for the very successful operation of the LHC and its injectors, as well as the support staff at CERN and at our institutions worldwide without whom ATLAS could not be operated efficiently.

The crucial computing support from all WLCG partners is acknowledged gratefully, in particular from CERN, the ATLAS Tier-1 facilities at TRIUMF/SFU (Canada), NDGF (Denmark, Norway, Sweden), CC-IN2P3 (France), KIT/GridKA (Germany), INFN-CNAF (Italy), NL-T1 (Netherlands), PIC (Spain), RAL (UK) and BNL (USA), the Tier-2 facilities worldwide and large non-WLCG resource providers. Major contributors of computing resources are listed in Ref. [118].

We gratefully acknowledge the support of ANPCyT, Argentina; YerPhI, Armenia; ARC, Australia; BMWFW and FWF, Austria; ANAS, Azerbaijan; CNPq and FAPESP, Brazil; NSERC, NRC and CFI, Canada; CERN; ANID, Chile; CAS, MOST and NSFC, China; Minciencias, Colombia; MEYS CR, Czech Republic; DNRf and DNSRC, Denmark; IN2P3-CNRS and CEA-DRF/IRFU, France; SRNSFG, Georgia; BMFTR, HGF and MPG, Germany; GSRI, Greece; RGC and Hong Kong SAR, China; ICHEP and Academy of Sciences and Humanities, Israel; INFN, Italy; MEXT and JSPS, Japan; CNRST, Morocco; NWO, Netherlands; RCN, Norway; MNiSW, Poland; FCT, Portugal; MNE/IFA, Romania; MSTDI, Serbia; MSSR, Slovakia; ARIS and MVZI, Slovenia; DSI/NRF, South Africa; MICIU/AEI, Spain; SRC and Wallenberg Foundation, Sweden; SERI, SNSF and Cantons of Bern and Geneva, Switzerland; NSTC, Taipei; TENMAK, Türkiye; STFC/UKRI, United Kingdom; DOE and NSF, United States of America.

Individual groups and members have received support from BCKDF, CANARIE, CRC and DRAC, Canada; CERN-CZ, FORTE and PRIMUS, Czech Republic; COST, ERC, ERDF, Horizon 2020, ICSC-NextGenerationEU and Marie Skłodowska-Curie Actions, European Union; Investissements d’Avenir Labex, Investissements d’Avenir Idex and ANR, France; DFG and AvH Foundation, Germany; Herakleitos, Thales and Aristeia programmes co-financed by EU-ESF and the Greek NSRF, Greece; BSF-NSF and MINERVA,

Israel; NCN and NAWA, Poland; La Caixa Banking Foundation, CERCA Programme Generalitat de Catalunya and PROMETEO and GenT Programmes Generalitat Valenciana, Spain; Göran Gustafssons Stiftelse, Sweden; The Royal Society and Leverhulme Trust, United Kingdom.

In addition, individual members wish to acknowledge support from CERN: European Organization for Nuclear Research (CERN DOCT); Chile: Agencia Nacional de Investigación y Desarrollo (FONDECYT 1230812, FONDECYT 1240864); China: Chinese Ministry of Science and Technology (MOST-2023YFA1605700, MOST-2023YFA1609300), National Natural Science Foundation of China (NSFC - 12175119, NSFC 12275265); Czech Republic: Czech Science Foundation (GACR - 24-11373S), Ministry of Education Youth and Sports (ERC-CZ-LL2327, FORTE CZ.02.01.01/00/22_008/0004632), PRIMUS Research Programme (PRIMUS/21/SCI/017); EU: H2020 European Research Council (ERC - 101002463); European Union: European Research Council (BARD No. 101116429, ERC - 948254, ERC 101089007), European Regional Development Fund (SMASH COFUND 101081355, SLO ERDF), Horizon 2020 Framework Programme (MUCCA - CHIST-ERA-19-XAI-00), European Union, Future Artificial Intelligence Research (FAIR-NextGenerationEU PE00000013), Italian Center for High Performance Computing, Big Data and Quantum Computing (ICSC, NextGenerationEU); France: Agence Nationale de la Recherche (ANR-21-CE31-0022, ANR-22-EDIR-0002); Germany: Baden-Württemberg Stiftung (BW Stiftung-Postdoc Elite-programme), Deutsche Forschungsgemeinschaft (DFG - 469666862, DFG - CR 312/5-2); China: Research Grants Council (GRF); Italy: Istituto Nazionale di Fisica Nucleare (ICSC, NextGenerationEU), Ministero dell'Università e della Ricerca (NextGenEU I53D23001490006 M4C2.1.1, NextGenEU I53D23000820006 M4C2.1.1, NextGenEU I53D23001490006 M4C2.1.1, SOE2024_0000023); Japan: Japan Society for the Promotion of Science (JSPS KAKENHI JP22H01227, JSPS KAKENHI JP22H04944, JSPS KAKENHI JP22KK0227, JSPS KAKENHI JP24K23939, JSPS KAKENHI JP24KK0251, JSPS KAKENHI JP25H00650, JSPS KAKENHI JP25H01291, JSPS KAKENHI JP25K01023); Norway: Research Council of Norway (RCN-314472); Poland: Ministry of Science and Higher Education (IDUB AGH, POB8, D4 no 9722), Polish National Science Centre (NCN 2021/42/E/ST2/00350, NCN OPUS 2023/51/B/ST2/02507, NCN OPUS nr 2022/47/B/ST2/03059, NCN UMO-2019/34/E/ST2/00393, UMO-2022/47/O/ST2/00148, UMO-2023/49/B/ST2/04085, UMO-2023/51/B/ST2/00920, UMO-2024/53/N/ST2/00869); Portugal: Foundation for Science and Technology (FCT); Spain: Ministry of Science and Innovation (MCIN & NextGenEU PCI2022-135018-2, MICIN & FEDER PID2021-125273NB, RYC2019-028510-I, RYC2020-030254-I, RYC2021-031273-I, RYC2022-038164-I); Sweden: Carl Trygger Foundation (Carl Trygger Foundation CTS 22:2312), Swedish Research Council (Swedish Research Council 2023-04654, VR 2021-03651, VR 2022-03845, VR 2022-04683, VR 2023-03403, VR 2024-05451), Knut and Alice Wallenberg Foundation (KAW 2018.0458, KAW 2022.0358, KAW 2023.0366); Switzerland: Swiss National Science Foundation (SNSF - PCEFP2_194658); United Kingdom: Royal Society (NIF-R1-231091); United States of America: U.S. Department of Energy (ECA DE-AC02-76SF00515), Neubauer Family Foundation.

References

- [1] ATLAS Collaboration, *Observation of a new particle in the search for the Standard Model Higgs boson with the ATLAS detector at the LHC*, *Phys. Lett. B* **716** (2012) 1, arXiv: [1207.7214 \[hep-ex\]](#).
- [2] CMS Collaboration, *Observation of a new boson at a mass of 125 GeV with the CMS experiment at the LHC*, *Phys. Lett. B* **716** (2012) 30, arXiv: [1207.7235 \[hep-ex\]](#).
- [3] L. Evans and P. Bryant, *LHC Machine*, *JINST* **3** (2008) S08001.
- [4] ATLAS Collaboration, *A detailed map of Higgs boson interactions by the ATLAS experiment ten years after the discovery*, *Nature* **607** (2022) 52, arXiv: [2207.00092 \[hep-ex\]](#), Erratum: *Nature* **612** (2022) E24.
- [5] CMS Collaboration, *A portrait of the Higgs boson by the CMS experiment ten years after the discovery*, *Nature* **607** (2022) 60, arXiv: [2207.00043 \[hep-ex\]](#), Erratum: *Nature* **623** (2023) E4.
- [6] ATLAS Collaboration, *Study of the spin and parity of the Higgs boson in diboson decays with the ATLAS detector*, *Eur. Phys. J. C* **75** (2015) 476, arXiv: [1506.05669 \[hep-ex\]](#), Erratum: *Eur. Phys. J. C* **76** (2016) 152.
- [7] CMS Collaboration, *Constraints on the spin-parity and anomalous HVV couplings of the Higgs boson in proton collisions at 7 and 8 TeV*, *Phys. Rev. D* **92** (2015) 012004, arXiv: [1411.3441 \[hep-ex\]](#).
- [8] ATLAS and CMS Collaborations, *Combined Measurement of the Higgs Boson Mass in pp Collisions at $\sqrt{s} = 7$ and 8 TeV with the ATLAS and CMS Experiments*, *Phys. Rev. Lett.* **114** (2015) 191803, arXiv: [1503.07589 \[hep-ex\]](#).
- [9] ATLAS Collaboration, *Combined Measurement of the Higgs Boson Mass from the $H \rightarrow \gamma\gamma$ and $H \rightarrow ZZ^* \rightarrow 4\ell$ Decay Channels with the ATLAS Detector Using $\sqrt{s} = 7, 8$, and 13 TeV pp Collision Data*, *Phys. Rev. Lett.* **131** (2023) 251802, arXiv: [hep-ex/2308.04775](#).
- [10] CMS Collaboration, *Measurement of the Higgs boson mass and width using the four-lepton final state in proton–proton collisions at $\sqrt{s} = 13$ TeV*, *Phys. Rev. D* **111** (2024) 092014, arXiv: [hep-ex/2409.13663](#).
- [11] CMS Collaboration, *A measurement of the Higgs boson mass in the diphoton decay channel*, *Phys. Lett. B* **805** (2020) 135425, arXiv: [2002.06398 \[hep-ex\]](#).
- [12] D. de Florian et al., *Handbook of LHC Higgs Cross Sections: 4. Deciphering the Nature of the Higgs Sector*, (2017), arXiv: [1610.07922 \[hep-ph\]](#).
- [13] M. Carena, I. Low and C. E. Wagner, *Implications of a modified Higgs to diphoton decay width*, *JHEP* **08** (2012) 060, arXiv: [hep-ph/1206.1082](#).
- [14] C.-W. Chiang and K. Yagyu, *Higgs boson decays to $\gamma\gamma$ and $Z\gamma$ in models with Higgs extensions*, *Phys. Rev. D* **87** (2013) 033003, arXiv: [hep-ph/1207.1065](#).
- [15] C.-S. Chen, C.-Q. Geng, D. Huang and L.-H. Tsai, *New scalar contributions to $h \rightarrow Z\gamma$* , *Phys. Rev. D* **87** (2013) 075019, arXiv: [hep-ph/1301.4694](#).

- [16] A. Djouadi, V. Driesen, W. Hollik and A. Kraft, *The Higgs-photon-Z boson coupling revisited*, *Eur. Phys. J. C* **1** (1998) 163, arXiv: [hep-ph/9701342](#).
- [17] H. T. Hung, T. T. Hong, H. H. Phuong, H. L. T. Mai and L. T. Hue, *Neutral Higgs boson decays $H \rightarrow Z\gamma, \gamma\gamma$ in 3-3-1 models*, *Phys. Rev. D* **100** (2019) 075014, arXiv: [1907.06735](#).
- [18] P. Archer-Smith, D. Stolarski and R. Vega-Morales, *On new physics contributions to the Higgs decay to $Z\gamma$* , *JHEP* **2021** (2021), arXiv: [2012.01440](#).
- [19] X.-G. He, Z.-L. Huang, M.-W. Li and C.-W. Liu, *The SM expected branching ratio for $h \rightarrow \gamma\gamma$ and an excess for $h \rightarrow Z\gamma$* , *JHEP* **10** (2024) 135, arXiv: [hep-ph/2402.08190](#).
- [20] A. Azatov, R. Contino, A. Di Iura and J. Galloway, *New prospects for Higgs compositeness in $h \rightarrow Z\gamma$* , *Phys. Rev. D* **88** (2013) 075019, arXiv: [hep-ph/1308.2676](#).
- [21] I. Low, J. Lykken and G. Shaughnessy, *Singlet scalars as Higgs boson imposters at the Large Hadron Collider*, *Phys. Rev. D* **84** (2011) 035027, arXiv: [hep-ph/1105.4587](#).
- [22] I. Low, J. Lykken and G. Shaughnessy, *Have we observed the Higgs boson (imposter)?*, *Phys. Rev. D* **86** (2012) 093012, arXiv: [hep-ph/1207.1093](#).
- [23] ATLAS Collaboration, *A search for the $Z\gamma$ decay mode of the Higgs boson in pp collisions at $\sqrt{s} = 13$ TeV with the ATLAS detector*, *Phys. Lett. B* **809** (2020) 135754, arXiv: [2005.05382 \[hep-ex\]](#).
- [24] CMS Collaboration, *Search for Higgs boson decays to a Z boson and a photon in proton–proton collisions at $\sqrt{s} = 13$ TeV*, *JHEP* **05** (2023) 233, arXiv: [2204.12945 \[hep-ex\]](#).
- [25] ATLAS Collaboration and CMS Collaboration, *Evidence for the Higgs Boson Decay to a Z Boson and a Photon at the LHC*, *Phys. Rev. Lett.* **132** (2024) 021803, arXiv: [hep-ex/2309.03501](#).
- [26] T. Chen and C. Guestrin, ‘XGBoost: A Scalable Tree Boosting System’, *Proceedings of the 22nd ACM SIGKDD International Conference on Knowledge Discovery and Data Mining*, ACM, 2016 785, arXiv: [1603.02754](#).
- [27] ATLAS Collaboration, *The ATLAS Experiment at the CERN Large Hadron Collider*, *JINST* **3** (2008) S08003.
- [28] ATLAS Collaboration, *The ATLAS experiment at the CERN Large Hadron Collider: a description of the detector configuration for Run 3*, *JINST* **19** (2024) P05063, arXiv: [2305.16623 \[physics.ins-det\]](#).
- [29] ATLAS Collaboration, *Performance of the ATLAS trigger system in 2015*, *Eur. Phys. J. C* **77** (2017) 317, arXiv: [1611.09661 \[hep-ex\]](#).
- [30] ATLAS Collaboration, *The ATLAS trigger system for LHC Run 3 and trigger performance in 2022*, *JINST* **19** (2024) P06029, arXiv: [2401.06630 \[hep-ex\]](#).
- [31] ATLAS Collaboration, *Software and computing for Run 3 of the ATLAS experiment at the LHC*, *Eur. Phys. J. C* **85** (2025) 234, arXiv: [2404.06335 \[hep-ex\]](#).
- [32] ATLAS Collaboration, *Performance of electron and photon triggers in ATLAS during LHC Run 2*, *Eur. Phys. J. C* **80** (2020) 47, arXiv: [1909.00761 \[hep-ex\]](#).

- [33] ATLAS Collaboration, *Performance of the ATLAS muon triggers in Run 2*, [JINST **15** \(2020\) P09015](#), arXiv: [2004.13447 \[physics.ins-det\]](#).
- [34] S. Agostinelli et al., *Geant4-a simulation toolkit*, [Nucl. Instrum. Meth. A **506** \(2003\) 250](#).
- [35] ATLAS Collaboration, *The ATLAS Simulation Infrastructure*, [Eur. Phys. J. C **70** \(2010\) 823](#), arXiv: [1005.4568 \[physics.ins-det\]](#).
- [36] C. Anastasiou, C. Duhr, F. Dulat, F. Herzog and B. Mistlberger, *Higgs Boson Gluon-Fusion Production in QCD at Three Loops*, [Phys. Rev. Lett. **114** \(2015\) 212001](#), arXiv: [1503.06056 \[hep-ph\]](#).
- [37] C. Anastasiou et al., *High precision determination of the gluon fusion Higgs boson cross-section at the LHC*, [JHEP **05** \(2016\) 058](#), arXiv: [1602.00695 \[hep-ph\]](#).
- [38] F. Dulat, A. Lazopoulos and B. Mistlberger, *iHixs 2 – Inclusive Higgs cross sections*, [Comput. Phys. Commun. **233** \(2018\) 243](#), arXiv: [1802.00827 \[hep-ph\]](#).
- [39] R. V. Harlander and K. J. Ozeren, *Finite top mass effects for hadronic Higgs production at next-to-next-to-leading order*, [JHEP **11** \(2009\) 088](#), arXiv: [0909.3420 \[hep-ph\]](#).
- [40] R. V. Harlander and K. J. Ozeren, *Top mass effects in Higgs production at next-to-next-to-leading order QCD: Virtual corrections*, [Phys. Lett. B **679** \(2009\) 467](#), arXiv: [0907.2997 \[hep-ph\]](#).
- [41] R. V. Harlander, H. Mantler, S. Marzani and K. J. Ozeren, *Higgs production in gluon fusion at next-to-next-to-leading order QCD for finite top mass*, [Eur. Phys. J. C **66** \(2010\) 359](#), arXiv: [0912.2104 \[hep-ph\]](#).
- [42] A. Pak, M. Rogal and M. Steinhauser, *Finite top quark mass effects in NNLO Higgs boson production at LHC*, [JHEP **02** \(2010\) 025](#), arXiv: [0911.4662 \[hep-ph\]](#).
- [43] S. Actis, G. Passarino, C. Sturm and S. Uccirati, *NLO electroweak corrections to Higgs boson production at hadron colliders*, [Phys. Lett. B **670** \(2008\) 12](#), arXiv: [0809.1301 \[hep-ph\]](#).
- [44] S. Actis, G. Passarino, C. Sturm and S. Uccirati, *NNLO computational techniques: The cases $H \rightarrow \gamma\gamma$ and $H \rightarrow gg$* , [Nucl. Phys. B **811** \(2009\) 182](#), arXiv: [hep-ph/0809.3667](#).
- [45] C. Anastasiou, R. Boughezal and F. Petriello, *Mixed QCD-electroweak corrections to Higgs boson production in gluon fusion*, [JHEP **04** \(2009\) 003](#), arXiv: [hep-ph/0811.3458](#).
- [46] U. Aglietti, R. Bonciani, G. Degrossi and A. Vicini, *Two-loop light fermion contribution to Higgs production and decays*, [Phys. Lett. B **595** \(2004\) 432](#), arXiv: [hep-ph/0404071](#).
- [47] M. Bonetti, K. Melnikov and L. Tancredi, *Higher order corrections to mixed QCD-EW contributions to Higgs boson production in gluon fusion*, [Phys. Rev. D **97** \(2018\) 056017](#), arXiv: [1801.10403 \[hep-ph\]](#), Erratum: [Phys. Rev. D **97** \(2018\) 099906\(E\)](#).
- [48] M. Ciccolini, A. Denner and S. Dittmaier, *Strong and Electroweak Corrections to the Production of a Higgs Boson+2Jets via Weak Interactions at the Large Hadron Collider*, [Phys. Rev. Lett. **99** \(2007\) 161803](#), arXiv: [hep-ph/0707.0381](#).

- [49] M. Ciccolini, A. Denner and S. Dittmaier,
Electroweak and QCD corrections to Higgs production via vector-boson fusion at the CERN LHC,
[*Phys. Rev. D* **77** \(2008\) 013002](#), arXiv: [0710.4749 \[hep-ph\]](#).
- [50] P. Bolzoni, F. Maltoni, S.-O. Moch and M. Zaro,
Higgs Boson Production via Vector-Boson Fusion at Next-to-Next-to-Leading Order in QCD,
[*Phys. Rev. Lett.* **105** \(2010\) 011801](#), arXiv: [1003.4451 \[hep-ph\]](#).
- [51] M. L. Ciccolini, S. Dittmaier and M. Krämer,
Electroweak radiative corrections to associated WH and ZH production at hadron colliders,
[*Phys. Rev. D* **68** \(2003\) 073003](#), arXiv: [hep-ph/0306234](#).
- [52] O. Brein, A. Djouadi and R. Harlander,
NNLO QCD corrections to the Higgs-strahlung processes at hadron colliders,
[*Phys. Lett. B* **579** \(2004\) 149](#), arXiv: [hep-ph/0307206](#).
- [53] O. Brein, R. V. Harlander, M. Wiesemann and T. Zirke,
Top-quark mediated effects in hadronic Higgs-Strahlung, [*Eur. Phys. J. C* **72** \(2012\) 1868](#),
arXiv: [1111.0761 \[hep-ph\]](#).
- [54] L. Altenkamp, S. Dittmaier, R. V. Harlander, H. Rzehak and T. J. E. Zirke,
Gluon-induced Higgs-strahlung at next-to-leading order QCD, [*JHEP* **02** \(2013\) 078](#),
arXiv: [1211.5015 \[hep-ph\]](#).
- [55] A. Denner, S. Dittmaier, S. Kallweit and A. Mück, *HAWK 2.0: A Monte Carlo program for Higgs production in vector-boson fusion and Higgs strahlung at hadron colliders*,
[*Comput. Phys. Commun.* **195** \(2015\) 161](#), arXiv: [1412.5390 \[hep-ph\]](#).
- [56] O. Brein, R. V. Harlander and T. J. E. Zirke, *vh@nnlo-Higgs Strahlung at hadron colliders*,
[*Comput. Phys. Commun.* **184** \(2013\) 998](#), arXiv: [hep-ph/1210.5347](#).
- [57] R. V. Harlander, A. Kulesza, V. Theeuwes and T. Zirke,
Soft gluon resummation for gluon-induced Higgs Strahlung, [*JHEP* **11** \(2014\) 082](#),
arXiv: [1410.0217 \[hep-ph\]](#).
- [58] R. V. Harlander, J. Klappert, S. Liebler and L. Simon,
vh@nnlo-v2: new physics in Higgs Strahlung, [*JHEP* **05** \(2018\) 089](#),
arXiv: [1802.04817 \[hep-ph\]](#).
- [59] W. Beenakker et al., *NLO QCD corrections to $t\bar{t}H$ production in hadron collisions*,
[*Nucl. Phys. B* **653** \(2003\) 151](#), arXiv: [hep-ph/0211352](#).
- [60] S. Dawson, C. Jackson, L. H. Orr, L. Reina and D. Wackerroth, *Associated Higgs boson production with top quarks at the CERN Large Hadron Collider: NLO QCD corrections*,
[*Phys. Rev. D* **68** \(2003\) 034022](#), arXiv: [hep-ph/0305087](#).
- [61] Y. Zhang, W.-G. Ma, R.-Y. Zhang, C. Chen and L. Guo,
QCD NLO and EW NLO corrections to $t\bar{t}H$ production with top quark decays at hadron collider,
[*Phys. Lett. B* **738** \(2014\) 1](#), arXiv: [hep-ph/1407.1110](#).
- [62] S. Frixione, V. Hirschi, D. Pagani, H.-S. Shao and M. Zaro,
Electroweak and QCD corrections to top-pair hadroproduction in association with heavy bosons,
[*JHEP* **06** \(2015\) 184](#), arXiv: [hep-ph/1504.03446](#).
- [63] M. Wiesemann et al., *Higgs production in association with bottom quarks*, [*JHEP* \(2015\) 132](#),
arXiv: [1409.5301](#).

- [64] S. Dittmaier, M. Krämer and M. Spira,
Higgs radiation off bottom quarks at the Fermilab Tevatron and the CERN LHC,
[Phys. Rev. D **70** \(2004\) 074010](#).
- [65] S. Dawson, C. B. Jackson, L. Reina and D. Wackeroth,
Exclusive Higgs boson production with bottom quarks at hadron colliders,
[Phys. Rev. D **69** \(2004\) 074027](#), arXiv: [hep-ph/0311067](#).
- [66] P. Nason and C. Oleari,
NLO Higgs boson production via vector-boson fusion matched with shower in POWHEG,
[JHEP **02** \(2010\) 037](#), arXiv: [0911.5299 \[hep-ph\]](#).
- [67] S. Alioli, P. Nason, C. Oleari and E. Re, *A general framework for implementing NLO calculations in shower Monte Carlo programs: the POWHEG BOX*, [JHEP **06** \(2010\) 043](#), (using ATLAS svn revisions r2856 for v1, r3080 for v2 ggF, r3052 for v2 VBF, and r3133 for v2 VH),
arXiv: [hep-ph/1002.2581](#).
- [68] P. Nason, *A new method for combining NLO QCD with shower Monte Carlo algorithms*,
[JHEP **11** \(2004\) 040](#), arXiv: [hep-ph/0409146](#).
- [69] S. Frixione, P. Nason and C. Oleari,
Matching NLO QCD computations with parton shower simulations: the POWHEG method,
[JHEP **11** \(2007\) 070](#), arXiv: [0709.2092 \[hep-ph\]](#).
- [70] H. B. Hartanto, B. Jäger, L. Reina and D. Wackeroth,
Higgs boson production in association with top quarks in the POWHEG BOX,
[Phys. Rev. D **91** \(2015\) 094003](#), arXiv: [1501.04498 \[hep-ph\]](#).
- [71] R. D. Ball et al., *The PDF4LHC21 combination of global PDF fits for the LHC Run III*,
[J. Phys. G **49** \(2022\) 080501](#).
- [72] C. Bierlich et al., *A comprehensive guide to the physics and usage of PYTHIA 8.3*,
[SciPost Phys. Codeb. \(2022\) 8](#), arXiv: [hep-ph/2203.11601](#).
- [73] C.-F. Q. L.-B. Chen and R.-L. Zhu, *Reconstructing the 125 GeV SM Higgs boson through $\ell\bar{\ell}\gamma$* ,
[Phys. Lett. B **726** \(2013\) 306](#), arXiv: [1211.6058](#).
- [74] J. Bellm et al., *Herwig 7.2 release note*, [Eur. Phys. J. C **80** \(2020\)](#).
- [75] E. Bothmann et al., *Event generation with Sherpa 2.2*, [SciPost Phys. **7** \(2019\) 034](#),
arXiv: [1905.09127 \[hep-ph\]](#).
- [76] NNPDF Collaboration, R. D. Ball et al., *Parton distributions for the LHC run II*,
[JHEP **04** \(2015\) 040](#), arXiv: [1410.8849 \[hep-ph\]](#).
- [77] ATLAS Collaboration, *AtlFast3: The Next Generation of Fast Simulation in ATLAS*,
[Comput. Softw. Big Sci. **6** \(2022\) 7](#), arXiv: [2109.02551 \[hep-ex\]](#).
- [78] J. Alwall et al., *The automated computation of tree-level and next-to-leading order differential cross sections, and their matching to parton shower simulations*, [JHEP **07** \(2014\) 079](#),
arXiv: [hep-ph/1405.0301](#).
- [79] R. D. Ball et al., *Parton distributions with QED corrections*, [Nucl. Phys. B **877** \(2013\) 290](#),
arXiv: [1308.0598](#).
- [80] ATLAS Collaboration, *ATLAS Pythia 8 tunes to 7 TeV data*, ATL-PHYS-PUB-2014-021, 2014,
URL: <https://cds.cern.ch/record/1966419>.

- [81] K. Werner, F.-M. Liu and T. Pierog, *Parton ladder splitting and the rapidity dependence of transverse momentum spectra in deuteron-gold collisions at RHIC*, *Phys. Rev. C* **74** (2006) 044902, arXiv: [hep-ph/0506232](#) [[hep-ph](#)].
- [82] T. Pierog, I. Karpenko, J. M. Katzy, E. Yatsenko and K. Werner, *EPOS LHC: Test of collective hadronization with data measured at the CERN Large Hadron Collider*, *Phys. Rev. D* **92** (2015) 034906, arXiv: [1306.0121](#) [[hep-ph](#)].
- [83] ATLAS Collaboration, *The Pythia 8 A3 tune description of ATLAS minimum bias and inelastic measurements incorporating the Donnachie–Landshoff diffractive model*, ATL-PHYS-PUB-2016-017, 2016, URL: <https://cds.cern.ch/record/2206965>.
- [84] R. D. Ball et al., *The PDF4LHC21 combination of global PDF fits for the LHC Run III*, *J. Phys. G* **49** (2022) 080501, arXiv: [2203.05506](#) [[hep-ph](#)].
- [85] G. Luisoni, P. Nason, C. Oleari and F. Tramontano, *$HW^\pm/HZ + 0$ and 1 jet at NLO with the POWHEG BOX interfaced to GoSam and their merging within MiNLO*, *JHEP* **10** (2013) 083, arXiv: [hep-ph/1306.2542](#).
- [86] M. K. S. Dittmaier and M. Spira, *Higgs radiation off bottom quarks at the Fermilab Tevatron and the CERN LHC*, *Phys. Rev. D* **70** (2004) 74010.
- [87] L. Altenkamp, S. Dittmaier, R. V. Harlander, H. Rzehak and T. J. E. Zirke, *Gluon-induced Higgs-strahlung at next-to-leading order QCD*, *JHEP* **2013** (2013) 78, arXiv: [1211.5015](#).
- [88] R. V. Harlander, A. Kulesza, V. Theeuwes and T. Zirke, *Soft gluon resummation for gluon-induced Higgs Strahlung*, *JHEP* **2014** (2014) 82, arXiv: [1410.0217](#).
- [89] H. B. Hartanto, B. Jäger, L. Reina and D. Wackerroth, *Higgs boson production in association with top quarks in the POWHEG BOX*, *Phys. Rev. D* **91** (2015) 094003, arXiv: [1501.04498](#).
- [90] B. Jäger, L. Reina and D. Wackerroth, *Higgs boson production in association with b jets in the POWHEG BOX*, *Phys. Rev. D* **93** (2016) 014030, arXiv: [1509.05843](#).
- [91] ATLAS Collaboration, *Vertex Reconstruction Performance of the ATLAS Detector at $\sqrt{s} = 13$ TeV*, ATL-PHYS-PUB-2015-026, 2015, URL: <https://cds.cern.ch/record/2037717>.
- [92] ATLAS Collaboration, *Muon reconstruction and identification efficiency in ATLAS using the full Run 2 pp collision data set at $\sqrt{s} = 13$ TeV*, *Eur. Phys. J. C* **81** (2021) 578, arXiv: [2012.00578](#) [[hep-ex](#)].
- [93] ATLAS Collaboration, *Studies of the muon momentum calibration and performance of the ATLAS detector with pp collisions at $\sqrt{s} = 13$ TeV*, *Eur. Phys. J. C* **83** (2023) 686, arXiv: [2212.07338](#) [[hep-ex](#)].
- [94] ATLAS Collaboration, *Electron and photon performance measurements with the ATLAS detector using the 2015–2017 LHC proton–proton collision data*, *JINST* **14** (2019) P12006, arXiv: [1908.00005](#) [[hep-ex](#)].
- [95] ATLAS Collaboration, *Electron and photon efficiencies in LHC Run 2 with the ATLAS experiment*, *JHEP* **05** (2024) 162, arXiv: [2308.13362](#) [[hep-ex](#)].

- [96] ATLAS Collaboration, *Electron and photon energy calibration with the ATLAS detector using LHC Run 2 data*, [JINST **19** \(2024\) P02009](#), arXiv: [2309.05471 \[hep-ex\]](#).
- [97] ATLAS Collaboration, *Jet reconstruction and performance using particle flow with the ATLAS Detector*, [Eur. Phys. J. C **77** \(2017\) 466](#), arXiv: [1703.10485 \[hep-ex\]](#).
- [98] M. Cacciari, G. P. Salam and G. Soyez, *The anti- k_t jet clustering algorithm*, [JHEP **04** \(2008\) 063](#), arXiv: [0802.1189 \[hep-ph\]](#).
- [99] M. Cacciari, G. P. Salam and G. Soyez, *FastJet user manual*, [Eur. Phys. J. C **72** \(2012\) 1896](#), arXiv: [1111.6097 \[hep-ph\]](#).
- [100] ATLAS Collaboration, *Jet energy scale and resolution measured in proton–proton collisions at $\sqrt{s} = 13$ TeV with the ATLAS detector*, [Eur. Phys. J. C **81** \(2021\) 689](#), arXiv: [2007.02645 \[hep-ex\]](#).
- [101] ATLAS Collaboration, *Performance of pile-up mitigation techniques for jets in pp collisions at $\sqrt{s} = 8$ TeV using the ATLAS detector*, [Eur. Phys. J. C **76** \(2016\) 581](#), arXiv: [1510.03823 \[hep-ex\]](#).
- [102] ATLAS Collaboration, *Forward jet vertex tagging using the particle flow algorithm*, ATL-PHYS-PUB-2019-026, 2019, URL: <https://cds.cern.ch/record/2683100>.
- [103] Particle Data Group, *Review of Particle Physics*, [PTEP **2020** \(2020\) 083C01](#).
- [104] OPAL Collaboration, *Search for anomalous production of di-lepton events with missing transverse momentum in e^+e^- collisions at $\sqrt{s} = 161$ and 172 GeV*, [Eur. Phys. J. C **4** \(1998\) 47](#), arXiv: [hep-ex/9710010](#).
- [105] M. Vesterinen and T. Wyatt, *A novel technique for studying the Z boson transverse momentum distribution at hadron colliders*, [Nucl. Instrum. Meth. A **602** \(2009\) 432](#), arXiv: [hep-ph/0807.4956](#).
- [106] D. Rainwater, R. Szalapski and D. Zeppenfeld, *Probing color-singlet exchange in Z + 2-jet events at the CERN LHC*, [Phys. Rev. D **54** \(1996\) 6680](#), arXiv: [hep-ph/9605444](#).
- [107] ATLAS Collaboration, *Search for Scalar Diphoton Resonances in the Mass Range 65-600 GeV with the ATLAS Detector in pp Collision Data at $\sqrt{s} = 8$ TeV*, [Phys. Rev. Lett. **113** \(2014\) 171801](#), arXiv: [hep-ex/1407.6583](#).
- [108] ATLAS Collaboration, *Measurement of the inclusive isolated prompt photon cross section in pp collisions at $\sqrt{s} = 7$ TeV with the ATLAS detector*, [Phys. Rev. D **83** \(2011\) 052005](#), arXiv: [1012.4389 \[hep-ex\]](#).
- [109] A. Wald, *Sequential Tests of Statistical Hypotheses*, [Annals Math. Statist. **16** \(1945\) 117](#).
- [110] ATLAS Collaboration, *Measurement of the properties of Higgs boson production at $\sqrt{s} = 13$ TeV in the $H \rightarrow \gamma\gamma$ channel using 139fb^{-1} of pp collision data with the ATLAS experiment*, [JHEP **07** \(2023\) 088](#), arXiv: [2207.00348 \[hep-ex\]](#).
- [111] M. Frate, K. Cranmer, S. Kalia, A. Vandenberg-Rodes and D. Whiteson, *Modeling Smooth Backgrounds and Generic Localized Signals with Gaussian Processes*, 2017, arXiv: [physics.data-an/1709.05681](#).

- [112] ATLAS Collaboration,
A search for the dimuon decay of the Standard Model Higgs boson with the ATLAS detector,
Phys. Lett. B **812** (2021) 135980, arXiv: [2007.07830 \[hep-ex\]](#).
- [113] G. Avoni et al., *The new LUCID-2 detector for luminosity measurement and monitoring in ATLAS*,
JINST **13** (2018) P07017.
- [114] ATLAS Collaboration,
Preliminary analysis of the luminosity calibration of the ATLAS 13.6 TeV data recorded in 2022,
ATL-DAPR-PUB-2023-001, 2023, URL: <https://cds.cern.ch/record/2853525>.
- [115] ATLAS Collaboration,
Preliminary analysis of the luminosity calibration for the ATLAS 13.6 TeV data recorded in 2023,
ATL-DAPR-PUB-2024-001, 2024, URL: <https://cds.cern.ch/record/2900949>.
- [116] G. Cowan, K. Cranmer, E. Gross and O. Vitells,
Asymptotic formulae for likelihood-based tests of new physics, *Eur. Phys. J. C* **71** (2011) 1554,
arXiv: [1007.1727 \[physics.data-an\]](#), Erratum: *Eur. Phys. J. C* **73** (2013) 2501.
- [117] ATLAS Collaboration, *Search for Higgs boson decays to a photon and a Z boson in pp collisions at $\sqrt{s} = 7$ and 8 TeV with the ATLAS detector*, *Phys. Lett. B* **732** (2014) 8,
arXiv: [1402.3051 \[hep-ex\]](#).
- [118] ATLAS Collaboration, *ATLAS Computing Acknowledgements*, ATL-SOFT-PUB-2025-001, 2025,
URL: <https://cds.cern.ch/record/2922210>.

The ATLAS Collaboration

G. Aad ¹⁰⁴, E. Aakvaag ¹⁷, B. Abbott ¹²³, S. Abdelhameed ^{119a}, K. Abeling ⁵⁵, N.J. Abicht ⁴⁹, S.H. Abidi ³⁰, M. Aboeela ⁴⁵, A. Aboulhorma ^{36e}, H. Abramowicz ¹⁵⁷, Y. Abulaiti ¹²⁰, B.S. Acharya ^{69a,69b,m}, A. Ackermann ^{63a}, C. Adam Bourdarios ⁴, L. Adameczyk ^{86a}, S.V. Addepalli ¹⁴⁹, M.J. Addison ¹⁰³, J. Adelman ¹¹⁸, A. Adiguzel ^{22c}, T. Adye ¹³⁷, A.A. Affolder ¹³⁹, Y. Afik ⁴⁰, M.N. Agaras ¹³, A. Aggarwal ¹⁰², C. Agheorghiesei ^{28c}, F. Ahmadov ^{39,ad}, S. Ahuja ⁹⁷, X. Ai ^{143b}, G. Aielli ^{76a,76b}, A. Aikot ¹⁶⁹, M. Ait Tamlihat ^{36e}, B. Aitbenkikh ^{36a}, M. Akbiyik ¹⁰², T.P.A. Åkesson ¹⁰⁰, A.V. Akimov ¹⁵¹, D. Akiyama ¹⁷⁴, N.N. Akolkar ²⁵, S. Aktas ¹⁷², G.L. Alberghi ^{24b}, J. Albert ¹⁷¹, U. Alberti ²⁰, P. Albicocco ⁵³, G.L. Albouy ⁶⁰, S. Alderweireldt ⁵², Z.L. Alegria ¹²⁴, M. Aleksa ³⁷, I.N. Aleksandrov ³⁹, C. Alexa ^{28b}, T. Alexopoulos ¹⁰, F. Alfonsi ^{24b}, M. Algren ⁵⁶, M. Alhroob ¹⁷³, B. Ali ¹³⁵, H.M.J. Ali ^{93,w}, S. Ali ³², S.W. Alibocus ⁹⁴, M. Aliev ^{34c}, G. Alimonti ^{71a}, W. Alkakh ⁵⁵, C. Allaire ⁶⁶, B.M.M. Allbrooke ¹⁵², J.S. Allen ¹⁰³, J.F. Allen ⁵², P.P. Allport ²¹, A. Aloisio ^{72a,72b}, F. Alonso ⁹², C. Alpighiani ¹⁴², Z.M.K. Alsolami ⁹³, A. Alvarez Fernandez ¹⁰², M. Alves Cardoso ⁵⁶, M.G. Alviggi ^{72a,72b}, M. Aly ¹⁰³, Y. Amaral Coutinho ^{83b}, A. Ambler ¹⁰⁶, C. Amelung ³⁷, M. Amerl ¹⁰³, C.G. Ames ¹¹¹, T. Amezza ¹³⁰, D. Amidei ¹⁰⁸, B. Amini ⁵⁴, K. Amirie ¹⁶¹, A. Amirkhanov ³⁹, S.P. Amor Dos Santos ^{133a}, K.R. Amos ¹⁶⁹, D. Amperiadou ¹⁵⁸, S. An ⁸⁴, C. Anastopoulos ¹⁴⁵, T. Andeen ¹¹, J.K. Anders ⁹⁴, A.C. Anderson ⁵⁹, A. Andreazza ^{71a,71b}, S. Angelidakis ⁹, A. Angerami ⁴², A.V. Anisenkov ³⁹, A. Annovi ^{74a}, C. Antel ³⁷, E. Antipov ¹⁵¹, M. Antonelli ⁵³, F. Anulli ^{75a}, M. Aoki ⁸⁴, T. Aoki ¹⁵⁹, M.A. Aparo ¹⁵², L. Aperio Bella ⁴⁸, M. Apicella ³¹, C. Appelt ¹⁵⁷, A. Apyan ²⁷, M. Arampatzi ¹⁰, S.J. Arbiol Val ⁸⁷, C. Arcangeletti ⁵³, A.T.H. Arce ⁵¹, J-F. Arguin ¹¹⁰, S. Argyropoulos ¹⁵⁸, J.-H. Arling ⁴⁸, O. Arnaez ⁴, H. Arnold ¹⁵¹, G. Artoni ^{75a,75b}, H. Asada ¹¹³, K. Asai ¹²¹, S. Asatryan ¹⁷⁹, N.A. Asbah ³⁷, R.A. Ashby Pickering ¹⁷³, A.M. Aslam ⁹⁷, K. Assamagan ³⁰, R. Astalos ^{29a}, K.S.V. Astrand ¹⁰⁰, S. Atashi ¹⁶⁵, R.J. Atkin ^{34a}, H. Atmani ^{36f}, P.A. Atlasiddha ¹³¹, K. Augsten ¹³⁵, A.D. Auriol ⁴¹, V.A. Austrup ¹⁰³, A.S. Avad ⁹⁶, G. Avolio ³⁷, K. Axiotis ⁵⁶, A. Azzam ¹³, D. Babal ^{29b}, H. Bachacou ¹³⁸, K. Bachas ^{158,q}, A. Bachiu ³⁵, E. Bachmann ⁵⁰, M.J. Backes ^{63a}, A. Badea ⁴⁰, T.M. Baer ¹⁰⁸, P. Bagnaia ^{75a,75b}, M. Bahmani ¹⁹, D. Bahner ⁵⁴, K. Bai ¹²⁶, J.T. Baines ¹³⁷, L. Baines ⁹⁶, O.K. Baker ¹⁷⁸, E. Bakos ¹⁶, D. Bakshi Gupta ⁸, L.E. Balabram Filho ^{83b}, V. Balakrishnan ¹²³, R. Balasubramanian ⁴, E.M. Baldin ³⁸, P. Balek ^{86a}, E. Ballabene ^{24b,24a}, F. Balli ¹³⁸, L.M. Baltes ^{63a}, W.K. Balunas ³³, J. Balz ¹⁰², I. Bamwidhi ^{119b}, E. Banas ⁸⁷, M. Bandieramonte ¹³², A. Bandyopadhyay ²⁵, S. Bansal ²⁵, L. Barak ¹⁵⁷, M. Barakat ⁴⁸, E.L. Barberio ¹⁰⁷, D. Barberis ^{18b}, M. Barbero ¹⁰⁴, M.Z. Barel ¹¹⁷, T. Barillari ¹¹², M-S. Barisits ³⁷, T. Barklow ¹⁴⁹, P. Baron ¹³⁶, D.A. Baron Moreno ¹⁰³, A. Baroncelli ⁶², A.J. Barr ¹²⁹, J.D. Barr ⁹⁸, F. Barreiro ¹⁰¹, J. Barreiro Guimarães da Costa ¹⁴, M.G. Barros Teixeira ^{133a}, S. Barsov ³⁸, F. Bartels ^{63a}, R. Bartoldus ¹⁴⁹, A.E. Barton ⁹³, P. Bartos ^{29a}, M. Baselga ⁴⁹, S. Bashiri ⁸⁷, A. Bassalat ^{66,b}, M.J. Basso ^{162a}, S. Bataju ⁴⁵, R. Bate ¹⁷⁰, R.L. Bates ⁵⁹, S. Batlamous ¹⁰¹, M. Battaglia ¹³⁹, D. Battulga ¹⁹, M. Baue ^{75a,75b}, M. Bauer ⁷⁹, P. Bauer ²⁵, L.T. Bayer ⁴⁸, L.T. Bazzano Hurrell ³¹, J.B. Beacham ¹¹², T. Beau ¹³⁰, J.Y. Beauchamp ⁹², P.H. Beauchemin ¹⁶⁴, P. Bechtle ²⁵, H.P. Beck ^{20,p}, K. Becker ¹⁷³, A.J. Beddall ⁸², V.A. Bednyakov ³⁹, C.P. Bee ¹⁵¹, L.J. Beemster ¹⁶, M. Begalli ^{83d}, M. Begel ³⁰, J.K. Behr ⁴⁸, J.F. Beirer ³⁷, F. Beisiegel ²⁵, M. Belfkir ^{119b}, G. Bella ¹⁵⁷, L. Bellagamba ^{24b}, A. Bellerive ³⁵, C.D. Bellgraph ⁶⁸, P. Bellos ²¹, K. Beloborodov ³⁸, I. Benaoumeur ²¹, D. Benckekroun ^{36a}, F. Bendebba ^{36a}, Y. Benhammou ¹⁵⁷, K.C. Benkendorfer ⁶¹, L. Beresford ⁴⁸,

M. Beretta ⁵³, E. Bergeaas Kuutmann ¹⁶⁷, N. Berger ⁴, B. Bergmann ¹³⁵, J. Beringer ^{18a},
G. Bernardi ⁵, C. Bernius ¹⁴⁹, F.U. Bernlochner ²⁵, A. Berrocal Guardia ¹³, T. Berry ⁹⁷,
P. Berta ¹³⁶, A. Berthold ⁵⁰, A. Berti ^{133a}, R. Bertrand ¹⁰⁴, S. Bethke ¹¹², A. Betti ^{75a,75b},
A.J. Bevan ⁹⁶, L. Bezio ⁵⁶, N.K. Bhalla ⁵⁴, S. Bharthuar ¹¹², S. Bhatta ¹⁵¹, P. Bhattacharai ¹⁴⁹,
Z.M. Bhatti ¹²⁰, K.D. Bhide ⁵⁴, V.S. Bhopalkar ¹²⁴, R.M. Bianchi ¹³², G. Bianco ^{24b,24a},
O. Biebel ¹¹¹, M. Biglietti ^{77a}, C.S. Billingsley ⁴⁵, Y. Bimgdi ^{36f}, M. Bindi ⁵⁵, A. Bingham ¹⁷⁷,
A. Bingul ^{22b}, C. Bini ^{75a,75b}, G.A. Bird ³³, M. Birman ¹⁷⁵, M. Biros ¹³⁶, S. Biryukov ¹⁵²,
T. Bisanz ⁴⁹, E. Bisceglie ^{24b,24a}, J.P. Biswal ¹³⁷, D. Biswas ¹⁴⁷, I. Bloch ⁴⁸, A. Blue ⁵⁹,
U. Blumenschein ⁹⁶, V.S. Bobrovnikov ³⁹, L. Boccardo ^{57b,57a}, M. Boehler ⁵⁴, B. Boehm ¹⁷²,
D. Bogavac ¹³, A.G. Bogdanchikov ³⁸, L.S. Boggia ¹³⁰, V. Boisvert ⁹⁷, P. Bokan ³⁷, T. Bold ^{86a},
M. Bomben ⁵, M. Bona ⁹⁶, M. Boonekamp ¹³⁸, A.G. Borbély ⁵⁹, I.S. Bordulev ³⁸,
G. Borissov ⁹³, D. Bortoletto ¹²⁹, D. Boscherini ^{24b}, M. Bosman ¹³, K. Bouaouda ^{36a},
N. Bouchhar ¹⁶⁹, L. Boudet ⁴, J. Boudreau ¹³², E.V. Bouhova-Thacker ⁹³, D. Boumediene ⁴¹,
R. Bouquet ^{57b,57a}, A. Boveia ¹²², J. Boyd ³⁷, D. Boye ³⁰, I.R. Boyko ³⁹, L. Bozianu ⁵⁶,
J. Bracinik ²¹, N. Brahimi ⁴, G. Brandt ¹⁷⁷, O. Brandt ³³, B. Brau ¹⁰⁵, J.E. Brau ¹²⁶,
R. Brenner ¹⁷⁵, L. Brenner ¹¹⁷, R. Brenner ¹⁶⁷, S. Bressler ¹⁷⁵, G. Brianti ^{78a,78b}, D. Britton ⁵⁹,
D. Britzger ¹¹², I. Brock ²⁵, R. Brock ¹⁰⁹, G. Brooijmans ⁴², A.J. Brooks ⁶⁸, E.M. Brooks ^{162b},
E. Brost ³⁰, L.M. Brown ^{171,162a}, L.E. Bruce ⁶¹, T.L. Bruckler ¹²⁹, P.A. Bruckman de Renstrom ⁸⁷,
B. Brüers ⁴⁸, A. Bruni ^{24b}, G. Bruni ^{24b}, D. Brunner ^{47a,47b}, M. Bruschi ^{24b}, N. Bruscino ^{75a,75b},
T. Buanes ¹⁷, Q. Buat ¹⁴², D. Buchin ¹¹², A.G. Buckley ⁵⁹, O. Bulekov ⁸², B.A. Bullard ¹⁴⁹,
S. Burdin ⁹⁴, C.D. Burgard ⁴⁹, A.M. Burger ⁹¹, B. Burghgrave ⁸, O. Burlayenko ⁵⁴,
J. Burleson ¹⁶⁸, J.C. Burzynski ¹⁴⁸, E.L. Busch ⁴², V. Büscher ¹⁰², P.J. Bussey ⁵⁹,
J.M. Butler ²⁶, C.M. Buttar ⁵⁹, J.M. Butterworth ⁹⁸, W. Buttinger ¹³⁷, C.J. Buxo Vazquez ¹⁰⁹,
A.R. Buzykaev ³⁹, S. Cabrera Urbán ¹⁶⁹, L. Cadamuro ⁶⁶, H. Cai ³⁷, Y. Cai ^{24b,114c,24a},
Y. Cai ^{114a}, V.M.M. Cairo ³⁷, O. Cakir ^{3a}, N. Calace ³⁷, P. Calafiura ^{18a}, G. Calderini ¹³⁰,
P. Calfayan ³⁵, L. Calic ¹⁰⁰, G. Callea ⁵⁹, L.P. Caloba ^{83b}, D. Calvet ⁴¹, S. Calvet ⁴¹,
R. Camacho Toro ¹³⁰, S. Camarda ³⁷, D. Camarero Munoz ²⁷, P. Camarri ^{76a,76b},
C. Camincher ¹⁷¹, M. Campanelli ⁹⁸, A. Camplani ⁴³, V. Canale ^{72a,72b}, A.C. Canbay ^{3a},
E. Canonero ⁹⁷, J. Cantero ¹⁶⁹, Y. Cao ¹⁶⁸, F. Capocasa ²⁷, M. Capua ^{44b,44a}, A. Carbone ^{71a,71b},
R. Cardarelli ^{76a}, J.C.J. Cardenas ⁸, M.P. Cardiff ²⁷, G. Carducci ^{44b,44a}, T. Carli ³⁷,
G. Carlino ^{72a}, J.I. Carlotto ¹³, B.T. Carlson ^{132,r}, E.M. Carlson ¹⁷¹, J. Carmignani ⁹⁴,
L. Carminati ^{71a,71b}, A. Carnelli ⁴, M. Carnesale ³⁷, S. Caron ¹¹⁶, E. Carquin ^{140g}, I.B. Carr ¹⁰⁷,
S. Carrá ^{73a,73b}, G. Carratta ^{24b,24a}, C. Carrion Martinez ¹⁶⁹, A.M. Carroll ¹²⁶, M.P. Casado ^{13,h},
P. Casolaro ^{72a,72b}, M. Caspar ⁴⁸, F.L. Castillo ⁴, L. Castillo Garcia ¹³, V. Castillo Gimenez ¹⁶⁹,
N.F. Castro ^{133a,133e}, A. Catinaccio ³⁷, J.R. Catmore ¹²⁸, T. Cavaliere ⁴, V. Cavaliere ³⁰,
L.J. Caviedes Betancourt ^{23b}, E. Celebi ⁸², S. Cella ³⁷, V. Cepaitis ⁵⁶, K. Cerny ¹²⁵,
A.S. Cerqueira ^{83a}, A. Cerri ^{74a,74b,am}, L. Cerrito ^{76a,76b}, F. Cerutti ^{18a}, B. Cervato ^{71a,71b},
A. Cervelli ^{24b}, G. Cesarini ⁵³, S.A. Cetin ⁸², P.M. Chabrilat ¹³⁰, R. Chakkappai ⁶⁶,
S. Chakraborty ¹⁷³, A. Chambers ⁶¹, J. Chan ^{18a}, W.Y. Chan ¹⁵⁹, J.D. Chapman ³³,
E. Chapon ¹³⁸, B. Chargeishvili ^{155b}, D.G. Charlton ²¹, C. Chauhan ¹³⁶, Y. Che ^{114a},
S. Chekanov ⁶, S.V. Chekulaev ^{162a}, G.A. Chelkov ^{39,a}, B. Chen ¹⁵⁷, B. Chen ¹⁷¹, H. Chen ^{114a},
H. Chen ³⁰, J. Chen ^{144a}, J. Chen ¹⁴⁸, M. Chen ¹²⁹, S. Chen ⁸⁹, S.J. Chen ^{114a}, X. Chen ^{144a},
X. Chen ^{15,ah}, Z. Chen ⁶², C.L. Cheng ¹⁷⁶, H.C. Cheng ^{64a}, S. Cheong ¹⁴⁹, A. Cheplakov ³⁹,
E. Cherepanova ¹¹⁷, R. Cherkaoui El Moursli ^{36e}, E. Cheu ⁷, K. Cheung ⁶⁵, L. Chevalier ¹³⁸,
V. Chiarella ⁵³, G. Chiarelli ^{74a}, G. Chiodini ^{70a}, A.S. Chisholm ²¹, A. Chitan ^{28b},
M. Chitishvili ¹⁶⁹, M.V. Chizhov ^{39,s}, K. Choi ¹¹, Y. Chou ¹⁴², E.Y.S. Chow ¹¹⁶, K.L. Chu ¹⁷⁵,
M.C. Chu ^{64a}, X. Chu ^{14,114c}, Z. Chubinidze ⁵³, J. Chudoba ¹³⁴, J.J. Chwastowski ⁸⁷,

D. Cieri ¹¹², K.M. Ciesla ^{86a}, V. Cindro ⁹⁵, A. Ciocio ^{18a}, F. Cirotto ^{72a,72b}, Z.H. Citron ¹⁷⁵,
M. Citterio ^{71a}, D.A. Ciubotaru ^{28b}, A. Clark ⁵⁶, P.J. Clark ⁵², N. Clarke Hall ⁹⁸, C. Clarry ¹⁶¹,
S.E. Clawson ⁴⁸, C. Clement ^{47a,47b}, Y. Coadou ¹⁰⁴, M. Cobal ^{69a,69c}, A. Coccaro ^{57b},
R.F. Coelho Barrue ^{133a}, R. Coelho Lopes De Sa ¹⁰⁵, S. Coelli ^{71a}, L.S. Colangeli ¹⁶¹, B. Cole ⁴²,
P. Collado Soto ¹⁰¹, J. Collot ⁶⁰, R. Coluccia ^{70a,70b}, P. Conde Muiño ^{133a,133g}, M.P. Connell ^{34c},
S.H. Connell ^{34c}, E.I. Conroy ¹²⁹, M. Contreras Cossio ¹¹, F. Conventi ^{72a,aj},
A.M. Cooper-Sarkar ¹²⁹, L. Corazzina ^{75a,75b}, F.A. Corchia ^{24b,24a}, A. Cordeiro Oudot Choi ¹⁴²,
L.D. Corpe ⁴¹, M. Corradi ^{75a,75b}, F. Corriveau ^{106,ab}, A. Cortes-Gonzalez ¹⁵⁹, M.J. Costa ¹⁶⁹,
F. Costanza ⁴, D. Costanzo ¹⁴⁵, J. Couthures ⁴, G. Cowan ⁹⁷, K. Cranmer ¹⁷⁶, L. Cremer ⁴⁹,
D. Cremonini ^{24b,24a}, S. Crépe-Renaudin ⁶⁰, F. Crescioli ¹³⁰, T. Cresta ^{73a,73b}, M. Cristinziani ¹⁴⁷,
M. Cristoforetti ^{78a,78b}, E. Critelli ⁹⁸, V. Croft ¹¹⁷, G. Crosetti ^{44b,44a}, A. Cueto ¹⁰¹, H. Cui ⁹⁸,
Z. Cui ⁷, B.M. Cunnett ¹⁵², W.R. Cunningham ⁵⁹, F. Curcio ¹⁶⁹, J.R. Curran ⁵²,
M.J. Da Cunha Sargedas De Sousa ^{57b,57a}, J.V. Da Fonseca Pinto ^{83b}, C. Da Via ¹⁰³,
W. Dabrowski ^{86a}, T. Dado ³⁷, S. Dahbi ¹⁵⁴, T. Dai ¹⁰⁸, D. Dal Santo ²⁰, C. Dallapiccola ¹⁰⁵,
M. Dam ⁴³, G. D'amen ³⁰, V. D'Amico ¹¹¹, J. Damp ¹⁰², J.R. Dandoy ³⁵, M. D'Andrea ^{57b,57a},
D. Dannheim ³⁷, G. D'anniballe ^{74a,74b}, M. Danninger ¹⁴⁸, V. Dao ¹⁵¹, G. Darbo ^{57b},
S.J. Das ³⁰, F. Dattola ⁴⁸, S. D'Auria ^{71a,71b}, A. D'Avanzo ^{72a,72b}, T. Davidek ¹³⁶,
J. Davidson ¹⁷³, I. Dawson ⁹⁶, K. De ⁸, C. De Almeida Rossi ¹⁶¹, R. De Asmundis ^{72a},
N. De Biase ⁴⁸, S. De Castro ^{24b,24a}, N. De Groot ¹¹⁶, P. de Jong ¹¹⁷, H. De la Torre ¹¹⁸,
A. De Maria ^{114a}, A. De Salvo ^{75a}, U. De Sanctis ^{76a,76b}, F. De Santis ^{70a,70b}, A. De Santo ¹⁵²,
J.B. De Vivie De Regie ⁶⁰, J. Debevc ⁹⁵, D.V. Dedovich ³⁹, J. Degens ⁹⁴, A.M. Deiana ⁴⁵,
J. Del Peso ¹⁰¹, L. Delagrangé ¹³⁰, F. Deliot ¹³⁸, C.M. Delitzsch ⁴⁹, M. Della Pietra ^{72a,72b},
D. Della Volpe ⁵⁶, A. Dell'Acqua ³⁷, L. Dell'Asta ^{71a,71b}, M. Delmastro ⁴, C.C. Delogu ¹⁰²,
P.A. Delsart ⁶⁰, S. Demers ¹⁷⁸, M. Demichev ³⁹, S.P. Denisov ³⁸, H. Denizli ^{22a,1},
L. D'Eramo ⁴¹, D. Derendarz ⁸⁷, F. Derue ¹³⁰, P. Dervan ⁹⁴, A.M. Desai ¹, K. Desch ²⁵,
F.A. Di Bello ^{57b,57a}, A. Di Ciaccio ^{76a,76b}, L. Di Ciaccio ⁴, A. Di Domenico ^{75a,75b},
C. Di Donato ^{72a,72b}, A. Di Girolamo ³⁷, G. Di Gregorio ³⁷, A. Di Luca ^{78a,78b},
B. Di Micco ^{77a,77b}, R. Di Nardo ^{77a,77b}, K.F. Di Petrillo ⁴⁰, M. Diamantopoulou ³⁵, F.A. Dias ¹¹⁷,
M.A. Diaz ^{140a,140b}, A.R. Didenko ³⁹, M. Didenko ¹⁶⁹, S.D. Diefenbacher ^{18a}, E.B. Diehl ¹⁰⁸,
S. Díez Cornell ⁴⁸, C. Díez Pardos ¹⁴⁷, C. Dimitriadi ¹⁵⁰, A. Dimitrievska ²¹, A. Dimri ¹⁵¹,
Y. Ding ⁶², J. Dingfelder ²⁵, T. Dingley ¹²⁹, I-M. Dinu ^{28b}, S.J. Dittmeier ^{63b}, F. Dittus ³⁷,
M. Divisek ¹³⁶, B. Dixit ⁹⁴, F. Djama ¹⁰⁴, T. Djobava ^{155b}, C. Doglioni ^{103,100},
A. Dohnalova ^{29a}, Z. Dolezal ¹³⁶, K. Domijan ^{86a}, K.M. Dona ⁴⁰, M. Donadelli ^{83d},
B. Dong ¹⁰⁹, J. Donini ⁴¹, A. D'Onofrio ^{72a,72b}, M. D'Onofrio ⁹⁴, J. Dopke ¹³⁷, A. Doria ^{72a},
N. Dos Santos Fernandes ^{133a}, I.A. Dos Santos Luz ^{83e}, P. Dougan ¹⁰³, M.T. Dova ⁹²,
A.T. Doyle ⁵⁹, M.P. Drescher ⁵⁵, E. Dreyer ¹⁷⁵, I. Drivas-koulouris ¹⁰, M. Drnevich ¹²⁰,
D. Du ⁶², T.A. du Pree ¹¹⁷, Z. Duan ^{114a}, M. Dubau ⁴, F. Dubinin ³⁹, M. Dubovsky ^{29a},
E. Duchovni ¹⁷⁵, G. Duckeck ¹¹¹, P.K. Duckett ⁹⁸, O.A. Ducu ^{28b}, D. Duda ⁵², A. Dudarev ³⁷,
M.M. Dudek ⁸⁷, E.R. Duden ²⁷, M. D'uffizi ¹⁰³, L. Duflost ⁶⁶, M. Dührssen ³⁷, I. Duminica ^{28g},
A.E. Dumitriu ^{28b}, M. Dunford ^{63a}, K. Dunne ^{47a,47b}, A. Duperrin ¹⁰⁴, H. Duran Yildiz ^{3a},
A. Durglishvili ^{155b}, G.I. Dyckes ^{18a}, M. Dyndal ^{86a}, B.S. Dziedzic ³⁷, Z.O. Earnshaw ¹⁵²,
G.H. Eberwein ¹²⁹, B. Eckerova ^{29a}, S. Eggebrecht ⁵⁵, E. Egidio Purcino De Souza ^{83e},
G. Eigen ¹⁷, K. Einsweiler ^{18a}, T. Ekelof ¹⁶⁷, P.A. Ekman ¹⁰⁰, S. El Farkh ^{36b}, Y. El Ghazali ⁶²,
H. El Jarrari ³⁷, A. El Moussaouy ^{36a}, D. Elitez ³⁷, M. Ellert ¹⁶⁷, F. Ellinghaus ¹⁷⁷,
T.A. Elliot ⁹⁷, N. Ellis ³⁷, J. Elmsheuser ³⁰, M. Elsayy ^{119a}, M. Elsing ³⁷, D. Emeliyanov ¹³⁷,
Y. Enari ⁸⁴, S. Epari ¹¹⁰, D. Ernani Martins Neto ⁸⁷, F. Ernst ³⁷, M. Errenst ¹⁷⁷, M. Escalier ⁶⁶,
C. Escobar ¹⁶⁹, E. Etzion ¹⁵⁷, G. Evans ^{133a,133b}, H. Evans ⁶⁸, L.S. Evans ⁴⁸, A. Ezhilov ³⁸,

S. Ezzarqtouni ^{id}36a, F. Fabbri ^{id}24b,24a, L. Fabbri ^{id}24b,24a, G. Facini ^{id}98, V. Fadeyev ^{id}139, R.M. Fakhrutdinov ^{id}38, D. Fakoudis ^{id}102, S. Falciano ^{id}75a, L.F. Falda Ulhoa Coelho ^{id}133a, F. Fallavollita ^{id}112, G. Falsetti ^{id}44b,44a, J. Faltova ^{id}136, C. Fan ^{id}168, K.Y. Fan ^{id}64b, Y. Fan ^{id}14, Y. Fang ^{id}14,114c, M. Fanti ^{id}71a,71b, M. Faraj ^{id}69a,69b, Z. Farazpay ^{id}99, A. Farbin ^{id}8, A. Farilla ^{id}77a, K. Farman ^{id}154, T. Farooque ^{id}109, J.N. Farr ^{id}178, S.M. Farrington ^{id}137,52, F. Fassi ^{id}36e, D. Fassouliotis ^{id}9, L. Fayard ^{id}66, P. Federic ^{id}136, P. Federicova ^{id}134, O.L. Fedin ^{id}38,a, M. Feickert ^{id}176, L. Feligioni ^{id}104, D.E. Fellers ^{id}18a, C. Feng ^{id}143a, Y. Feng ^{id}14, Z. Feng ^{id}117, M.J. Fenton ^{id}165, L. Ferencz ^{id}48, B. Fernandez Barbadillo ^{id}93, P. Fernandez Martinez ^{id}67, M.J.V. Fernoux ^{id}104, J. Ferrando ^{id}93, A. Ferrari ^{id}167, P. Ferrari ^{id}117,116, R. Ferrari ^{id}73a, D. Ferrere ^{id}56, C. Ferretti ^{id}108, M.P. Fewell ^{id}1, D. Fiacco ^{id}75a,75b, F. Fiedler ^{id}102, P. Fiedler ^{id}135, S. Filimonov ^{id}39, M.S. Filip ^{id}28b,t, A. Filipčič ^{id}95, E.K. Filmer ^{id}162a, F. Filthaut ^{id}116, M.C.N. Fiolhais ^{id}133a,133c,c, L. Fiorini ^{id}169, W.C. Fisher ^{id}109, T. Fitschen ^{id}103, P.M. Fitzhugh ^{id}138, I. Fleck ^{id}147, P. Fleischmann ^{id}108, T. Flick ^{id}177, M. Flores ^{id}34d,ag, L.R. Flores Castillo ^{id}64a, L. Flores Sanz De Acedo ^{id}37, F.M. Follega ^{id}78a,78b, N. Fomin ^{id}33, J.H. Foo ^{id}161, A. Formica ^{id}138, A.C. Forti ^{id}103, E. Fortin ^{id}37, A.W. Fortman ^{id}18a, L. Foster ^{id}18a, L. Fountas ^{id}9,i, D. Fournier ^{id}66, H. Fox ^{id}93, P. Francavilla ^{id}74a,74b, S. Francescato ^{id}61, S. Franchellucci ^{id}56, M. Franchini ^{id}24b,24a, S. Franchino ^{id}63a, D. Francis ^{id}37, L. Franco ^{id}116, L. Franconi ^{id}48, M. Franklin ^{id}61, G. Frattari ^{id}27, Y.Y. Frid ^{id}157, J. Friend ^{id}59, N. Fritzsche ^{id}37, A. Froch ^{id}56, D. Froidevaux ^{id}37, J.A. Frost ^{id}129, Y. Fu ^{id}109, S. Fuenzalida Garrido ^{id}140g, M. Fujimoto ^{id}151, K.Y. Fung ^{id}64a, E. Furtado De Simas Filho ^{id}83e, M. Furukawa ^{id}159, J. Fuster ^{id}169, A. Gaa ^{id}55, A. Gabrielli ^{id}24b,24a, A. Gabrielli ^{id}161, P. Gadow ^{id}37, G. Gagliardi ^{id}57b,57a, L.G. Gagnon ^{id}18a, S. Gaid ^{id}88b, S. Galantzan ^{id}157, J. Gallagher ^{id}1, E.J. Gallas ^{id}129, A.L. Gallen ^{id}167, B.J. Gallop ^{id}137, K.K. Gan ^{id}122, S. Ganguly ^{id}159, Y. Gao ^{id}52, Z. Gao ^{id}114a, A. Garabaglu ^{id}142, F.M. Garay Walls ^{id}140a,140b, C. García ^{id}169, A. Garcia Alonso ^{id}117, A.G. Garcia Caffaro ^{id}178, J.E. García Navarro ^{id}169, M.A. Garcia Ruiz ^{id}23b, M. Garcia-Sciveres ^{id}18a, G.L. Gardner ^{id}131, R.W. Gardner ^{id}40, N. Garelli ^{id}164, R.B. Garg ^{id}149, J.M. Gargan ^{id}33, C.A. Garner ^{id}161, C.M. Garvey ^{id}34a, V.K. Gassmann ^{id}164, G. Gaudio ^{id}73a, V. Gautam ^{id}13, P. Gauzzi ^{id}75a,75b, J. Gavranovic ^{id}95, I.L. Gavrilenko ^{id}133a, A. Gavrilyuk ^{id}38, C. Gay ^{id}170, G. Gaycken ^{id}126, E.N. Gazis ^{id}10, A. Gekow ^{id}122, C. Gemme ^{id}57b, M.H. Genest ^{id}60, A.D. Gentry ^{id}115, S. George ^{id}97, T. Geralis ^{id}46, A.A. Gerwin ^{id}123, P. Gessinger-Befurt ^{id}37, M.E. Geyik ^{id}177, M. Ghani ^{id}173, K. Ghorbanian ^{id}96, A. Ghosal ^{id}147, A. Ghosh ^{id}165, A. Ghosh ^{id}7, B. Giacobbe ^{id}24b, S. Giagu ^{id}75a,75b, T. Giani ^{id}117, A. Giannini ^{id}62, S.M. Gibson ^{id}97, M. Gignac ^{id}139, D.T. Gil ^{id}86b, A.K. Gilbert ^{id}86a, B.J. Gilbert ^{id}42, D. Gillberg ^{id}35, G. Gilles ^{id}117, D.M. Gingrich ^{id}2,ai, M.P. Giordani ^{id}69a,69c, P.F. Giraud ^{id}138, G. Giugliarelli ^{id}69a,69c, D. Giugni ^{id}71a, F. Giuli ^{id}76a,76b, I. Gkialas ^{id}9,i, L.K. Gladilin ^{id}38, C. Glasman ^{id}101, M. Glazewska ^{id}20, R.M. Gleason ^{id}165, G. Glemža ^{id}48, M. Glisic ^{id}126, I. Gnesi ^{id}44b, Y. Go ^{id}30, M. Goblirsch-Kolb ^{id}37, B. Gocke ^{id}49, D. Godin ^{id}110, B. Gokturk ^{id}22a, S. Goldfarb ^{id}107, T. Golling ^{id}56, M.G.D. Gololo ^{id}34c, D. Golubkov ^{id}38, J.P. Gombas ^{id}109, A. Gomes ^{id}133a,133b, G. Gomes Da Silva ^{id}147, A.J. Gomez Delegido ^{id}37, R. Gonçalves ^{id}133a, L. Gonella ^{id}21, A. Gongadze ^{id}155c, F. Gonnella ^{id}21, J.L. Gonski ^{id}149, R.Y. González Andana ^{id}52, S. González de la Hoz ^{id}169, M.V. Gonzalez Rodrigues ^{id}48, R. Gonzalez Suarez ^{id}167, S. Gonzalez-Sevilla ^{id}56, L. Goossens ^{id}37, B. Gorini ^{id}37, E. Gorini ^{id}70a,70b, A. Gorišek ^{id}95, T.C. Gosart ^{id}131, A.T. Goshaw ^{id}51, M.I. Gostkin ^{id}39, S. Goswami ^{id}124, C.A. Gottardo ^{id}37, S.A. Gotz ^{id}111, M. Goughri ^{id}36b, A.G. Goussiou ^{id}142, N. Govender ^{id}34c, R.P. Grabarczyk ^{id}129, I. Grabowska-Bold ^{id}86a, K. Graham ^{id}35, E. Gramstad ^{id}128, S. Grancagnolo ^{id}70a,70b, C.M. Grant ^{id}1, P.M. Gravila ^{id}28f, F.G. Gravili ^{id}70a,70b, H.M. Gray ^{id}18a, M. Greco ^{id}112, M.J. Green ^{id}1, C. Grefe ^{id}25, A.S. Grefsrud ^{id}17, I.M. Gregor ^{id}48, K.T. Greif ^{id}165, P. Grenier ^{id}149, S.G. Grewe ^{id}112, A.A. Grillo ^{id}139, K. Grimm ^{id}32, S. Grinstein ^{id}13,x, J.-F. Grivaz ^{id}66, E. Gross ^{id}175, J. Grosse-Knetter ^{id}55, L. Guan ^{id}108, G. Guerrieri ^{id}37, R. Guevara ^{id}128, R. Gugel ^{id}102, J.A.M. Guhit ^{id}108, A. Guida ^{id}19, E. Guilloton ^{id}173, S. Guindon ^{id}37, F. Guo ^{id}14,114c, J. Guo ^{id}144a,

L. Guo ^{id48}, L. Guo ^{id114b,v}, Y. Guo ^{id108}, A. Gupta ^{id49}, R. Gupta ^{id132}, S. Gupta ^{id27}, S. Gurbuz ^{id25},
 S.S. Gurdasani ^{id48}, G. Gustavino ^{id75a,75b}, P. Gutierrez ^{id123}, L.F. Gutierrez Zagazeta ^{id131},
 M. Gutsche ^{id50}, C. Gutschow ^{id98}, C. Gwenlan ^{id129}, C.B. Gwilliam ^{id94}, E.S. Haaland ^{id128},
 A. Haas ^{id120}, M. Habedank ^{id59}, C. Haber ^{id18a}, H.K. Hadavand ^{id8}, A. Haddad ^{id41}, A. Hadeef ^{id50},
 A.I. Hagan ^{id93}, J.J. Hahn ^{id147}, E.H. Haines ^{id98}, M. Haleem ^{id172}, J. Haley ^{id124}, G.D. Hallewell ^{id104},
 J.A. Hallford ^{id48}, K. Hamano ^{id171}, H. Hamdaoui ^{id167}, M. Hamer ^{id25}, S.E.D. Hammoud ^{id66},
 E.J. Hampshire ^{id97}, J. Han ^{id143a}, L. Han ^{id114a}, L. Han ^{id62}, S. Han ^{id14}, K. Hanagaki ^{id84},
 M. Hance ^{id139}, D.A. Hangal ^{id42}, H. Hanif ^{id148}, M.D. Hank ^{id131}, J.B. Hansen ^{id43}, P.H. Hansen ^{id43},
 D. Harada ^{id56}, T. Harenberg ^{id177}, S. Harkusha ^{id179}, M.L. Harris ^{id105}, Y.T. Harris ^{id25}, J. Harrison ^{id13},
 N.M. Harrison ^{id122}, P.F. Harrison ^{id173}, M.L.E. Hart ^{id98}, N.M. Hartman ^{id112}, N.M. Hartmann ^{id111},
 R.Z. Hasan ^{id97,137}, Y. Hasegawa ^{id146}, F. Haslbeck ^{id129}, S. Hassan ^{id17}, R. Hauser ^{id109},
 M. Haviernik ^{id136}, C.M. Hawkes ^{id21}, R.J. Hawkins ^{id37}, Y. Hayashi ^{id159}, D. Hayden ^{id109},
 C. Hayes ^{id108}, R.L. Hayes ^{id117}, C.P. Hays ^{id129}, J.M. Hays ^{id96}, H.S. Hayward ^{id94}, M. He ^{id14,114c},
 Y. He ^{id48}, Y. He ^{id98}, N.B. Heatley ^{id96}, V. Hedberg ^{id100}, C. Heidegger ^{id54}, K.K. Heidegger ^{id54},
 J. Heilman ^{id35}, S. Heim ^{id48}, T. Heim ^{id18a}, J.J. Heinrich ^{id126}, L. Heinrich ^{id112}, J. Hejbal ^{id134},
 M. Helbig ^{id50}, A. Held ^{id176}, S. Hellesund ^{id17}, C.M. Helling ^{id170}, S. Hellman ^{id47a,47b},
 A.M. Henriques Correia ^{id37}, H. Herde ^{id100}, Y. Hernández Jiménez ^{id151}, L.M. Herrmann ^{id25},
 T. Herrmann ^{id50}, G. Herten ^{id54}, R. Hertenberger ^{id111}, L. Hervas ^{id37}, M.E. Hesping ^{id102},
 N.P. Hessey ^{id162a}, J. Hessler ^{id112}, M. Hidaoui ^{id36b}, N. Hidic ^{id136}, E. Hill ^{id161}, T.S. Hillersoy ^{id17},
 S.J. Hillier ^{id21}, J.R. Hinds ^{id109}, F. Hinterkeuser ^{id25}, M. Hirose ^{id127}, S. Hirose ^{id163},
 D. Hirschbuehl ^{id177}, T.G. Hitchings ^{id103}, B. Hiti ^{id95}, J. Hobbs ^{id151}, R. Hobincu ^{id28e}, N. Hod ^{id175},
 A.M. Hodges ^{id168}, M.C. Hodgkinson ^{id145}, B.H. Hodgkinson ^{id129}, A. Hoecker ^{id37}, D.D. Hofer ^{id108},
 J. Hofer ^{id169}, J. Hofner ^{id102}, M. Holzbock ^{id37}, L.B.A.H. Hommels ^{id33}, V. Homsak ^{id129},
 B.P. Honan ^{id103}, J.J. Hong ^{id68}, T.M. Hong ^{id132}, B.H. Hooberman ^{id168}, W.H. Hopkins ^{id6},
 M.C. Hoppesch ^{id168}, Y. Horii ^{id113}, M.E. Horstmann ^{id112}, S. Hou ^{id154}, M.R. Housenga ^{id168},
 J. Howarth ^{id59}, J. Hoya ^{id6}, M. Hrabovsky ^{id125}, T. Hryn'ova ^{id4}, P.J. Hsu ^{id65}, S.-C. Hsu ^{id142},
 T. Hsu ^{id66}, M. Hu ^{id18a}, Q. Hu ^{id62}, S. Huang ^{id33}, X. Huang ^{id14,114c}, Y. Huang ^{id136}, Y. Huang ^{id114b},
 Y. Huang ^{id14}, Z. Huang ^{id66}, Z. Hubacek ^{id135}, F. Huegging ^{id25}, T.B. Huffman ^{id129},
 M. Hufnagel Maranha De Faria ^{id83a}, C.A. Hugli ^{id48}, M. Huhtinen ^{id37}, S.K. Huiberts ^{id17},
 R. Hulsken ^{id106}, C.E. Hultquist ^{id18a}, D.L. Humphreys ^{id105}, N. Huseynov ^{id12}, J. Huston ^{id109},
 J. Huth ^{id61}, L. Huth ^{id48}, R. Hyneman ^{id7}, G. Iacobucci ^{id56}, G. Iakovidis ^{id30},
 L. Iconomidou-Fayard ^{id66}, J.P. Iddon ^{id37}, P. Iengo ^{id72a,72b}, R. Iguchi ^{id159}, Y. Iiyama ^{id159},
 T. Iizawa ^{id159}, Y. Ikegami ^{id84}, D. Iliadis ^{id158}, N. Ilıc ^{id161}, H. Imam ^{id36a}, G. Inacio Goncalves ^{id83d},
 S.A. Infante Cabanas ^{id140c}, T. Ingebretsen Carlson ^{id47a,47b}, J.M. Inglis ^{id96}, G. Introzzi ^{id73a,73b},
 M. Iodice ^{id77a}, V. Ippolito ^{id75a,75b}, R.K. Irwin ^{id94}, M. Ishino ^{id159}, W. Islam ^{id176}, C. Issever ^{id19},
 S. Istin ^{id22a,ao}, K. Itabashi ^{id84}, H. Ito ^{id174}, R. Iuppa ^{id78a,78b}, A. Ivina ^{id175}, V. Izzo ^{id72a}, P. Jacka ^{id135},
 P. Jackson ^{id1}, P. Jain ^{id48}, K. Jakobs ^{id54}, T. Jakoubek ^{id175}, J. Jamieson ^{id59}, W. Jang ^{id159},
 S. Jankovych ^{id136}, M. Javurkova ^{id105}, P. Jawahar ^{id103}, L. Jeanty ^{id126}, J. Jejelava ^{id155a,ae}, P. Jenni ^{id54,f},
 C.E. Jessiman ^{id35}, C. Jia ^{id143a}, H. Jia ^{id170}, J. Jia ^{id151}, X. Jia ^{id112,114c}, Z. Jia ^{id114a}, C. Jiang ^{id52},
 Q. Jiang ^{id64b}, S. Jiggins ^{id48}, M. Jimenez Ortega ^{id169}, J. Jimenez Pena ^{id13}, S. Jin ^{id114a}, A. Jinaru ^{id28b},
 O. Jinnouchi ^{id141}, P. Johansson ^{id145}, K.A. Johns ^{id7}, J.W. Johnson ^{id139}, F.A. Jolly ^{id48},
 D.M. Jones ^{id152}, E. Jones ^{id48}, K.S. Jones ^{id8}, P. Jones ^{id33}, R.W.L. Jones ^{id93}, T.J. Jones ^{id94},
 H.L. Joos ^{id55}, R. Joshi ^{id122}, J. Jovicevic ^{id16}, X. Ju ^{id18a}, J.J. Junggeburth ^{id37}, T. Junkermann ^{id63a},
 A. Juste Rozas ^{id13,x}, M.K. Juzek ^{id87}, S. Kabana ^{id140f}, A. Kaczmarska ^{id87}, S.A. Kadir ^{id149},
 M. Kado ^{id112}, H. Kagan ^{id122}, M. Kagan ^{id149}, A. Kahn ^{id131}, C. Kahra ^{id102}, T. Kaji ^{id159},
 E. Kajomovitz ^{id156}, N. Kakati ^{id175}, N. Kakoty ^{id13}, I. Kalaitzidou ^{id54}, S. Kandel ^{id8}, N.J. Kang ^{id139},
 D. Kar ^{id34h}, E. Karentzos ^{id25}, K. Karki ^{id8}, O. Karkout ^{id117}, S.N. Karpov ^{id39}, Z.M. Karpova ^{id39},

V. Kartvelishvili ⁹³, A.N. Karyukhin ³⁸, E. Kasimi ¹⁵⁸, J. Katzy ⁴⁸, S. Kaur ³⁵, K. Kawade ¹⁴⁶, M.P. Kawale ¹²³, C. Kawamoto ⁸⁹, T. Kawamoto ⁶², E.F. Kay ³⁷, F.I. Kaya ¹⁶⁴, S. Kazakos ¹⁰⁹, V.F. Kazanin ³⁸, J.M. Keaveney ^{34a}, R. Keeler ¹⁷¹, G.V. Kehris ⁶¹, J.S. Keller ³⁵, J.M. Kelly ¹⁷¹, J.J. Kempster ¹⁵², O. Kepka ¹³⁴, J. Kerr ^{162b}, B.P. Kerridge ¹³⁷, B.P. Kerševan ⁹⁵, L. Keszeghova ^{29a}, R.A. Khan ¹³², A. Khanov ¹²⁴, A.G. Kharlamov ³⁸, T. Kharlamova ³⁸, E.E. Khoda ¹⁴², M. Kholodenko ^{133a}, T.J. Khoo ¹⁹, G. Khorauli ¹⁷², Y. Khoulaki ^{36a}, Y.A.R. Khwaira ¹³⁰, B. Kibirige ^{34h}, D. Kim ⁶, D.W. Kim ^{18b}, Y.K. Kim ⁴⁰, N. Kimura ⁹⁸, M.K. Kingston ⁵⁵, A. Kirchhoff ⁵⁵, C. Kirfel ²⁵, F. Kirfel ²⁵, J. Kirk ¹³⁷, A.E. Kiryunin ¹¹², S. Kita ¹⁶³, O. Kivernyk ²⁵, M. Klassen ¹⁶⁴, C. Klein ³⁵, L. Klein ¹⁷², M.H. Klein ⁴⁵, S.B. Klein ⁵⁶, U. Klein ⁹⁴, A. Klimentov ³⁰, T. Klioutchnikova ³⁷, P. Kluit ¹¹⁷, S. Kluth ¹¹², E. Kneringer ⁷⁹, T.M. Knight ¹⁶¹, A. Knue ⁴⁹, M. Kobel ⁵⁰, D. Kobylanskii ¹⁷⁵, S.F. Koch ¹²⁹, M. Kocian ¹⁴⁹, P. Kodyš ¹³⁶, D.M. Koeck ¹²⁶, T. Koffas ³⁵, O. Kolay ⁵⁰, I. Koletsou ⁴, T. Komarek ⁸⁷, K. Köneke ⁵⁵, A.X.Y. Kong ¹, T. Kono ¹²¹, N. Konstantinidis ⁹⁸, P. Kontaxakis ⁵⁶, B. Konya ¹⁰⁰, R. Kopeliansky ⁴², S. Koperny ^{86a}, K. Korcyl ⁸⁷, K. Kordas ^{158,d}, A. Korn ⁹⁸, S. Korn ⁵⁵, I. Korolkov ¹³, N. Korotkova ³⁸, B. Kortman ¹¹⁷, O. Kortner ¹¹², S. Kortner ¹¹², W.H. Kostecka ¹¹⁸, M. Kostov ^{29a}, V.V. Kostyukhin ¹⁴⁷, A. Kotskechagia ³⁷, A. Kotwal ⁵¹, A. Koulouris ³⁷, A. Kourkouveli-Charalampidi ^{73a,73b}, C. Kourkouvelis ⁹, E. Kourlitis ¹¹², O. Kovanda ¹²⁶, R. Kowalewski ¹⁷¹, W. Kozanecki ¹²⁶, A.S. Kozhin ³⁸, V.A. Kramarenko ³⁸, G. Kramberger ⁹⁵, P. Kramer ²⁵, M.W. Krasny ¹³⁰, A. Krasznahorkay ¹⁰⁵, A.C. Kraus ¹¹⁸, J.W. Kraus ¹⁷⁷, J.A. Kremer ⁴⁸, N.B. Krengel ¹⁴⁷, T. Kresse ⁵⁰, L. Kretschmann ¹⁷⁷, J. Kretzschmar ⁹⁴, P. Krieger ¹⁶¹, K. Krizka ²¹, K. Kroeninger ⁴⁹, H. Kroha ¹¹², J. Kroll ¹³⁴, J. Kroll ¹³¹, K.S. Krowpman ¹⁰⁹, U. Kruchonak ³⁹, H. Krüger ²⁵, N. Krumnack ⁸¹, M.C. Kruse ⁵¹, O. Kuchinskaja ³⁹, S. Kuday ^{3a}, S. Kuehn ³⁷, R. Kuesters ⁵⁴, T. Kuhl ⁴⁸, V. Kukhtin ³⁹, Y. Kulchitsky ³⁹, S. Kuleshov ^{140d,140b}, J. Kull ¹, E.V. Kumar ¹¹¹, M. Kumar ^{34h}, N. Kumari ⁴⁸, P. Kumari ^{162b}, A. Kupco ¹³⁴, A. Kupich ³⁸, O. Kuprash ⁵⁴, H. Kurashige ⁸⁵, L.L. Kurchaninov ^{162a}, O. Kurdysh ⁴, Y.A. Kurochkin ³⁸, A. Kurova ³⁸, M. Kuze ¹⁴¹, A.K. Kvam ¹⁰⁵, J. Kvita ¹²⁵, N.G. Kyriacou ¹⁴², C. Lacasta ¹⁶⁹, F. Lacava ^{75a,75b}, H. Lacker ¹⁹, D. Lacour ¹³⁰, N.N. Lad ⁹⁸, E. Ladygin ³⁹, A. Lafarge ⁴¹, B. Laforge ¹³⁰, T. Lagouri ¹⁷⁸, F.Z. Lahbabi ^{36a}, S. Lai ^{55,37}, W.S. Lai ⁹⁸, J.E. Lambert ¹⁷¹, S. Lammers ⁶⁸, W. Lampl ⁷, C. Lampoudis ^{158,d}, G. Lamprinoudis ¹⁰², A.N. Lancaster ¹¹⁸, E. Lançon ³⁰, U. Landgraf ⁵⁴, M.P.J. Landon ⁹⁶, V.S. Lang ⁵⁴, O.K.B. Langrekken ¹²⁸, A.J. Lankford ¹⁶⁵, F. Lanni ³⁷, K. Lantzsch ²⁵, A. Lanza ^{73a}, M. Lanzac Berrocal ¹⁶⁹, J.F. Laporte ¹³⁸, T. Lari ^{71a}, D. Larsen ¹⁷, L. Larson ¹¹, F. Lasagni Manghi ^{24b}, M. Lassnig ³⁷, S.D. Lawlor ¹⁴⁵, R. Lazaridou ¹⁶⁵, M. Lazzaroni ^{71a,71b}, E.T.T. Le ¹⁶⁵, H.D.M. Le ¹⁰⁹, E.M. Le Boulicaut ¹⁷⁸, L.T. Le Pottier ^{18a}, B. Leban ^{24b,24a}, F. Ledroit-Guillon ⁶⁰, T.F. Lee ^{162b}, L.L. Leeuw ^{34c}, M. Lefebvre ¹⁷¹, C. Leggett ^{18a}, G. Lehmann Miotto ³⁷, M. Leigh ⁵⁶, W.A. Light ¹⁰⁵, W. Leinonen ¹¹⁶, A. Leisos ^{158,u}, M.A.L. Leite ^{83c}, C.E. Leitgeb ¹⁹, R. Leitner ¹³⁶, K.J.C. Leney ⁴⁵, T. Lenz ²⁵, S. Leone ^{74a}, C. Leonidopoulos ⁵², A. Leopold ¹⁵⁰, J.H. Lepage Bourbonnais ³⁵, R. Les ¹⁰⁹, C.G. Lester ³³, M. Levchenko ³⁸, J. Levêque ⁴, L.J. Levinson ¹⁷⁵, G. Levrimi ^{24b,24a}, M.P. Lewicki ⁸⁷, C. Lewis ¹⁴², D.J. Lewis ⁴, L. Lewitt ¹⁴⁵, A. Li ³⁰, B. Li ^{143a}, C. Li ¹⁰⁸, C-Q. Li ¹¹², H. Li ^{143a}, H. Li ¹⁰³, H. Li ¹⁵, H. Li ⁶², H. Li ^{143a}, J. Li ^{144a}, K. Li ¹⁴, L. Li ^{144a}, R. Li ¹⁷⁸, S. Li ^{14,114c}, S. Li ^{144b,144a}, T. Li ⁵, X. Li ¹⁰⁶, Y. Li ¹⁴, Z. Li ¹⁵⁹, Z. Li ^{14,114c}, Z. Li ⁶², S. Liang ^{14,114c}, Z. Liang ¹⁴, M. Liberatore ¹³⁸, B. Liberti ^{76a}, G.B. Libotte ^{83d}, K. Lie ^{64c}, J. Lieber Marin ^{83e}, H. Lien ⁶⁸, H. Lin ¹⁰⁸, S.F. Lin ¹⁵¹, L. Linden ¹¹¹, R.E. Lindley ⁷, J.H. Lindon ³⁷, J. Ling ⁶¹, E. Lipeles ¹³¹, A. Lipniacka ¹⁷, A. Lister ¹⁷⁰, J.D. Little ⁶⁸, B. Liu ¹⁴, B.X. Liu ^{114b}, D. Liu ^{144b,144a}, D. Liu ¹³⁹, E.H.L. Liu ²¹, J.K.K. Liu ¹²⁰, K. Liu ^{144b}, K. Liu ^{144b,144a}, M. Liu ⁶², M.Y. Liu ⁶², P. Liu ¹⁴,

Q. Liu ^{149,142,144a}, S. Liu ¹⁵¹, X. Liu ⁶², X. Liu ^{143a}, Y. Liu ^{114b,114c}, Y. Liu ¹⁶⁸, Y.L. Liu ^{143a}, Y.W. Liu ⁶², Z. Liu ^{66,k}, S.L. Lloyd ⁹⁶, E.M. Lobodzinska ⁴⁸, P. Loch ⁷, E. Lodhi ¹⁶¹, K. Lohwasser ¹⁴⁵, E. Loiacono ⁴⁸, J.D. Lomas ²¹, J.D. Long ⁴², I. Longarini ¹⁶⁵, R. Longo ¹⁶⁸, A. Lopez Solis ¹³, N.A. Lopez-canelas ⁷, N. Lorenzo Martinez ⁴, A.M. Lory ¹¹¹, M. Losada ^{119a}, G. Löschcke Centeno ⁴, X. Lou ^{47a,47b}, X. Lou ^{14,114c}, A. Lounis ⁶⁶, P.A. Love ⁹³, M. Lu ⁶⁶, S. Lu ¹³¹, Y.J. Lu ¹⁵⁴, H.J. Lubatti ¹⁴², C. Luci ^{75a,75b}, F.L. Lucio Alves ^{114a}, F. Luehring ⁶⁸, B.S. Lunday ¹³¹, O. Lundberg ¹⁵⁰, J. Lunde ³⁷, N.A. Luongo ⁶, M.S. Lutz ³⁷, A.B. Lux ²⁶, D. Lynn ³⁰, R. Lysak ¹³⁴, V. Lysenko ¹³⁵, E. Lytken ¹⁰⁰, V. Lyubushkin ³⁹, T. Lyubushkina ³⁹, M.M. Lyukova ¹⁵¹, M.Firdaus M. Soberi ⁵², H. Ma ³⁰, K. Ma ⁶², L.L. Ma ^{143a}, W. Ma ⁶², Y. Ma ¹²⁴, J.C. MacDonald ¹⁰², P.C. Machado De Abreu Farias ^{83e}, D. Macina ³⁷, R. Madar ⁴¹, T. Madula ⁹⁸, J. Maeda ⁸⁵, T. Maeno ³⁰, P.T. Mafa ^{34c,j}, H. Maguire ¹⁴⁵, M. Maheshwari ³³, V. Maiboroda ⁶⁶, A. Maio ^{133a,133b,133d}, K. Maj ^{86a}, O. Majersky ⁴⁸, S. Majewski ¹²⁶, R. Makhmanazarov ³⁸, N. Makovec ⁶⁶, V. Maksimovic ¹⁶, B. Malaescu ¹³⁰, J. Malamant ¹²⁸, Pa. Malecki ⁸⁷, V.P. Maleev ³⁸, F. Malek ^{60,o}, M. Mali ⁹⁵, D. Malito ⁹⁷, U. Mallik ^{80,*}, A. Maloizel ⁵, S. Maltezos ¹⁰, A. Malvezzi Lopes ^{83d}, S. Malyukov ³⁹, J. Mamuzic ⁹⁵, G. Mancini ⁵³, M.N. Mancini ²⁷, G. Manco ^{73a,73b}, J.P. Mandalia ⁹⁶, S.S. Mandarry ¹⁵², I. Mandić ⁹⁵, L. Manhaes de Andrade Filho ^{83a}, I.M. Maniatis ¹⁷⁵, J. Manjarres Ramos ⁹¹, D.C. Mankad ¹⁷⁵, A. Mann ¹¹¹, T. Manoussos ³⁷, M.N. Mantinan ⁴⁰, S. Manzoni ³⁷, L. Mao ^{144a}, X. Mapekula ^{34c}, A. Marantis ¹⁵⁸, R.R. Marcelo Gregorio ⁹⁶, G. Marchiori ⁵, C. Marcon ^{71a}, E. Maricic ¹⁶, M. Marinescu ⁴⁸, S. Marium ⁴⁸, M. Marjanovic ¹²³, A. Markhoos ⁵⁴, M. Markovitch ⁶⁶, M.K. Maroun ¹⁰⁵, M.C. Marr ¹⁴⁸, G.T. Marsden ¹⁰³, E.J. Marshall ⁹³, Z. Marshall ^{18a}, S. Marti-Garcia ¹⁶⁹, J. Martin ⁹⁸, T.A. Martin ¹³⁷, V.J. Martin ⁵², B. Martin dit Latour ¹⁷, L. Martinelli ^{75a,75b}, M. Martinez ^{13,x}, P. Martinez Agullo ¹⁶⁹, V.I. Martinez Outschoorn ¹⁰⁵, P. Martinez Suarez ³⁷, S. Martin-Haugh ¹³⁷, G. Martinovicova ¹³⁶, V.S. Martoiu ^{28b}, A.C. Martyniuk ⁹⁸, A. Marzin ³⁷, D. Mascione ^{78a,78b}, L. Masetti ¹⁰², J. Masik ¹⁰³, A.L. Maslennikov ³⁹, S.L. Mason ⁴², P. Massarotti ^{72a,72b}, P. Mastrandrea ^{74a,74b}, A. Mastroberardino ^{44b,44a}, T. Masubuchi ¹²⁷, T.T. Mathew ¹²⁶, J. Matousek ¹³⁶, D.M. Mattern ⁴⁹, J. Maurer ^{28b}, T. Maurin ⁵⁹, A.J. Maury ⁶⁶, B. Maček ⁹⁵, C. Mavungu Tsava ¹⁰⁴, D.A. Maximov ³⁸, A.E. May ¹⁰³, E. Mayer ⁴¹, R. Mazini ^{34h}, I. Maznas ¹¹⁸, S.M. Mazza ¹³⁹, E. Mazzeo ³⁷, J.P. Mc Gowan ¹⁷¹, S.P. Mc Kee ¹⁰⁸, C.A. Mc Lean ⁶, C.C. McCracken ¹⁷⁰, E.F. McDonald ¹⁰⁷, A.E. McDougall ¹¹⁷, L.F. Mcelhinney ⁹³, J.A. Mcfayden ¹⁵², R.P. McGovern ¹³¹, R.P. McKenzie ^{34h}, T.C. McLachlan ⁴⁸, D.J. McLaughlin ⁹⁸, S.J. McMahon ¹³⁷, C.M. Mcpartland ⁹⁴, R.A. McPherson ^{171,ab}, S. Mehlhase ¹¹¹, A. Mehta ⁹⁴, D. Melini ¹⁶⁹, B.R. Mellado Garcia ^{34h}, A.H. Melo ⁵⁵, F. Meloni ⁴⁸, A.M. Mendes Jacques Da Costa ¹⁰³, L. Meng ⁹³, S. Menke ¹¹², M. Mentink ³⁷, E. Meoni ^{44b,44a}, G. Mercado ¹¹⁸, S. Merianos ¹⁵⁸, C. Merlassino ^{69a,69c}, C. Meroni ^{71a,71b}, J. Metcalfe ⁶, A.S. Mete ⁶, E. Meuser ¹⁰², C. Meyer ⁶⁸, J-P. Meyer ¹³⁸, Y. Miao ^{114a}, R.P. Middleton ¹³⁷, M. Mihovilovic ⁶⁶, L. Mijović ⁵², G. Mikenberg ¹⁷⁵, M. Mikestikova ¹³⁴, M. Mikuž ⁹⁵, H. Mildner ¹⁰², A. Milic ³⁷, D.W. Miller ⁴⁰, E.H. Miller ¹⁴⁹, A. Milov ¹⁷⁵, D.A. Milstead ^{47a,47b}, T. Min ^{114a}, A.A. Minaenko ³⁸, I.A. Minashvili ^{155b}, A.I. Mincer ¹²⁰, B. Mindur ^{86a}, M. Mineev ³⁹, Y. Mino ⁸⁹, L.M. Mir ¹³, M. Miralles Lopez ⁵⁹, M. Mironova ^{18a}, M.C. Missio ⁴¹, A. Mitra ¹⁷³, V.A. Mitsou ¹⁶⁹, Y. Mitsumori ¹¹³, O. Miu ¹⁶¹, P.S. Miyagawa ⁹⁶, T. Mkrtchyan ³⁷, M. Mlinarevic ⁹⁸, T. Mlinarevic ⁹⁸, M. Mlynarikova ¹³⁶, L. Mlynarska ^{86a}, C. Mo ^{144a}, S. Mobius ²⁰, M.H. Mohamed Farook ¹¹⁵, S. Mohapatra ⁴², S. Mohiuddin ¹²⁴, G. Mokgatitswane ^{34h}, L. Moleri ¹⁷⁵, U. Molinatti ¹²⁹, L.G. Mollier ²⁰, B. Mondal ¹³⁴, S. Mondal ¹³⁵, K. Mönig ⁴⁸, E. Monnier ¹⁰⁴, L. Monsonis Romero ¹⁶⁹, J. Montejo Berlingen ¹³, A. Montella ^{47a,47b}, M. Montella ¹²², F. Montereali ^{77a,77b}, F. Monticelli ⁹², S. Monzani ^{69a,69c}, A. Morancho Tarda ⁴³,

N. Morange ⁶⁶, A.L. Moreira De Carvalho ⁴⁸, M. Moreno Llácer ¹⁶⁹, C. Moreno Martinez ⁵⁶,
 J.M. Moreno Perez ^{23b}, P. Morettini ^{57b}, S. Morgenstern ³⁷, M. Morii ⁶¹, M. Morinaga ¹⁵⁹,
 M. Moritsu ⁹⁰, F. Morodei ^{75a,75b}, P. Moschovakos ³⁷, B. Moser ⁵⁴, M. Mosidze ^{155b},
 T. Moskalets ⁴⁵, P. Moskvitina ¹¹⁶, J. Moss ³², P. Moszkowicz ^{86a}, A. Moussa ^{36d}, Y. Moyal ¹⁷⁵,
 H. Moyano Gomez ¹³, E.J.W. Moyse ¹⁰⁵, T.G. Mroz ⁸⁷, O. Mtintsilana ^{34h}, S. Muanza ¹⁰⁴,
 M. Mucha ²⁵, J. Mueller ¹³², R. Müller ³⁷, G.A. Mullier ¹⁶⁷, A.J. Mullin ³³, J.J. Mullin ⁵¹,
 A.C. Mullins ⁴⁵, A.E. Mulski ⁶¹, D.P. Mungo ¹⁶¹, D. Munoz Perez ¹⁶⁹, F.J. Munoz Sanchez ¹⁰³,
 W.J. Murray ^{173,137}, M. Muškinja ⁹⁵, C. Mwewa ⁴⁸, A.G. Myagkov ^{38,a}, A.J. Myers ⁸,
 G. Myers ¹⁰⁸, M. Myska ¹³⁵, B.P. Nachman ¹⁴⁹, K. Nagai ¹²⁹, K. Nagano ⁸⁴, R. Nagasaka ¹⁵⁹,
 J.L. Nagle ^{30,al}, E. Nagy ¹⁰⁴, A.M. Nairz ³⁷, Y. Nakahama ⁸⁴, K. Nakamura ⁸⁴, K. Nakkalil ⁵,
 A. Nandi ^{63b}, H. Nanjo ¹²⁷, E.A. Narayanan ⁴⁵, Y. Narukawa ¹⁵⁹, I. Naryshkin ³⁸,
 L. Nasella ^{71a,71b}, S. Nasri ^{119b}, C. Nass ²⁵, G. Navarro ^{23a}, A. Nayaz ¹⁹, P.Y. Nechaeva ³⁸,
 S. Nechaeva ^{24b,24a}, F. Nechansky ¹³⁴, L. Nedic ¹²⁹, T.J. Neep ²¹, A. Negri ^{73a,73b},
 M. Negrini ^{24b}, C. Nellist ¹¹⁷, C. Nelson ¹⁰⁶, K. Nelson ¹⁰⁸, S. Nemecek ¹³⁴, M. Nessi ^{37,g},
 M.S. Neubauer ¹⁶⁸, J. Newell ⁹⁴, P.R. Newman ²¹, Y.W.Y. Ng ¹⁶⁸, B. Ngair ^{119a},
 H.D.N. Nguyen ¹¹⁰, J.D. Nichols ¹²³, R.B. Nickerson ¹²⁹, R. Nicolaidou ¹³⁸, J. Nielsen ¹³⁹,
 M. Niemeyer ⁵⁵, J. Niermann ³⁷, N. Nikiforou ³⁷, V. Nikolaenko ^{38,a}, I. Nikolic-Audit ¹³⁰,
 P. Nilsson ³⁰, I. Ninca ⁴⁸, G. Ninio ¹⁵⁷, A. Nisati ^{75a}, R. Nisius ¹¹², N. Nitika ¹⁷⁵,
 J-E. Nitschke ⁵⁰, E.K. Nkadimeng ^{34b}, T. Nobe ¹⁵⁹, D. Noll ^{18a}, T. Nommensen ¹⁵³,
 M.B. Norfolk ¹⁴⁵, B.J. Norman ³⁵, L.C. Nosler ^{18a}, M. Noury ^{36a}, J. Novak ⁹⁵, T. Novak ⁹⁵,
 R. Novotny ¹³⁵, L. Nozka ¹²⁵, K. Ntekas ¹⁶⁵, D. Ntounis ¹⁴⁹, N.M.J. Nunes De Moura Junior ^{83b},
 J. Ocariz ¹³⁰, I. Ochoa ^{133a}, S. Oerdek ^{48,y}, J.T. Offermann ⁴⁰, A. Ogrodnik ⁸⁷, A. Oh ¹⁰³,
 C.C. Ohm ¹⁵⁰, H. Oide ⁸⁴, M.L. Ojeda ³⁷, Y. Okumura ¹⁵⁹, L.F. Oleiro Seabra ^{133a},
 I. Oleksiyuk ⁵⁶, G. Oliveira Correa ¹³, D. Oliveira Damazio ³⁰, J.L. Oliver ¹⁶⁵, R. Omar ⁶⁸,
 Ö.O. Öncel ⁵⁴, A.P. O'Neill ²⁰, A. Onofre ^{133a,133e,e}, P.U.E. Onyisi ¹¹, M.J. Oreglia ⁴⁰,
 D. Orestano ^{77a,77b}, R. Orlandini ^{77a,77b}, R.S. Orr ¹⁶¹, L.M. Osojnak ⁴², Y. Osumi ¹¹³,
 G. Otero y Garzon ³¹, H. Otono ⁹⁰, M. Ouchrif ^{36d}, F. Ould-Saada ¹²⁸, T. Ovsiannikova ¹⁴²,
 M. Owen ⁵⁹, R.E. Owen ¹³⁷, V.E. Ozcan ^{22a}, F. Ozturk ⁸⁷, N. Ozturk ⁸, S. Ozturk ⁸²,
 H.A. Pacey ¹²⁹, K. Pachal ^{162a}, A. Pacheco Pages ¹³, C. Padilla Aranda ¹³, G. Padovano ^{75a,75b},
 S. Pagan Griso ^{18a}, G. Palacino ⁶⁸, A. Palazzo ^{70a,70b}, J. Pampel ²⁵, J. Pan ¹⁷⁸, T. Pan ^{64a},
 D.K. Panchal ¹¹, C.E. Pandini ⁶⁰, J.G. Panduro Vazquez ¹³⁷, H.D. Pandya ¹, H. Pang ¹³⁸,
 P. Pani ⁴⁸, G. Panizzo ^{69a,69c}, L. Panwar ¹³⁰, L. Paolozzi ⁵⁶, S. Parajuli ¹⁶⁸, A. Paramonov ⁶,
 C. Paraskevopoulos ⁵³, D. Paredes Hernandez ^{64b}, S.R. Paredes Saenz ⁵², A. Pareti ^{73a,73b},
 K.R. Park ⁴², T.H. Park ¹¹², F. Parodi ^{57b,57a}, J.A. Parsons ⁴², U. Parzefall ⁵⁴, B. Pascual Dias ⁴¹,
 L. Pascual Dominguez ¹⁰¹, E. Pasqualucci ^{75a}, S. Passaggio ^{57b}, F. Pastore ⁹⁷, P. Patel ⁸⁷,
 U.M. Patel ⁵¹, J.R. Pater ¹⁰³, T. Pauly ³⁷, F. Pauwels ¹³⁶, C.I. Pazos ¹⁶⁴, M. Pedersen ¹²⁸,
 R. Pedro ^{133a}, S.V. Peleganchuk ³⁸, O. Penc ¹³⁴, S. Peng ¹⁵, G.D. Penn ¹⁷⁸, K.E. Penski ¹¹¹,
 M. Penzin ³⁸, B.S. Peralva ^{83d}, A.P. Pereira Peixoto ¹⁴², L. Pereira Sanchez ¹⁴⁹,
 D.V. Perepelitsa ^{30,al}, G. Perera ¹⁰⁵, E. Perez Codina ³⁷, M. Perganti ¹⁰, H. Pernegger ³⁷,
 S. Perrella ^{75a,75b}, K. Peters ⁴⁸, R.F.Y. Peters ¹⁰³, B.A. Petersen ³⁷, T.C. Petersen ⁴³, E. Petit ¹⁰⁴,
 V. Petousis ¹³⁵, A.R. Petri ^{71a,71b}, C. Petridou ^{158,d}, T. Petru ¹³⁶, A. Petrukhin ¹⁴⁷, M. Pettee ^{18a},
 A. Petukhov ⁸², K. Petukhova ³⁷, R. Pezoa ^{140g}, L. Pezzotti ^{24b,24a}, G. Pezzullo ¹⁷⁸,
 L. Pfaffenbichler ³⁷, A.J. Pflieger ⁷⁹, T.M. Pham ¹⁷⁶, T. Pham ¹⁰⁷, P.W. Phillips ¹³⁷,
 G. Piacquadio ¹⁵¹, E. Pianori ^{18a}, F. Piazza ¹²⁶, R. Piegaia ³¹, D. Pietreanu ^{28b},
 A.D. Pilkington ¹⁰³, M. Pinamonti ^{69a,69c}, J.L. Pinfold ², G. Pinheiro Matos ⁴²,
 B.C. Pinheiro Pereira ^{133a}, J. Pinol Bel ¹³, A.E. Pinto Pinoargote ¹³⁰, L. Pintucci ^{69a,69c},
 K.M. Piper ¹⁵², A. Pirttikoski ⁵⁶, D.A. Pizzi ³⁵, L. Pizzimento ^{64b}, A. Plebani ³³,

M.-A. Pleier ^{id30}, V. Pleskot ^{id136}, E. Plotnikova³⁹, G. Poddar ^{id96}, R. Poettgen ^{id100}, L. Poggioli ^{id130},
S. Polacek ^{id136}, G. Polesello ^{id73a}, A. Poley ^{id148}, A. Polini ^{id24b}, C.S. Pollard ^{id173}, Z.B. Pollock ^{id122},
E. Pompa Pacchi ^{id123}, N.I. Pond ^{id98}, D. Ponomarenko ^{id68}, L. Pontecorvo ^{id37}, S. Popa ^{id28a},
G.A. Popeneciu ^{id28d}, A. Poreba ^{id37}, D.M. Portillo Quintero ^{id162a}, S. Pospisil ^{id135}, M.A. Postill ^{id145},
P. Postolache ^{id28c}, K. Potamianos ^{id173}, P.A. Potepa ^{id86a}, I.N. Potrap ^{id39}, C.J. Potter ^{id33}, H. Potti ^{id153},
J. Poveda ^{id169}, M.E. Pozo Astigarraga ^{id37}, R. Pozzi ^{id37}, A. Prades Ibanez ^{id76a,76b}, S.R. Pradhan ^{id145},
J. Pretel ^{id171}, D. Price ^{id103}, M. Primavera ^{id70a}, L. Primomo ^{id69a,69c}, M.A. Principe Martin ^{id101},
R. Privara ^{id125}, T. Procter ^{id86b}, M.L. Proffitt ^{id142}, N. Proklova ^{id131}, K. Prokofiev ^{id64c}, G. Proto ^{id112},
J. Proudfoot ^{id6}, M. Przybycien ^{id86a}, W.W. Przygoda ^{id86b}, A. Psallidas ^{id46}, J.E. Puddefoot ^{id145},
D. Pudzha ^{id53}, H.I. Purnell ^{id1}, D. Pyatiizbyantseva ^{id116}, J. Qian ^{id108}, R. Qian ^{id109}, D. Qichen ^{id129},
Y. Qin ^{id13}, T. Qiu ^{id52}, A. Quadt ^{id55}, M. Queitsch-Maitland ^{id103}, G. Quetant ^{id56}, R.P. Quinn ^{id170},
G. Rabanal Bolanos ^{id61}, D. Rafanoharana ^{id112}, F. Raffaeli ^{id76a,76b}, F. Ragusa ^{id71a,71b},
J.L. Rainbolt ^{id40}, S. Rajagopalan ^{id30}, E. Ramakoti ^{id39}, L. Rambelli ^{id57b,57a}, I.A. Ramirez-Berend ^{id35},
K. Ran ^{id48,114c}, D.S. Rankin ^{id131}, N.P. Rapheeha ^{id34h}, H. Rasheed ^{id28b}, D.F. Rassloff ^{id63a},
A. Rastogi ^{id18a}, S. Rave ^{id102}, S. Ravera ^{id57b,57a}, B. Ravina ^{id37}, I. Ravinovich ^{id175}, M. Raymond ^{id37},
A.L. Read ^{id128}, N.P. Readioff ^{id145}, D.M. Rebuzzi ^{id73a,73b}, A.S. Reed ^{id59}, K. Reeves ^{id27},
J.A. Reidelsturz ^{id177}, D. Reikher ^{id37}, A. Rej ^{id49}, C. Rembser ^{id37}, H. Ren ^{id62}, M. Renda ^{id28b},
F. Renner ^{id48}, A.G. Rennie ^{id59}, A.L. Rescia ^{id57b,57a}, S. Resconi ^{id71a}, M. Ressegotti ^{id57b,57a},
S. Rettie ^{id117}, W.F. Rettie ^{id35}, M.M. Revering ^{id33}, E. Reynolds ^{id18a}, O.L. Rezanova ^{id39},
P. Reznicek ^{id136}, H. Riani ^{id36d}, N. Ribaric ^{id51}, B. Ricci ^{id69a,69c}, E. Ricci ^{id78a,78b}, R. Richter ^{id112},
S. Richter ^{id47a,47b}, E. Richter-Was ^{id86b}, M. Ridel ^{id130}, S. Ridouani ^{id36d}, P. Rieck ^{id120}, P. Riedler ^{id37},
E.M. Riefel ^{id47a,47b}, J.O. Rieger ^{id117}, M. Rijssenbeek ^{id151}, M. Rimoldi ^{id37}, L. Rinaldi ^{id24b,24a},
P. Rincke ^{id167,55}, G. Ripellino ^{id167}, I. Riu ^{id13}, J.C. Rivera Vergara ^{id171}, F. Rizatdinova ^{id124},
E. Rizvi ^{id96}, B.R. Roberts ^{id18a}, S.S. Roberts ^{id139}, D. Robinson ^{id33}, M. Robles Manzano ^{id102},
A. Robson ^{id59}, A. Rocchi ^{id76a,76b}, C. Roda ^{id74a,74b}, S. Rodriguez Bosca ^{id37}, Y. Rodriguez Garcia ^{id23a},
A.M. Rodríguez Vera ^{id118}, S. Roe³⁷, J.T. Roemer ^{id37}, O. Røhne ^{id128}, R.A. Rojas ^{id37},
C.P.A. Roland ^{id130}, A. Romaniouk ^{id79}, E. Romano ^{id73a,73b}, M. Romano ^{id24b},
A.C. Romero Hernandez ^{id168}, N. Rompotis ^{id94}, L. Roos ^{id130}, S. Rosati ^{id75a}, B.J. Rosser ^{id40},
E. Rossi ^{id129}, E. Rossi ^{id72a,72b}, L.P. Rossi ^{id61}, L. Rossini ^{id54}, R. Rosten ^{id122}, M. Rotaru ^{id28b},
B. Rottler ^{id54}, D. Rousseau ^{id66}, D. Rouso ^{id48}, S. Roy-Garand ^{id161}, A. Rozanov ^{id104},
Z.M.A. Rozario ^{id59}, Y. Rozen ^{id156}, A. Rubio Jimenez ^{id169}, V.H. Ruelas Rivera ^{id19}, T.A. Ruggeri ^{id1},
A. Ruggiero ^{id129}, A. Ruiz-Martinez ^{id169}, A. Rummler ^{id37}, Z. Rurikova ^{id54}, N.A. Rusakovich ^{id39},
S. Ruscelli ^{id49}, H.L. Russell ^{id171}, G. Russo ^{id75a,75b}, J.P. Rutherford ^{id7}, S. Rutherford Colmenares ^{id33},
M. Rybar ^{id136}, P. Rybczynski ^{id86a}, A. Ryzhov ^{id45}, J.A. Sabater Iglesias ^{id56}, H.F.W. Sadrozinski ^{id139},
F. Safai Tehrani ^{id75a}, S. Saha ^{id1}, M. Sahinsoy ^{id82}, B. Sahoo ^{id175}, A. Saibel ^{id169}, B.T. Saifuddin ^{id123},
M. Saimpert ^{id138}, G.T. Saito ^{id83c}, M. Saito ^{id159}, T. Saito ^{id159}, A. Sala ^{id71a,71b}, A. Salnikov ^{id149},
J. Salt ^{id169}, A. Salvador Salas ^{id157}, F. Salvatore ^{id152}, A. Salzburger ^{id37}, D. Sammel ^{id54},
E. Sampson ^{id93}, D. Sampsonidis ^{id158,d}, D. Sampsonidou ^{id126}, M.A.A. Samy ^{id59}, J. Sánchez ^{id169},
V. Sanchez Sebastian ^{id169}, H. Sandaker ^{id128}, C.O. Sander ^{id48}, J.A. Sandesara ^{id176}, M. Sandhoff ^{id177},
C. Sandoval ^{id23b}, L. Sanfilippo ^{id63a}, D.P.C. Sankey ^{id137}, T. Sano ^{id89}, A. Sansoni ^{id53},
M. Santana Queiroz ^{id18b}, L. Santi ^{id37}, C. Santoni ^{id41}, H. Santos ^{id133a,133b}, A. Santra ^{id175},
E. Sanzani ^{id24b,24a}, K.A. Saoucha ^{id88b}, J.G. Saraiva ^{id133a,133d}, J. Sardain ^{id7}, O. Sasaki ^{id84},
K. Sato ^{id163}, C. Sauer³⁷, E. Sauvan ^{id4}, P. Savard ^{id161,ai}, R. Sawada ^{id159}, C. Sawyer ^{id137},
L. Sawyer ^{id99}, C. Sbarra ^{id24b}, A. Sbrizzi ^{id24b,24a}, T. Scanlon ^{id98}, J. Schaarschmidt ^{id142},
U. Schäfer ^{id102}, A.C. Schaffer ^{id66,45}, D. Schaile ^{id111}, R.D. Schamberger ^{id151}, C. Scharf ^{id19},
M.M. Schefer ^{id20}, V.A. Schegelsky ^{id38}, D. Scheirich ^{id136}, M. Schernau ^{id140f}, C. Scheulen ^{id56},
C. Schiavi ^{id57b,57a}, M. Schioppa ^{id44b,44a}, B. Schlag ^{id149}, S. Schlenker ^{id37}, J. Schmeing ^{id177},

E. Schmidt ¹¹², M.A. Schmidt ¹⁷⁷, K. Schmieden ¹⁰², C. Schmitt ¹⁰², N. Schmitt ¹⁰²,
 S. Schmitt ⁴⁸, N.A. Schneider ¹¹¹, L. Schoeffel ¹³⁸, A. Schoening ^{63b}, P.G. Scholer ³⁵,
 E. Schopf ¹⁴⁷, M. Schott ²⁵, S. Schramm ⁵⁶, T. Schroer ⁵⁶, H-C. Schultz-Coulon ^{63a},
 M. Schumacher ⁵⁴, B.A. Schumm ¹³⁹, Ph. Schune ¹³⁸, H.R. Schwartz ⁷, A. Schwartzman ¹⁴⁹,
 T.A. Schwarz ¹⁰⁸, Ph. Schwemling ¹³⁸, R. Schwienhorst ¹⁰⁹, F.G. Sciacca ²⁰, A. Sciandra ³⁰,
 G. Sciolla ²⁷, F. Scuri ^{74a}, C.D. Sebastiani ³⁷, K. Sedlaczek ¹¹⁸, S.C. Seidel ¹¹⁵, A. Seiden ¹³⁹,
 B.D. Seidlitz ⁴², C. Seitz ⁴⁸, J.M. Seixas ^{83b}, G. Sekhniaidze ^{72a}, L. Selem ⁶⁰,
 N. Semprini-Cesari ^{24b,24a}, A. Semushin ¹⁷⁹, D. Sengupta ⁵⁶, V. Senthilkumar ¹⁶⁹, L. Serin ⁶⁶,
 M. Sessa ^{72a,72b}, H. Severini ¹²³, F. Sforza ^{57b,57a}, A. Sfyrly ⁵⁶, Q. Sha ¹⁴, E. Shabalina ⁵⁵,
 H. Shaddix ¹¹⁸, A.H. Shah ³³, R. Shaheen ¹⁵⁰, J.D. Shahinian ¹³¹, M. Shamim ³⁷, L.Y. Shan ¹⁴,
 M. Shapiro ^{18a}, A. Sharma ³⁷, A.S. Sharma ¹⁷⁰, P. Sharma ³⁰, P.B. Shatalov ³⁸, K. Shaw ¹⁵²,
 S.M. Shaw ¹⁰³, Q. Shen ^{144a}, D.J. Sheppard ¹⁴⁸, P. Sherwood ⁹⁸, L. Shi ⁹⁸, X. Shi ¹⁴,
 S. Shimizu ⁸⁴, C.O. Shimmin ¹⁷⁸, I.P.J. Shipsey ^{129,*}, S. Shirabe ⁹⁰, M. Shiyakova ^{39,z},
 M.J. Shochet ⁴⁰, D.R. Shope ¹²⁸, B. Shrestha ¹²³, S. Shrestha ^{122,an}, I. Shreyber ³⁹,
 M.J. Shroff ¹⁷¹, P. Sicho ¹³⁴, A.M. Sickles ¹⁶⁸, E. Sideras Haddad ^{34h,166}, A.C. Sidley ¹¹⁷,
 A. Sidoti ^{24b}, F. Siegert ⁵⁰, Dj. Sijacki ¹⁶, F. Sili ⁶², J.M. Silva ⁵², I. Silva Ferreira ^{83b},
 M.V. Silva Oliveira ³⁰, S.B. Silverstein ^{47a}, S. Simion ⁶⁶, R. Simoniello ³⁷, E.L. Simpson ¹⁰³,
 H. Simpson ¹⁵², L.R. Simpson ⁶, S. Simsek ⁸², S. Sindhu ⁵⁵, P. Sinervo ¹⁶¹, S.N. Singh ²⁷,
 S. Singh ³⁰, S. Sinha ⁴⁸, S. Sinha ¹⁰³, M. Sioli ^{24b,24a}, K. Sioulas ⁹, I. Siral ³⁷, E. Sitnikova ⁴⁸,
 J. Sjölin ^{47a,47b}, A. Skaf ⁵⁵, E. Skorda ²¹, P. Skubic ¹²³, M. Slawinska ⁸⁷, I. Slazyk ¹⁷,
 I. Sliusar ¹²⁸, V. Smakhtin ¹⁷⁵, B.H. Smart ¹³⁷, S.Yu. Smirnov ^{140b}, Y. Smirnov ⁸²,
 L.N. Smirnova ^{38,a}, O. Smirnova ¹⁰⁰, A.C. Smith ⁴², D.R. Smith ¹⁶⁵, J.L. Smith ¹⁰³,
 M.B. Smith ³⁵, R. Smith ¹⁴⁹, H. Smitmanns ¹⁰², M. Smizanska ⁹³, K. Smolek ¹³⁵,
 P. Smolyanskiy ¹³⁵, A.A. Snesarev ³⁹, H.L. Snoek ¹¹⁷, S. Snyder ³⁰, R. Sobie ^{171,ab},
 A. Soffer ¹⁵⁷, C.A. Solans Sanchez ³⁷, E.Yu. Soldatov ³⁹, U. Soldevila ¹⁶⁹, A.A. Solodkov ^{34h},
 S. Solomon ²⁷, A. Soloshenko ³⁹, K. Solovieva ⁵⁴, O.V. Solovyanov ⁴¹, P. Sommer ⁵⁰,
 A. Sonay ¹³, A. Sopczak ¹³⁵, A.L. Sopio ⁵², F. Sopkova ^{29b}, J.D. Sorenson ¹¹⁵,
 I.R. Sotarriva Alvarez ¹⁴¹, V. Sothilingam ^{63a}, O.J. Soto Sandoval ^{140c,140b}, S. Sottocornola ⁶⁸,
 R. Soualah ^{88a}, Z. Soumami ^{36e}, D. South ⁴⁸, N. Soybelman ¹⁷⁵, S. Spagnolo ^{70a,70b},
 M. Spalla ¹¹², D. Sperlich ⁵⁴, B. Spisso ^{72a,72b}, D.P. Spiteri ⁵⁹, L. Splendori ¹⁰⁴, M. Spousta ¹³⁶,
 E.J. Staats ³⁵, R. Stamen ^{63a}, E. Stanecka ⁸⁷, W. Stanek-Maslouska ⁴⁸, M.V. Stange ⁵⁰,
 B. Stanislaus ^{18a}, M.M. Stanitzki ⁴⁸, B. Stapf ⁴⁸, E.A. Starchenko ³⁸, G.H. Stark ¹³⁹, J. Stark ⁹¹,
 P. Staroba ¹³⁴, P. Starovoitov ^{88b}, R. Staszewski ⁸⁷, C. Stauch ¹¹¹, G. Stavropoulos ⁴⁶,
 A. Stefl ³⁷, A. Stein ¹⁰², P. Steinberg ³⁰, B. Stelzer ^{148,162a}, H.J. Stelzer ¹³², O. Stelzer ^{162a},
 H. Stenzel ⁵⁸, T.J. Stevenson ¹⁵², G.A. Stewart ³⁷, J.R. Stewart ¹²⁴, G. Stoica ^{28b},
 M. Stolarski ^{133a}, S. Stonjek ¹¹², A. Straessner ⁵⁰, J. Strandberg ¹⁵⁰, S. Strandberg ^{47a,47b},
 M. Stratmann ¹⁷⁷, M. Strauss ¹²³, T. Streblor ¹⁰⁴, P. Strizenec ^{29b}, R. Ströhmer ¹⁷²,
 D.M. Strom ¹²⁶, R. Stroynowski ⁴⁵, A. Strubig ^{47a,47b}, S.A. Stucci ³⁰, B. Stugu ¹⁷, J. Stupak ¹²³,
 N.A. Styles ⁴⁸, D. Su ¹⁴⁹, S. Su ⁶², X. Su ⁶², D. Suchy ^{29a}, A.D. Sudhakar Ponnu ⁵⁵,
 K. Sugizaki ¹³¹, V.V. Sulin ³⁸, D.M.S. Sultan ¹²⁹, L. Sultanaliyeva ²⁵, S. Sultansoy ^{3b},
 S. Sun ¹⁷⁶, W. Sun ¹⁴, N. Sur ¹⁰⁰, M.R. Sutton ¹⁵², M. Svatos ¹³⁴, P.N. Swallow ³³,
 M. Swiatlowski ^{162a}, T. Swirski ¹⁷², A. Swoboda ³⁷, I. Sykora ^{29a}, M. Sykora ¹³⁶, T. Sykora ¹³⁶,
 D. Ta ¹⁰², K. Tackmann ^{48,y}, A. Taffard ¹⁶⁵, R. Tahirout ^{162a}, Y. Takubo ⁸⁴, M. Talby ¹⁰⁴,
 A.A. Talyshev ³⁸, K.C. Tam ^{64b}, N.M. Tamir ¹⁵⁷, A. Tanaka ¹⁵⁹, J. Tanaka ¹⁵⁹, R. Tanaka ⁶⁶,
 M. Tanasini ¹⁵¹, Z. Tao ¹⁷⁰, S. Tapia Araya ^{140g}, S. Tapprogge ¹⁰²,
 A. Tarek Abouelfadl Mohamed ³⁷, S. Tarem ¹⁵⁶, K. Tariq ¹⁴, G. Tarna ³⁷, G.F. Tartarelli ^{71a},
 M.J. Tartarin ⁹¹, P. Tas ¹³⁶, M. Tasevsky ¹³⁴, E. Tassi ^{44b,44a}, A.C. Tate ¹⁶⁸, Y. Tayalati ^{36e,aa},

G.N. Taylor ¹⁰⁷, W. Taylor ^{162b}, R.J. Taylor Vara ¹⁶⁹, A.S. Tegetmeier ⁹¹, P. Teixeira-Dias ⁹⁷, J.J. Teoh ¹⁶¹, K. Terashi ¹⁵⁹, J. Terron ¹⁰¹, S. Terzo ¹³, M. Testa ⁵³, R.J. Teuscher ^{161,ab}, A. Thaler ⁷⁹, O. Theiner ⁵⁶, T. Theveneaux-Pelzer ¹⁰⁴, D.W. Thomas ⁹⁷, J.P. Thomas ²¹, E.A. Thompson ^{18a}, P.D. Thompson ²¹, E. Thomson ¹³¹, R.E. Thornberry ⁴⁵, C. Tian ⁶², Y. Tian ⁵⁶, V. Tikhomirov ⁸², Yu.A. Tikhonov ³⁹, S. Timoshenko ³⁸, D. Timoshyn ¹³⁶, E.X.L. Ting ¹, P. Tipton ¹⁷⁸, A. Tishelman-Charny ³⁰, K. Todome ¹⁴¹, S. Todorova-Nova ¹³⁶, L. Toffolin ^{69a,69c}, M. Togawa ⁸⁴, J. Tojo ⁹⁰, S. Tokár ^{29a}, O. Toldaiev ⁶⁸, G. Tolkachev ¹⁰⁴, M. Tomoto ⁸⁴, L. Tompkins ^{149,n}, E. Torrence ¹²⁶, H. Torres ⁹¹, D.I. Torres Arza ^{140g}, E. Torró Pastor ¹⁶⁹, M. Toscani ³¹, C. Toscirì ⁴⁰, M. Tost ¹¹, D.R. Tovey ¹⁴⁵, T. Trefzger ¹⁷², P.M. Tricarico ¹³, A. Tricoli ³⁰, I.M. Trigger ^{162a}, S. Trincaz-Duvoid ¹³⁰, D.A. Trischuk ²⁷, A. Tropina ³⁹, L. Truong ^{34c}, M. Trzebinski ⁸⁷, A. Trzupek ⁸⁷, F. Tsai ¹⁵¹, M. Tsai ¹⁰⁸, A. Tsiamis ¹⁵⁸, P.V. Tsiareshka ³⁹, S. Tsigaridas ^{162a}, A. Tsirigotis ^{158,u}, V. Tsiskaridze ^{155a}, E.G. Tskhadadze ^{155a}, Y. Tsujikawa ⁸⁹, I.I. Tsukerman ³⁸, V. Tsulaia ^{18a}, S. Tsuno ⁸⁴, K. Tsuru ¹²¹, D. Tsybychev ¹⁵¹, Y. Tu ^{64b}, A. Tudorache ^{28b}, V. Tudorache ^{28b}, S.B. Tuncay ¹²⁹, S. Turchikhin ^{57b,57a}, I. Turk Cakir ^{3a}, R. Turra ^{71a}, T. Turtuvshin ^{39,ac}, P.M. Tuts ⁴², S. Tzamarias ^{158,d}, Y. Uematsu ⁸⁴, F. Ukegawa ¹⁶³, P.A. Ulloa Poblete ^{140c,140b}, E.N. Umaka ³⁰, G. Unal ³⁷, A. Undrus ³⁰, G. Unel ¹⁶⁵, J. Urban ^{29b}, P. Urrejola ^{140e}, G. Usai ⁸, R. Ushioda ¹⁶⁰, M. Usman ¹¹⁰, F. Ustuner ⁵², Z. Uysal ⁸², V. Vacek ¹³⁵, B. Vachon ¹⁰⁶, T. Vafeiadis ³⁷, A. Vaitkus ⁹⁸, C. Valderanis ¹¹¹, E. Valdes Santurio ^{47a,47b}, M. Valente ³⁷, S. Valentinetti ^{24b,24a}, A. Valero ¹⁶⁹, E. Valiente Moreno ¹⁶⁹, A. Vallier ⁹¹, J.A. Valls Ferrer ¹⁶⁹, D.R. Van Arneeman ¹¹⁷, A. Van Der Graaf ⁴⁹, H.Z. Van Der Schyf ^{34h}, P. Van Gemmeren ⁶, M. Van Rijnbach ³⁷, S. Van Stroud ⁹⁸, I. Van Vulpen ¹¹⁷, P. Vana ¹³⁶, M. Vanadia ^{76a,76b}, U.M. Vande Voorde ¹⁵⁰, W. Vandelli ³⁷, E.R. Vandewall ¹²⁴, D. Vannicola ¹⁵⁷, L. Vannoli ⁵³, R. Vari ^{75a}, M. Varma ¹⁷⁸, E.W. Varnes ⁷, C. Varni ¹¹⁸, D. Varouchas ⁶⁶, L. Varriale ¹⁶⁹, K.E. Varvell ¹⁵³, M.E. Vasile ^{28b}, L. Vaslin ⁸⁴, M.D. Vassilev ¹⁴⁹, A. Vasyukov ³⁹, L.M. Vaughan ¹²⁴, R. Vavricka ¹³⁶, T. Vazquez Schroeder ¹³, J. Veatch ³², V. Vecchio ¹⁰³, M.J. Veen ¹⁰⁵, I. Veliscek ³⁰, I. Velkovska ⁹⁵, L.M. Veloce ¹⁶¹, F. Veloso ^{133a,133c}, S. Veneziano ^{75a}, A. Ventura ^{70a,70b}, A. Verbytskyi ¹¹², M. Verducci ^{74a,74b}, C. Vergis ⁹⁶, M. Verissimo De Araujo ^{83b}, W. Verkerke ¹¹⁷, J.C. Vermeulen ¹¹⁷, C. Vernieri ¹⁴⁹, M. Vessella ¹⁶⁵, M.C. Vetterli ^{148,ai}, A. Vgenopoulos ¹⁰², N. Viaux Maira ^{140g,af}, T. Vickey ¹⁴⁵, O.E. Vickey Boeriu ¹⁴⁵, G.H.A. Viehhauser ¹²⁹, L. Vigani ^{63b}, M. Vigl ¹¹², M. Villa ^{24b,24a}, M. Villaplana Perez ¹⁶⁹, E.M. Villhauer ⁴⁰, E. Vilucchi ⁵³, M. Vincent ¹⁶⁹, M.G. Vincter ³⁵, A. Visible ¹¹⁷, A. Visive ¹¹⁷, C. Vittori ³⁷, I. Vivarelli ^{24b,24a}, M.I. Vivas Albornoz ⁴⁸, E. Voevodina ¹¹², F. Vogel ¹¹¹, J.C. Voigt ⁵⁰, P. Vokac ¹³⁵, Yu. Volkotrub ^{86b}, L. Vomberg ²⁵, E. Von Toerne ²⁵, B. Vormwald ³⁷, K. Vorobev ⁵¹, M. Vos ¹⁶⁹, K. Voss ¹⁴⁷, M. Vozak ³⁷, L. Vozdecky ¹²³, N. Vranjes ¹⁶, M. Vranjes Milosavljevic ¹⁶, M. Vreeswijk ¹¹⁷, N.K. Vu ^{144b,144a}, R. Vuillermet ³⁷, O. Vujinovic ¹⁰², I. Vukotic ⁴⁰, I.K. Vyas ³⁵, J.F. Wack ³³, S. Wada ¹⁶³, C. Wagner ¹⁴⁹, J.M. Wagner ^{18a}, W. Wagner ¹⁷⁷, S. Wahdan ¹⁷⁷, H. Wahlberg ⁹², C.H. Waits ¹²³, J. Walder ¹³⁷, R. Walker ¹¹¹, K. Walkingshaw Pass ⁵⁹, W. Walkowiak ¹⁴⁷, A. Wall ¹³¹, E.J. Wallin ¹⁰⁰, T. Wamorkar ^{18a}, K. Wandall-Christensen ¹⁶⁹, A. Wang ⁶², A.Z. Wang ¹³⁹, C. Wang ¹⁰², C. Wang ¹¹, H. Wang ^{18a}, J. Wang ^{64c}, P. Wang ¹⁰³, P. Wang ⁹⁸, R. Wang ⁶¹, R. Wang ⁶, S.M. Wang ¹⁵⁴, S. Wang ¹⁴, T. Wang ¹¹⁶, T. Wang ⁶², W.T. Wang ¹²⁹, W. Wang ¹⁴, X. Wang ¹⁶⁸, X. Wang ^{144a}, X. Wang ⁴⁸, Y. Wang ^{114a}, Y. Wang ⁶², Z. Wang ¹⁰⁸, Z. Wang ^{144b}, Z. Wang ¹⁰⁸, Z. Wang ¹⁴, C. Wanotayaroj ⁸⁴, A. Warburton ¹⁰⁶, A.L. Warnerbring ¹⁴⁷, S. Waterhouse ⁹⁷, A.T. Watson ²¹, H. Watson ⁵², M.F. Watson ²¹, E. Watton ³⁷, G. Watts ¹⁴², B.M. Waugh ⁹⁸, J.M. Webb ⁵⁴, C. Weber ³⁰, H.A. Weber ¹⁹, M.S. Weber ²⁰, S.M. Weber ^{63a}, C. Wei ⁶², Y. Wei ⁵⁴, A.R. Weidberg ¹²⁹, E.J. Weik ¹²⁰,

J. Weingarten ⁴⁹, C. Weiser ⁵⁴, C.J. Wells ⁴⁸, T. Wenaus ³⁰, T. Wengler ³⁷, N.S. Wenke ¹¹², N. Wermes ²⁵, M. Wessels ^{63a}, A.M. Wharton ⁹³, A.S. White ⁶¹, A. White ⁸, M.J. White ¹, D. Whiteson ¹⁶⁵, L. Wickremasinghe ¹²⁷, W. Wiedenmann ¹⁷⁶, M. WIELERS ¹³⁷, R. Wierda ¹⁵⁰, C. Wiglesworth ⁴³, H.G. Wilkens ³⁷, J.J.H. Wilkinson ³³, D.M. Williams ⁴², H.H. Williams ¹³¹, S. Williams ³³, S. Willocq ¹⁰⁵, B.J. Wilson ¹⁰³, D.J. Wilson ¹⁰³, P.J. Windischhofer ⁴⁰, F.I. Winkel ³¹, F. Winklmeier ¹²⁶, B.T. Winter ⁵⁴, M. Wittgen ¹⁴⁹, M. Wobisch ⁹⁹, T. Wojtkowski ⁶⁰, Z. Wolfs ¹¹⁷, J. Wollrath ³⁷, M.W. Wolter ⁸⁷, H. Wolters ^{133a,133c}, M.C. Wong ¹³⁹, E.L. Woodward ⁴², S.D. Worm ⁴⁸, B.K. Wosiek ⁸⁷, K.W. Woźniak ⁸⁷, S. Wozniowski ⁵⁵, K. Wraight ⁵⁹, C. Wu ¹⁶¹, C. Wu ²¹, J. Wu ¹⁵⁹, M. Wu ^{114b}, M. Wu ¹¹⁶, S.L. Wu ¹⁷⁶, S. Wu ^{14,ak}, X. Wu ⁶², Y.Q. Wu ¹⁶¹, Y. Wu ⁶², Z. Wu ⁴, Z. Wu ^{114a}, J. Wuerzinger ¹¹², T.R. Wyatt ¹⁰³, B.M. Wynne ⁵², S. Xella ⁴³, L. Xia ^{114a}, M. Xie ⁶², A. Xiong ¹²⁶, D. Xu ¹⁴, H. Xu ⁶², L. Xu ⁶², R. Xu ¹³¹, T. Xu ¹⁰⁸, Y. Xu ¹⁴², Z. Xu ⁵², R. Xue ¹³², B. Yabsley ¹⁵³, S. Yacoob ^{34a}, Y. Yamaguchi ⁸⁴, E. Yamashita ¹⁵⁹, H. Yamauchi ¹⁶³, T. Yamazaki ^{18a}, Y. Yamazaki ⁸⁵, S. Yan ⁵⁹, Z. Yan ¹⁰⁵, H.J. Yang ^{144a,144b}, H.T. Yang ⁶², S. Yang ⁶², T. Yang ^{64c}, X. Yang ³⁷, X. Yang ¹⁴, Y. Yang ¹⁵⁹, Y. Yang ⁶², W-M. Yao ^{18a}, C.L. Yardley ¹⁵², J. Ye ¹⁴, S. Ye ³⁰, X. Ye ⁶², Y. Yeh ⁹⁸, I. Yeletsikh ³⁹, B. Yeo ^{18b}, M.R. Yexley ⁹⁸, T.P. Yildirim ¹²⁹, K. Yorita ¹⁷⁴, C.J.S. Young ³⁷, C. Young ¹⁴⁹, N.D. Young ¹²⁶, Y. Yu ⁶², J. Yuan ^{14,114c}, M. Yuan ¹⁰⁸, R. Yuan ^{144b,144a}, L. Yue ⁹⁸, M. Zaazoua ⁶², B. Zabinski ⁸⁷, I. Zahir ^{36a}, A. Zaio ^{57b,57a}, Z.K. Zak ⁸⁷, T. Zakareishvili ¹⁶⁹, S. Zambito ⁵⁶, J.A. Zamora Saa ^{140d}, J. Zang ¹⁵⁹, R. Zanzottera ^{71a,71b}, O. Zaplatilek ¹³⁵, C. Zeitnitz ¹⁷⁷, H. Zeng ¹⁴, J.C. Zeng ¹⁶⁸, D.T. Zenger Jr ²⁷, O. Zenin ³⁸, T. Ženiš ^{29a}, S. Zenz ⁹⁶, D. Zerwas ⁶⁶, M. Zhai ^{14,114c}, D.F. Zhang ¹⁴⁵, G. Zhang ^{14,ak}, J. Zhang ^{143a}, J. Zhang ⁶, K. Zhang ^{14,114c}, L. Zhang ⁶², L. Zhang ^{114a}, P. Zhang ^{14,114c}, R. Zhang ^{114a}, S. Zhang ⁹¹, T. Zhang ¹⁵⁹, Y. Zhang ¹⁴², Y. Zhang ⁹⁸, Y. Zhang ⁶², Y. Zhang ^{114a}, Z. Zhang ^{18a}, Z. Zhang ^{143a}, Z. Zhang ⁶⁶, H. Zhao ¹⁴², T. Zhao ^{143a}, Y. Zhao ³⁵, Z. Zhao ⁶², Z. Zhao ⁶², A. Zhemchugov ³⁹, J. Zheng ^{114a}, K. Zheng ¹⁶⁸, X. Zheng ⁶², Z. Zheng ¹⁴⁹, D. Zhong ¹⁶⁸, B. Zhou ¹⁰⁸, H. Zhou ⁷, N. Zhou ^{144a}, Y. Zhou ¹⁵, Y. Zhou ^{114a}, Y. Zhou ⁷, C.G. Zhu ^{143a}, J. Zhu ¹⁰⁸, X. Zhu ^{144b}, Y. Zhu ^{144a}, Y. Zhu ⁶², X. Zhuang ¹⁴, K. Zhukov ⁶⁸, N.I. Zimine ³⁹, J. Zinsser ^{63b}, M. Ziolkowski ¹⁴⁷, L. Živković ¹⁶, A. Zoccoli ^{24b,24a}, K. Zoch ⁶¹, A. Zografos ³⁷, T.G. Zorbas ¹⁴⁵, O. Zormpa ⁴⁶, L. Zwalinski ³⁷.

¹Department of Physics, University of Adelaide, Adelaide; Australia.

²Department of Physics, University of Alberta, Edmonton AB; Canada.

^{3(a)}Department of Physics, Ankara University, Ankara; ^(b)Division of Physics, TOBB University of Economics and Technology, Ankara; Türkiye.

⁴LAPP, Université Savoie Mont Blanc, CNRS/IN2P3, Annecy; France.

⁵APC, Université Paris Cité, CNRS/IN2P3, Paris; France.

⁶High Energy Physics Division, Argonne National Laboratory, Argonne IL; United States of America.

⁷Department of Physics, University of Arizona, Tucson AZ; United States of America.

⁸Department of Physics, University of Texas at Arlington, Arlington TX; United States of America.

⁹Physics Department, National and Kapodistrian University of Athens, Athens; Greece.

¹⁰Physics Department, National Technical University of Athens, Zografou; Greece.

¹¹Department of Physics, University of Texas at Austin, Austin TX; United States of America.

¹²Institute of Physics, Azerbaijan Academy of Sciences, Baku; Azerbaijan.

¹³Institut de Física d'Altes Energies (IFAE), Barcelona Institute of Science and Technology, Barcelona; Spain.

¹⁴Institute of High Energy Physics, Chinese Academy of Sciences, Beijing; China.

- ¹⁵Physics Department, Tsinghua University, Beijing; China.
- ¹⁶Institute of Physics, University of Belgrade, Belgrade; Serbia.
- ¹⁷Department for Physics and Technology, University of Bergen, Bergen; Norway.
- ^{18(a)}Physics Division, Lawrence Berkeley National Laboratory, Berkeley CA; ^(b)University of California, Berkeley CA; United States of America.
- ¹⁹Institut für Physik, Humboldt Universität zu Berlin, Berlin; Germany.
- ²⁰Albert Einstein Center for Fundamental Physics and Laboratory for High Energy Physics, University of Bern, Bern; Switzerland.
- ²¹School of Physics and Astronomy, University of Birmingham, Birmingham; United Kingdom.
- ^{22(a)}Department of Physics, Bogazici University, Istanbul; ^(b)Department of Physics Engineering, Gaziantep University, Gaziantep; ^(c)Department of Physics, Istanbul University, Istanbul; Türkiye.
- ^{23(a)}Facultad de Ciencias y Centro de Investigaciones, Universidad Antonio Nariño, Bogotá; ^(b)Departamento de Física, Universidad Nacional de Colombia, Bogotá; Colombia.
- ^{24(a)}Dipartimento di Fisica e Astronomia A. Righi, Università di Bologna, Bologna; ^(b)INFN Sezione di Bologna; Italy.
- ²⁵Physikalisches Institut, Universität Bonn, Bonn; Germany.
- ²⁶Department of Physics, Boston University, Boston MA; United States of America.
- ²⁷Department of Physics, Brandeis University, Waltham MA; United States of America.
- ^{28(a)}Transilvania University of Brasov, Brasov; ^(b)Horia Hulubei National Institute of Physics and Nuclear Engineering, Bucharest; ^(c)Department of Physics, Alexandru Ioan Cuza University of Iasi, Iasi; ^(d)National Institute for Research and Development of Isotopic and Molecular Technologies, Physics Department, Cluj-Napoca; ^(e)National University of Science and Technology Politehnica, Bucharest; ^(f)West University in Timisoara, Timisoara; ^(g)Faculty of Physics, University of Bucharest, Bucharest; Romania.
- ^{29(a)}Faculty of Mathematics, Physics and Informatics, Comenius University, Bratislava; ^(b)Department of Subnuclear Physics, Institute of Experimental Physics of the Slovak Academy of Sciences, Kosice; Slovak Republic.
- ³⁰Physics Department, Brookhaven National Laboratory, Upton NY; United States of America.
- ³¹Universidad de Buenos Aires, Facultad de Ciencias Exactas y Naturales, Departamento de Física, y CONICET, Instituto de Física de Buenos Aires (IFIBA), Buenos Aires; Argentina.
- ³²California State University, CA; United States of America.
- ³³Cavendish Laboratory, University of Cambridge, Cambridge; United Kingdom.
- ^{34(a)}Department of Physics, University of Cape Town, Cape Town; ^(b)iThemba Labs, Western Cape; ^(c)Department of Mechanical Engineering Science, University of Johannesburg, Johannesburg; ^(d)National Institute of Physics, University of the Philippines Diliman (Philippines); ^(e)Department of Physics, Stellenbosch University, Matieland; ^(f)University of South Africa, Department of Physics, Pretoria; ^(g)University of Zululand, KwaDlangezwa; ^(h)School of Physics, University of the Witwatersrand, Johannesburg; South Africa.
- ³⁵Department of Physics, Carleton University, Ottawa ON; Canada.
- ^{36(a)}Faculté des Sciences Ain Chock, Université Hassan II de Casablanca; ^(b)Faculté des Sciences, Université Ibn-Tofail, Kénitra; ^(c)Faculté des Sciences Semlalia, Université Cadi Ayyad, LPHEA-Marrakech; ^(d)LPMR, Faculté des Sciences, Université Mohamed Premier, Oujda; ^(e)Faculté des sciences, Université Mohammed V, Rabat; ^(f)Institute of Applied Physics, Mohammed VI Polytechnic University, Ben Guerir; Morocco.
- ³⁷CERN, Geneva; Switzerland.
- ³⁸Affiliated with an institute formerly covered by a cooperation agreement with CERN.
- ³⁹Affiliated with an international laboratory covered by a cooperation agreement with CERN.
- ⁴⁰Enrico Fermi Institute, University of Chicago, Chicago IL; United States of America.

- ⁴¹LPC, Université Clermont Auvergne, CNRS/IN2P3, Clermont-Ferrand; France.
- ⁴²Nevis Laboratory, Columbia University, Irvington NY; United States of America.
- ⁴³Niels Bohr Institute, University of Copenhagen, Copenhagen; Denmark.
- ⁴⁴(^a) Dipartimento di Fisica, Università della Calabria, Rende; (^b) INFN Gruppo Collegato di Cosenza, Laboratori Nazionali di Frascati; Italy.
- ⁴⁵Physics Department, Southern Methodist University, Dallas TX; United States of America.
- ⁴⁶National Centre for Scientific Research "Demokritos", Agia Paraskevi; Greece.
- ⁴⁷(^a) Department of Physics, Stockholm University; (^b) Oskar Klein Centre, Stockholm; Sweden.
- ⁴⁸Deutsches Elektronen-Synchrotron DESY, Hamburg and Zeuthen; Germany.
- ⁴⁹Fakultät Physik, Technische Universität Dortmund, Dortmund; Germany.
- ⁵⁰Institut für Kern- und Teilchenphysik, Technische Universität Dresden, Dresden; Germany.
- ⁵¹Department of Physics, Duke University, Durham NC; United States of America.
- ⁵²SUPA - School of Physics and Astronomy, University of Edinburgh, Edinburgh; United Kingdom.
- ⁵³INFN e Laboratori Nazionali di Frascati, Frascati; Italy.
- ⁵⁴Physikalisches Institut, Albert-Ludwigs-Universität Freiburg, Freiburg; Germany.
- ⁵⁵II. Physikalisches Institut, Georg-August-Universität Göttingen, Göttingen; Germany.
- ⁵⁶Département de Physique Nucléaire et Corpusculaire, Université de Genève, Genève; Switzerland.
- ⁵⁷(^a) Dipartimento di Fisica, Università di Genova, Genova; (^b) INFN Sezione di Genova; Italy.
- ⁵⁸II. Physikalisches Institut, Justus-Liebig-Universität Giessen, Giessen; Germany.
- ⁵⁹SUPA - School of Physics and Astronomy, University of Glasgow, Glasgow; United Kingdom.
- ⁶⁰LPSC, Université Grenoble Alpes, CNRS/IN2P3, Grenoble INP, Grenoble; France.
- ⁶¹Laboratory for Particle Physics and Cosmology, Harvard University, Cambridge MA; United States of America.
- ⁶²Department of Modern Physics and State Key Laboratory of Particle Detection and Electronics, University of Science and Technology of China, Hefei; China.
- ⁶³(^a) Kirchhoff-Institut für Physik, Ruprecht-Karls-Universität Heidelberg, Heidelberg; (^b) Physikalisches Institut, Ruprecht-Karls-Universität Heidelberg, Heidelberg; Germany.
- ⁶⁴(^a) Department of Physics, Chinese University of Hong Kong, Shatin, N.T., Hong Kong; (^b) Department of Physics, University of Hong Kong, Hong Kong; (^c) Department of Physics and Institute for Advanced Study, Hong Kong University of Science and Technology, Clear Water Bay, Kowloon, Hong Kong; China.
- ⁶⁵Department of Physics, National Tsing Hua University, Hsinchu; Taiwan.
- ⁶⁶IJCLab, Université Paris-Saclay, CNRS/IN2P3, 91405, Orsay; France.
- ⁶⁷Centro Nacional de Microelectrónica (IMB-CNM-CSIC), Barcelona; Spain.
- ⁶⁸Department of Physics, Indiana University, Bloomington IN; United States of America.
- ⁶⁹(^a) INFN Gruppo Collegato di Udine, Sezione di Trieste, Udine; (^b) ICTP, Trieste; (^c) Dipartimento Politecnico di Ingegneria e Architettura, Università di Udine, Udine; Italy.
- ⁷⁰(^a) INFN Sezione di Lecce; (^b) Dipartimento di Matematica e Fisica, Università del Salento, Lecce; Italy.
- ⁷¹(^a) INFN Sezione di Milano; (^b) Dipartimento di Fisica, Università di Milano, Milano; Italy.
- ⁷²(^a) INFN Sezione di Napoli; (^b) Dipartimento di Fisica, Università di Napoli, Napoli; Italy.
- ⁷³(^a) INFN Sezione di Pavia; (^b) Dipartimento di Fisica, Università di Pavia, Pavia; Italy.
- ⁷⁴(^a) INFN Sezione di Pisa; (^b) Dipartimento di Fisica E. Fermi, Università di Pisa, Pisa; Italy.
- ⁷⁵(^a) INFN Sezione di Roma; (^b) Dipartimento di Fisica, Sapienza Università di Roma, Roma; Italy.
- ⁷⁶(^a) INFN Sezione di Roma Tor Vergata; (^b) Dipartimento di Fisica, Università di Roma Tor Vergata, Roma; Italy.
- ⁷⁷(^a) INFN Sezione di Roma Tre; (^b) Dipartimento di Matematica e Fisica, Università Roma Tre, Roma; Italy.
- ⁷⁸(^a) INFN-TIFPA; (^b) Università degli Studi di Trento, Trento; Italy.

- ⁷⁹Universität Innsbruck, Department of Astro and Particle Physics, Innsbruck; Austria.
- ⁸⁰University of Iowa, Iowa City IA; United States of America.
- ⁸¹Department of Physics and Astronomy, Iowa State University, Ames IA; United States of America.
- ⁸²Istinye University, Sariyer, Istanbul; Türkiye.
- ⁸³(^a) Departamento de Engenharia Elétrica, Universidade Federal de Juiz de Fora (UFJF), Juiz de Fora; (^b) Universidade Federal do Rio De Janeiro COPPE/EE/IF, Rio de Janeiro; (^c) Instituto de Física, Universidade de São Paulo, São Paulo; (^d) Rio de Janeiro State University, Rio de Janeiro; (^e) Federal University of Bahia, Bahia; Brazil.
- ⁸⁴KEK, High Energy Accelerator Research Organization, Tsukuba; Japan.
- ⁸⁵Graduate School of Science, Kobe University, Kobe; Japan.
- ⁸⁶(^a) AGH University of Krakow, Faculty of Physics and Applied Computer Science, Krakow; (^b) Marian Smoluchowski Institute of Physics, Jagiellonian University, Krakow; Poland.
- ⁸⁷Institute of Nuclear Physics Polish Academy of Sciences, Krakow; Poland.
- ⁸⁸(^a) Khalifa University of Science and Technology, Abu Dhabi; (^b) University of Sharjah, Sharjah; United Arab Emirates.
- ⁸⁹Faculty of Science, Kyoto University, Kyoto; Japan.
- ⁹⁰Research Center for Advanced Particle Physics and Department of Physics, Kyushu University, Fukuoka ; Japan.
- ⁹¹L2IT, Université de Toulouse, CNRS/IN2P3, UPS, Toulouse; France.
- ⁹²Instituto de Física La Plata, Universidad Nacional de La Plata and CONICET, La Plata; Argentina.
- ⁹³Physics Department, Lancaster University, Lancaster; United Kingdom.
- ⁹⁴Oliver Lodge Laboratory, University of Liverpool, Liverpool; United Kingdom.
- ⁹⁵Department of Experimental Particle Physics, Jožef Stefan Institute and Department of Physics, University of Ljubljana, Ljubljana; Slovenia.
- ⁹⁶Department of Physics and Astronomy, Queen Mary University of London, London; United Kingdom.
- ⁹⁷Department of Physics, Royal Holloway University of London, Egham; United Kingdom.
- ⁹⁸Department of Physics and Astronomy, University College London, London; United Kingdom.
- ⁹⁹Louisiana Tech University, Ruston LA; United States of America.
- ¹⁰⁰Fysiska institutionen, Lunds universitet, Lund; Sweden.
- ¹⁰¹Departamento de Física Teórica C-15 and CIAFF, Universidad Autónoma de Madrid, Madrid; Spain.
- ¹⁰²Institut für Physik, Universität Mainz, Mainz; Germany.
- ¹⁰³School of Physics and Astronomy, University of Manchester, Manchester; United Kingdom.
- ¹⁰⁴CPPM, Aix-Marseille Université, CNRS/IN2P3, Marseille; France.
- ¹⁰⁵Department of Physics, University of Massachusetts, Amherst MA; United States of America.
- ¹⁰⁶Department of Physics, McGill University, Montreal QC; Canada.
- ¹⁰⁷School of Physics, University of Melbourne, Victoria; Australia.
- ¹⁰⁸Department of Physics, University of Michigan, Ann Arbor MI; United States of America.
- ¹⁰⁹Department of Physics and Astronomy, Michigan State University, East Lansing MI; United States of America.
- ¹¹⁰Group of Particle Physics, University of Montreal, Montreal QC; Canada.
- ¹¹¹Fakultät für Physik, Ludwig-Maximilians-Universität München, München; Germany.
- ¹¹²Max-Planck-Institut für Physik (Werner-Heisenberg-Institut), München; Germany.
- ¹¹³Graduate School of Science and Kobayashi-Maskawa Institute, Nagoya University, Nagoya; Japan.
- ¹¹⁴(^a) Department of Physics, Nanjing University, Nanjing; (^b) School of Science, Shenzhen Campus of Sun Yat-sen University; (^c) University of Chinese Academy of Science (UCAS), Beijing; China.
- ¹¹⁵Department of Physics and Astronomy, University of New Mexico, Albuquerque NM; United States of America.

- ¹¹⁶Institute for Mathematics, Astrophysics and Particle Physics, Radboud University/Nikhef, Nijmegen; Netherlands.
- ¹¹⁷Nikhef National Institute for Subatomic Physics and University of Amsterdam, Amsterdam; Netherlands.
- ¹¹⁸Department of Physics, Northern Illinois University, DeKalb IL; United States of America.
- ¹¹⁹(^a) New York University Abu Dhabi, Abu Dhabi; (^b) United Arab Emirates University, Al Ain; United Arab Emirates.
- ¹²⁰Department of Physics, New York University, New York NY; United States of America.
- ¹²¹Ochanomizu University, Otsuka, Bunkyo-ku, Tokyo; Japan.
- ¹²²Ohio State University, Columbus OH; United States of America.
- ¹²³Homer L. Dodge Department of Physics and Astronomy, University of Oklahoma, Norman OK; United States of America.
- ¹²⁴Department of Physics, Oklahoma State University, Stillwater OK; United States of America.
- ¹²⁵Palacký University, Joint Laboratory of Optics, Olomouc; Czech Republic.
- ¹²⁶Institute for Fundamental Science, University of Oregon, Eugene, OR; United States of America.
- ¹²⁷Graduate School of Science, University of Osaka, Osaka; Japan.
- ¹²⁸Department of Physics, University of Oslo, Oslo; Norway.
- ¹²⁹Department of Physics, Oxford University, Oxford; United Kingdom.
- ¹³⁰LPNHE, Sorbonne Université, Université Paris Cité, CNRS/IN2P3, Paris; France.
- ¹³¹Department of Physics, University of Pennsylvania, Philadelphia PA; United States of America.
- ¹³²Department of Physics and Astronomy, University of Pittsburgh, Pittsburgh PA; United States of America.
- ¹³³(^a) Laboratório de Instrumentação e Física Experimental de Partículas - LIP, Lisboa; (^b) Departamento de Física, Faculdade de Ciências, Universidade de Lisboa, Lisboa; (^c) Departamento de Física, Universidade de Coimbra, Coimbra; (^d) Centro de Física Nuclear da Universidade de Lisboa, Lisboa; (^e) Departamento de Física, Escola de Ciências, Universidade do Minho, Braga; (^f) Departamento de Física Teórica y del Cosmos, Universidad de Granada, Granada (Spain); (^g) Departamento de Física, Instituto Superior Técnico, Universidade de Lisboa, Lisboa; Portugal.
- ¹³⁴Institute of Physics of the Czech Academy of Sciences, Prague; Czech Republic.
- ¹³⁵Czech Technical University in Prague, Prague; Czech Republic.
- ¹³⁶Charles University, Faculty of Mathematics and Physics, Prague; Czech Republic.
- ¹³⁷Particle Physics Department, Rutherford Appleton Laboratory, Didcot; United Kingdom.
- ¹³⁸IRFU, CEA, Université Paris-Saclay, Gif-sur-Yvette; France.
- ¹³⁹Santa Cruz Institute for Particle Physics, University of California Santa Cruz, Santa Cruz CA; United States of America.
- ¹⁴⁰(^a) Departamento de Física, Pontificia Universidad Católica de Chile, Santiago; (^b) Millennium Institute for Subatomic physics at high energy frontier (SAPHIR), Santiago; (^c) Instituto de Investigación Multidisciplinario en Ciencia y Tecnología, y Departamento de Física, Universidad de La Serena; (^d) Universidad Andres Bello, Department of Physics, Santiago; (^e) Universidad San Sebastian, Recoleta; (^f) Instituto de Alta Investigación, Universidad de Tarapacá, Arica; (^g) Departamento de Física, Universidad Técnica Federico Santa María, Valparaíso; Chile.
- ¹⁴¹Department of Physics, Institute of Science, Tokyo; Japan.
- ¹⁴²Department of Physics, University of Washington, Seattle WA; United States of America.
- ¹⁴³(^a) Institute of Frontier and Interdisciplinary Science and Key Laboratory of Particle Physics and Particle Irradiation (MOE), Shandong University, Qingdao; (^b) School of Physics, Zhengzhou University; China.
- ¹⁴⁴(^a) State Key Laboratory of Dark Matter Physics, School of Physics and Astronomy, Shanghai Jiao Tong University, Key Laboratory for Particle Astrophysics and Cosmology (MOE), SKLPPC, Shanghai; (^b) State

Key Laboratory of Dark Matter Physics, Tsung-Dao Lee Institute, Shanghai Jiao Tong University, Shanghai; China.

¹⁴⁵Department of Physics and Astronomy, University of Sheffield, Sheffield; United Kingdom.

¹⁴⁶Department of Physics, Shinshu University, Nagano; Japan.

¹⁴⁷Department Physik, Universität Siegen, Siegen; Germany.

¹⁴⁸Department of Physics, Simon Fraser University, Burnaby BC; Canada.

¹⁴⁹SLAC National Accelerator Laboratory, Stanford CA; United States of America.

¹⁵⁰Department of Physics, Royal Institute of Technology, Stockholm; Sweden.

¹⁵¹Departments of Physics and Astronomy, Stony Brook University, Stony Brook NY; United States of America.

¹⁵²Department of Physics and Astronomy, University of Sussex, Brighton; United Kingdom.

¹⁵³School of Physics, University of Sydney, Sydney; Australia.

¹⁵⁴Institute of Physics, Academia Sinica, Taipei; Taiwan.

¹⁵⁵(^a) E. Andronikashvili Institute of Physics, Iv. Javakhishvili Tbilisi State University, Tbilisi; (^b) High Energy Physics Institute, Tbilisi State University, Tbilisi; (^c) University of Georgia, Tbilisi; Georgia.

¹⁵⁶Department of Physics, Technion, Israel Institute of Technology, Haifa; Israel.

¹⁵⁷Raymond and Beverly Sackler School of Physics and Astronomy, Tel Aviv University, Tel Aviv; Israel.

¹⁵⁸Department of Physics, Aristotle University of Thessaloniki, Thessaloniki; Greece.

¹⁵⁹International Center for Elementary Particle Physics and Department of Physics, University of Tokyo, Tokyo; Japan.

¹⁶⁰Graduate School of Science and Technology, Tokyo Metropolitan University, Tokyo; Japan.

¹⁶¹Department of Physics, University of Toronto, Toronto ON; Canada.

¹⁶²(^a) TRIUMF, Vancouver BC; (^b) Department of Physics and Astronomy, York University, Toronto ON; Canada.

¹⁶³Division of Physics and Tomonaga Center for the History of the Universe, Faculty of Pure and Applied Sciences, University of Tsukuba, Tsukuba; Japan.

¹⁶⁴Department of Physics and Astronomy, Tufts University, Medford MA; United States of America.

¹⁶⁵Department of Physics and Astronomy, University of California Irvine, Irvine CA; United States of America.

¹⁶⁶University of West Attica, Athens; Greece.

¹⁶⁷Department of Physics and Astronomy, University of Uppsala, Uppsala; Sweden.

¹⁶⁸Department of Physics, University of Illinois, Urbana IL; United States of America.

¹⁶⁹Instituto de Física Corpuscular (IFIC), Centro Mixto Universidad de Valencia - CSIC, Valencia; Spain.

¹⁷⁰Department of Physics, University of British Columbia, Vancouver BC; Canada.

¹⁷¹Department of Physics and Astronomy, University of Victoria, Victoria BC; Canada.

¹⁷²Fakultät für Physik und Astronomie, Julius-Maximilians-Universität Würzburg, Würzburg; Germany.

¹⁷³Department of Physics, University of Warwick, Coventry; United Kingdom.

¹⁷⁴Waseda University, Tokyo; Japan.

¹⁷⁵Department of Particle Physics and Astrophysics, Weizmann Institute of Science, Rehovot; Israel.

¹⁷⁶Department of Physics, University of Wisconsin, Madison WI; United States of America.

¹⁷⁷Fakultät für Mathematik und Naturwissenschaften, Fachgruppe Physik, Bergische Universität Wuppertal, Wuppertal; Germany.

¹⁷⁸Department of Physics, Yale University, New Haven CT; United States of America.

¹⁷⁹Yerevan Physics Institute, Yerevan; Armenia.

^a Also at Affiliated with an institute formerly covered by a cooperation agreement with CERN.

^b Also at An-Najah National University, Nablus; Palestine.

^c Also at Borough of Manhattan Community College, City University of New York, New York NY; United

States of America.

^d Also at Center for Interdisciplinary Research and Innovation (CIRI-AUTH), Thessaloniki; Greece.

^e Also at Centre of Physics of the Universities of Minho and Porto (CF-UM-UP); Portugal.

^f Also at CERN, Geneva; Switzerland.

^g Also at Département de Physique Nucléaire et Corpusculaire, Université de Genève, Genève; Switzerland.

^h Also at Departament de Física de la Universitat Autònoma de Barcelona, Barcelona; Spain.

ⁱ Also at Department of Financial and Management Engineering, University of the Aegean, Chios; Greece.

^j Also at Department of Mathematical Sciences, University of South Africa, Johannesburg; South Africa.

^k Also at Department of Modern Physics and State Key Laboratory of Particle Detection and Electronics, University of Science and Technology of China, Hefei; China.

^l Also at Department of Physics, Bolu Abant İzzet Baysal University, Bolu; Türkiye.

^m Also at Department of Physics, King's College London, London; United Kingdom.

ⁿ Also at Department of Physics, Stanford University, Stanford CA; United States of America.

^o Also at Department of Physics, Stellenbosch University; South Africa.

^p Also at Department of Physics, University of Fribourg, Fribourg; Switzerland.

^q Also at Department of Physics, University of Thessaly; Greece.

^r Also at Department of Physics, Westmont College, Santa Barbara; United States of America.

^s Also at Faculty of Physics, Sofia University, 'St. Kliment Ohridski', Sofia; Bulgaria.

^t Also at Faculty of Physics, University of Bucharest; Romania.

^u Also at Hellenic Open University, Patras; Greece.

^v Also at Henan University; China.

^w Also at Imam Mohammad Ibn Saud Islamic University; Saudi Arabia.

^x Also at Institutio Catalana de Recerca i Estudis Avancats, ICREA, Barcelona; Spain.

^y Also at Institut für Experimentalphysik, Universität Hamburg, Hamburg; Germany.

^z Also at Institute for Nuclear Research and Nuclear Energy (INRNE) of the Bulgarian Academy of Sciences, Sofia; Bulgaria.

^{aa} Also at Institute of Applied Physics, Mohammed VI Polytechnic University, Ben Guerir; Morocco.

^{ab} Also at Institute of Particle Physics (IPP); Canada.

^{ac} Also at Institute of Physics and Technology, Mongolian Academy of Sciences, Ulaanbaatar; Mongolia.

^{ad} Also at Institute of Physics, Azerbaijan Academy of Sciences, Baku; Azerbaijan.

^{ae} Also at Institute of Theoretical Physics, Ilia State University, Tbilisi; Georgia.

^{af} Also at Millennium Institute for Subatomic physics at high energy frontier (SAPHIR), Santiago; Chile.

^{ag} Also at National Institute of Physics, University of the Philippines Diliman (Philippines); Philippines.

^{ah} Also at The Collaborative Innovation Center of Quantum Matter (CICQM), Beijing; China.

^{ai} Also at TRIUMF, Vancouver BC; Canada.

^{aj} Also at Università di Napoli Parthenope, Napoli; Italy.

^{ak} Also at University of Chinese Academy of Sciences (UCAS), Beijing; China.

^{al} Also at University of Colorado Boulder, Department of Physics, Colorado; United States of America.

^{am} Also at University of Sienna; Italy.

^{an} Also at Washington College, Chestertown, MD; United States of America.

^{ao} Also at Yeditepe University, Physics Department, Istanbul; Türkiye.

* Deceased